



TÉCNICO
LISBOA

***Ex-vivo* Expansion of Umbilical Cord Blood
Hematopoietic Stem Cells**

Jorge Moura Sampaio

Thesis to obtain the Master of Science degree in

Biotechnology

Supervisors: Doctor Ana Margarida Pires Fernandes Platzgummer

Professor Cláudia Alexandra Martins Lobato da Silva

Examination Committee

Chairperson: Doutora Leonilde de Fátima Morais Moreira

Supervisor: Doutora Ana Margarida Pires Fernandes-Platzgummer

Member of the Committee: Doutor Francisco Ferreira dos Santos

September 2016

Acknowledgements

My appreciation goes to everyone in the SCBL group that accompanied me throughout this past year.

Firstly, I would like to thank Professor Joaquim Cabral for giving me the chance to work at the Stem Cell Bioengineering Laboratory (SCBL), and to my advisors, Professor Cláudia Lobato da Silva and Doctor Ana Fernandes-Platzgummer for trusting in my work from an early stage and for giving me advice.

A special thanks to Márcia Mata, my *chêfinha*, for having lots of patience, and teaching me how to get around the laboratory, for listening to all my ideas and answering all my questions, for her good mood, for her readiness to help me, and for teaching me everything she could. Without her presence, this master thesis would not be as valuable as it is.

Additionally, I would like to thank António Soure and Marta Costa for sharing their knowledge with me, for the valuable discussions and brainstorming, and for always keeping a good mood in the face of adversity.

I would also like to thank Carlos Rodrigues and João Silva for always believing in Éder, and for all the funny lunch talks about all kinds of topics. Speaking of funny, a big thanks to Sara Vieira and Margarida Barroso for all the good times, friendship, patience, and for being on my side this past year. To Ricardo Ribeiro, Pedro Fontes and Bárbara Fernandes, a big thanks also for being part of this two-year journey on the Masters course.

A big hug to my dear friends, André Barateiro, Beatriz Pinheiro, Henrique Pereira, Mariana Dias, Rita Dias, Rita Esteves, José Amaro, André Costa, Andreia Teixeira. Also to my bros, Afonso Rodrigues and João Palma. These past years have been incredible.

To Joana Ferreira, the love of my life, for always being by my side when I needed the most, and for driving me to be a better person every day.

Finally, I would like to thank my parents and my grandma, for all the values they taught me, for all the efforts they did so I could accomplish my objectives, for their unconditional support and love. To my grandpa Jorge, who I know would be proud.

Abstract

The major obstacle to the widespread use of umbilical cord blood (UCB) in hematopoietic stem (HSC) cell therapy is the low cell dose available, which often leads to graft failure. The engrafting capability of a UCB unit can be enhanced by *ex-vivo* expansion by a rational combination of many factors such as initial stem/progenitor cell enrichments and oxygen tension, culture duration, cytokine cocktails, blocking *in vitro* differentiation of early progenitor cells and co-culture with stromal feeder layers. Interactions of vascular/stromal cells with HSCs are known to be of great importance for their maintenance, thus making stromal cells ideal to mimic HSCs adult niche – the bone marrow (BM) – in *in vitro* conditions. With the objective of expanding Mesenchymal Stem/Stromal Cells (MSCs) on a xenogeneic (xeno)-free manner, chemically defined medium (StemPro®), and Human platelet lysate (HPL)-supplemented media were used to expand BM MSCs. HPL-supplemented media was able to expand and establish BM MSC-derived feeder-layers capable of supporting HSC expansion, indicative that HSC/MSC co-culture can be done in a fully xeno-free manner throughout all steps of the process. To surpass availability issues associated with BM MSCs, HPL-supplemented media was also able to expand MSCs from alternative sources, usually regarded as biological waste, such as adipose tissue (AT) and umbilical cord matrix (UCM), and establish functional feeder layers. Additionally, a two-level face-centred cube design (FC-CD) approach was used for the optimization of a cytokine cocktail to supplement StemSpan SFEM II expansion medium, in the presence or absence of MSC-derived stromal feeder layers.

Resumo

O maior obstáculo para o uso generalizado de sangue do cordão umbilical (UCB) em terapia com células estaminais hematopoiéticas (HSCs) é baixa dose de células disponível, o que muitas vezes leva à falência do enxerto. A capacidade de enxerto de uma unidade de UCB pode ser reforçada por expansão ex-vivo por uma combinação racional de vários factores, tais como a tensão de oxigénio, duração da cultura, cocktails de citocinas e co-cultura com células mesenquimais. As interações de células mesenquimais/estromais com HSCs são conhecidos por ser de grande importância para a sua manutenção, essas células ideais para aumentar os números de HSCs em laboratório. Com o objetivo de expandir MSCs da medula óssea de uma maneira livre de xenogênicos, meio quimicamente definido (StemPro®) e meio suplementado com lisado plaquetário humano (HPL) foram usados para expandir MSCs. Meio suplementado com HPL foi capaz de expandir e estabelecer camadas aderentes de MSCs capazes de suportar a expansão HSCs, indicativo de que a co-cultura de HSC/MSc pode ser feito de uma forma totalmente xeno livre em todas as etapas do processo. Para superar problemas de disponibilidade associados com MSCs provenientes da medula óssea, meio suplementado com HPL também foi usado para expandir MSCs a partir de fontes alternativas, tais como tecido adiposo (AT) e da matriz do cordão umbilical (UCM). Além disso, um design experimental baseado num face-centred cube design (FC-CD) foi utilizado para a otimização de um cocktail de citocinas para suplementar o meio de expansão StemSpan SFEM II, na presença ou ausência de MSCs.

Keywords

Bone Marrow

Mesenchymal stem/stromal cells

Hematopoietic stem cells

Umbilical Cord Blood

Ex-vivo expansion

Cell Therapy

Palavras-Chave

Células estaminais mesenquimais

Medula Óssea

Células estaminais Hematopoiéticas

Sangue do Cordão Umbilical

Expansão *ex-vivo*

Terapia Celular

Table of Contents

Acknowledgements	i
Abstract	ii
Resumo	iii
Keywords	iv
Palavras-Chave	v
Table of Contents	vi
List of Tables	viii
List of Figures	ix
List of Abbreviations	xiii
I. Aim of Studies	1
II. Introduction	2
II.1 Brief History	2
II.2. Bone Marrow Niche	2
II.2.1 Endosteal Region	3
II.2.2 Perivascular Regions and Mesenchymal Stem/Progenitor Cells	4
II.2.4 Oxygen Gradient and Functional Zones	6
II.3. Human Hematopoietic Lineages	7
II.4. In vitro assays	8
II.5. HSC Transplantation.	11
II.5.1 Mobilized Peripheral Blood.	11
II.5.2 Umbilical Cord Blood.	12
II.6. Ex-vivo expansion of HSCs.	13
II.5.1 Stromal feeder layers	15
III. Materials and Methods.	17
III.1. Human Samples.	17
III.1.1. Processing Umbilical Cord Blood.	17
III.1.2. Purification of CD34 ⁺ -enriched cells.	17
III.2. Cell Counting.	17
III.3. MSC cell culture.	18
III.3.1. Thawing.	18
III.3.1. Ex-vivo expansion in static conditions.	18
III.4. HSC/MSK Expansion Systems.	18
III.4.1. Establishment of MSC-derived feeder layers.	18
III.4.3. Expansion of CD34 ⁺ -enriched cells in Static conditions.	19
III.5. In vitro assays.	19
III.5.1. Proliferative analysis	19
III.5.2. Phenotypic analysis	19

III.5.3. Clonogenic Potential assay	19
IV. Hematopoietic supportive capacity of different mesenchymal stem/stromal cell populations	21
IV.1 Background	22
IV.2 Establishment of xenogeneic (xeno)-free bone marrow (BM) MSC-derived feeder layers for HSC expansion	22
- StemPro® MSC SFM (Life Technologies™)	22
- Human Platelet Lysate (HPL) – BSSub™-XF (AventaCell BioMedical Co. Ltd.)	25
IV.3 Establishment of xenogeneic (xeno)-free feeder layers from alternative MSC sources for HSC expansion	30
V. Systematic delineation of optimal cytokine concentrations through a two-level face-centered cube design (FC-CD).	35
V.1 Background and Experimental Design	36
V.2. No Stroma model	39
V.3. Stroma model	43
V.4. Discussion	47
VI. Conclusions and Future Trends	48
VII. Supplementary Figures	49
VIII. References	50

List of Tables

Table 1 - Summary of the main results focusing on UCB expansion under static conditions, either on liquid suspension cultures or in the presence of mesenchymal stem/stromal cells feeder layers. Adapted From: Andrade, P. Z., Santos et al. Stem cell bioengineering strategies to widen the therapeutic applications of hematopoietic stem/progenitor cells from umbilical cord blood: *J. Tissue Eng. Regen. Med.* 9, 988–1003 (2015).

Table 2 - Summary of cytokines and other molecules used in human hematopoietic stem/progenitor cell culture ex-vivo with their reported functions. Adapted From: Andrade, P. Z., Santos et al. Stem cell bioengineering strategies to widen the therapeutic applications of hematopoietic stem/progenitor cells from umbilical cord blood: *J. Tissue Eng. Regen. Med.* 9, 988–1003 (2015).

Table 3 - Number of cells measured at day 0 (D0) and day 7 (D7), and viability at day 7, of XF and SS MSCs inactivated in different media and mitomycin-C concentration.

Table 4 - Design matrix for the optimization of the cytokine cocktail, and cube representation of the design used in the present studies: SCF, Flt-3L, TPO were tested either at 0 ng mL⁻¹ (low level, -1) or 100 mL⁻¹ (high level, +1), respectively. Mid level (0) = 50 ng mL⁻¹.

Table 5 – Results for each response variable in the no stroma model, after 7 days in culture measured as fold increase in: Total nucleated cells (TNC), CD34+, BFU-E, CFU-GM and CFU-mix

Table 6 - Results for each response variable in the stroma model, after 7 days in culture measured as fold increase in: Total nucleated cells (TNC), CD34+, BFU-E, CFU-GM and CFU-mix.

List of Figures

Figure 1 - Schematic diagram of hematopoietic and niche cellular components in the bone marrow. Moore & Lemischka. Stem cells and their niches. *Science* 311, 1880–1885 (2006).

Figure 2 - SNO-HSC signalling in the bone marrow endosteal niche. Purple: Promotes stem cell differentiation; Blue: Maintains HSC immaturity. Hofmeister et al. Ex-vivo expansion of umbilical cord blood stem cells for transplantation: growing knowledge from the hematopoietic niche. *Bone Marrow Transplant.* 39, 11–23 (2007).

Figure 3 - The adult bone marrow HSC niche. Dormant HSCs are found around arterioles where factors such as CXCL12 and SCF secreted by perivascular, endothelial, Schwann, and sympathetic neuronal cells promote their maintenance. Less quiescent or activated HSCs are located near sinusoidal niches which are likely diverse in their influence for self-renewal, proliferation, and differentiation. Hematopoietic cells such as macrophages or megakaryocytes are examples of HSC-derived progeny that can feed back to the niche to influence HSC migration or proliferation. GFAP, glial fibrillary acidic protein; TGF- β 1, transforming growth factor beta-1. Boulais, P. E. & Frenette, P. S. Making sense of hematopoietic stem cell niches. *Blood* 125, 2621–2629 (2015).

Figure 4 - Oxygen gradient within the bone marrow niche. Mohyeldin et al. Oxygen in stem cell biology: a critical component of the stem cell niche. *Cell Stem Cell* 7, 150–161 (2010).

Figure 5 – Simplified scheme of HSC distribution in the bone marrow. Adapted from: Li et al. Coexistence of Quiescent and Active Adult Stem Cells in Mammals. *Science* 327, 542–545 (2010).

Figure 6 – Classical human hematopoiesis lineages model. HSC: Hematopoietic Stem Cell; MPP: Multipotent Progenitor; MLP: Multi-Lymphoid Progenitor; CMP: Common Myeloid Progenitor; GMP: Granulocyte-Monocyte Progenitor; MEP: Megakaryocyte-Erythroid Progenitor; Adapted From: Doulatov et al. Hematopoiesis: A Human Perspective. *Cell Stem Cell* 10, 120–136 (2012).

Figure 7 - CFU-GEMM colonies.

Figure 8 - CFU-GM Colonies. Normal (top) and Large (Bottom) colonies

Figure 9 - BFU-E colonies

Figure 10 – CAFC colony assay. Cobblestone areas are shown (straight-lined circles) as well as two areas with output (phase bright) cells shown in dashed circles. Adapted from: van Os et al. In vitro assays for cobblestone area-forming cells, LTC-IC, and CFU-C. *Methods Mol. Biol.* Clifton NJ 430, 143–157 (2008).

Figure 11 - Schematic of ex vivo expansion techniques for cord blood transplantation. Adapted From: Munoz, J. et al. Concise Review: Umbilical Cord Blood Transplantation: Past, Present, and Future. Stem Cells Transl. Med. 3, 1435–1443 (2014).

Figure 12 – Plastic adherent BM MSC cell culture, expanded in a) StemPro – XF MSCs b) DMEM 10% FBS – SS MSCs

Figure 13 – Representative image of a senescent XF MSC-derived feeder layer

Figure 14 – Comparison of BM MSC feeder layers expanded either in DMEM 10%FBS treated with 0.5 ug.mL⁻¹ of mitomycin-C (a) or in StemPro® MSC SFM XenoFree treated with 5 ug.mL⁻¹ of mitomycin-C (b).

Figure 15 - BM MSCs expanded in DMEM 5%HPL-XF prior to mitomycin-C treatment

Figure 16 - BM MSC feeder layers expanded in DMEM 5%HPL-XF: a) BM MSC at day-7, without mitomycin-C treatment; b) BM MSC at day-7, 0.5 µg mitomycin-c treatment.

Figure 17 – DMEM 5%HPL-XF expanded BM MSCs stromal layers: Fold increase in total number of cells (Left) and Viability measurement (Right) after 7 days in co-culture media, for non-inactivated samples (BM no MitoC), 5 ug.mL⁻¹ inactivated samples (BM Inactivated), and inactivated samples left for 48h in HPL prior to 7-day culture (BM MitoC + 48h).

Figure 18 – Side-by-side comparison of the ex-vivo hematopoietic supportive capacity of BM MSC feeder layers expanded either in DMEM 10% FBS or DMEM 5% HPL-XF, and in the absence of stroma (noSTR): Outputs measured as fold increase in total nucleated cells (TNC, results presented as Mean ± SEM), and clonogenic potential as measured by Burst forming units – erythroid (BFU-E), Colony forming units – granulocyte monocyte (CFU-GM), and Colony forming units – mix (CFU-Mix).

Figure 19 - Proportion of hematopoietic subpopulations for fresh CD34+-enriched UCB sample (day 0).

Figure 20 – Proportion of hematopoietic subpopulations for expanded CD34+-enriched UCB samples (day 7), in co-culture with BM MSC expanded feeder layers in DMEM 10%FBS, DMEM 5% HPL or in the absence of stroma (noSTR).

Figure 21 – Fold increase in hematopoietic subpopulations for expanded CD34+-enriched UCB samples (day 7), in co-culture with BM MSC expanded feeder layers in DMEM 10%FBS, DMEM 5% HPL or in the absence of stroma (noSTR).

Figure 22 - 60% Confluent AT MSCs expanded in DMEM 5%HPL-XF prior to inactivation

Figure 23 – DMEM 5%HPL-XF expanded AT MSC-derived feeder layers at day 7: A) 50 µg.mL⁻¹ Mitomycin-C treatment; B) 5 µg.mL⁻¹ Mitomycin-C treatment; C) 0.5 µg.mL⁻¹ Mitomycin-C treatment; D) Without Mitomycin-C Inactivation

Figure 24 - DMEM 5%HPL-XF expanded AT MSCs stromal layers: Fold increase in total number of cells and Viability % measurement after 7 days in co-culture media, for non-inactivated samples (AT no MitoC), and 5 ug.mL⁻¹ inactivated samples (AT 5 ug.mL⁻¹)

Figure 25 - UCM MSC expanded in HPL-XF prior to inactivation.

Figure 26 - DMEM 5%HPL-XF expanded UCM MSC-derived feeder layers at day 7: a) 50 µg.mL⁻¹ mitomycin-c treatment; b) 5 µg.mL⁻¹ mitomycin-c treatment; c) 0.5 µg.mL⁻¹ mitomycin-c treatment; d) Without mitomycin-c treatment;

Figure 27 - DMEM 5%HPL-XF expanded UCM MSCs stromal layers, inactivated with 5 µg.mL⁻¹ mitomycin-c: a) Fold increase in total number of cells and b) Viability measurement after 7 days in co-culture media, for non-inactivated samples (UCM no MitoC), 5 ug.mL⁻¹ inactivated samples (UCM StemSpan), and inactivated samples left for 48h in HPL prior to 7-day culture (BM HPL 48h)

Figure 28 – Representation of the hierarchy levels in the polynomial: Adapted from: gelifesciences. Understanding Design of Experiments (DoE) in Protein Purification

Figure 29 – Pareto chart of effects for SCF (1), FLT3-L (2) and TPO (3) factors, within each response variable: FI Total nucleated cells (TNC), FI CD34+, FI BFU-E, FI CFU-GM and FI CFU-mix. Linear effects denoted as (L), and quadratic effects as (Q). P-value = 0.05. No stroma model

Figure 30 – Adjusted Pareto Chart (left) and ANOVA table (right) for FI TNC response variable. No stroma model

Figure 31 – Normal probability plot of residuals, for the FI TNC response variable of no stroma model

Figure 32 – Regression coefficients for the FI TNC response variable of no stroma model.

Figure 33 - Fitted response surface plot for SCF and TPO with (left) or without (Right) the quadratic effect for SCF, for the no stroma model

Figure 34 - Fitted response surface plot for FLT3-L and TPO (left) and SCF and Flt3-L (Right) for the no stroma model

Figure 35 – Pareto chart of effects for the FI TNC response variable. Before (left) and After (right) adjustment. Stroma model.

Figure 36 – ANOVA table for the FI TNC response variable after adjustment, for the stroma model.

Figure 37 – Normal probability plot of residuals, for the FI TNC response variable for the stroma model.

Figure 38 – Regression coefficients for the FI TNC response variable for the stroma model.

Figure 39 - Fitted response surface plot for SCF and Flt3-L for the stroma model

Figure 40 - Fitted response surface plot for SCF and TPO, with FLT3-L fixed at 50ng.mL (left) or at 100 ng.mL (right) for the stroma model

Figure 41 - Fitted response surface plot for FLT3-I and TPO for the stroma model

List of Abbreviations

AT	Adipose Tissue
bFGF	basic Fibroblast Growth Factor
BFU-E	Burst-Forming Unit – Erythroid
BM	Bone Marrow
CAFCs	Cobblestone-Area Forming Cells
CD	Cluster of Differentiation
CFU-GM	Colony-Forming Unit – Granulocyte/Macrophage
CFU-Mix	Colony-Forming Unit – Granulocyte, erythroid, macrophage, megakaryocyte
cGMP	current Good Manufacturing Practice
DAPI	4',6-diamidino-2-phenylindole
DMEM	Dulbecco's Modified Eagle's Medium
FBS	Fetal Bovine Serum
FC-CD	Face-centred cube design
FLT-3	FMS-like tyrosine kinase 3
G-CSF	Granulocyte colony-stimulating factor
GM-CSF	Granulocyte–macrophage colony-stimulating factor
GMP	Good Manufacturing Practice
GvHD	Graft-versus-host disease
GvT	Graft-versus-Tumour
HLA	Major Histocompatibility Complex
HPL	Human Platelet Lysate
HSC	Hematopoietic Stem Cell
IL	Interleukin
ICAM1	Intercellular adhesion molecule 1
IPO	Instituto Português de Oncologia
MACS	Magnetic-Activated Cell Sorting
M-CSF	Macrophage colony-stimulating factor
MCP-1	Monocyte chemoattractant protein-1
MIP-1a	Macrophage inflammatory protein-1a
MNCs	Mononuclear Cells
MPPs	Multipotent Progenitors
MSCs	Mesenchymal Stem/Stromal Cells

PBS	Phosphate Buffered Saline
QBSF	Quality Biological Serum-Free
SC	Serum-containing
SCBL	Stem Cell Bioengineering Laboratory
SCF	Stem Cell Factor
SDF-1	Stromal cell-Derived Factor 1
SEM	Standard Error of the Mean
SNO	Spindle-shaped N-cadherin ⁺ Osteoblasts
TGFb	Transforming growth factor-b
TNFa	Tumour necrosis factor-a
TPO	Thrombopoietin
UCB	Umbilical Cord Blood
UCM	Umbilical cord matrix
VCAM1	Vascular cell adhesion molecule 1

I. Aim of Studies

This thesis aims at the optimization of a serum-free hematopoietic stem cells (HSC)/mesenchymal stem/stromal cells (MSC) co-culture system towards the maximization of umbilical cord blood (UCB) hematopoietic stem/progenitor cell expansion for the improvement of their therapeutic potential in treating hematological malignancies. Cell culture was mainly performed under static conditions to provide important insights towards the translation of HSC/MSC co-culture system to a scalable bioreactor system, in order to allow clinical-scale production for HSC transplantation.

In **Chapter IV**, laboratory work focused on expanding MSC for establishing stromal feeder layers on a GMP-compliant fashion was performed by using several commercially available xeno-free expansion media for MSC, and analyse how these xeno-free populations of MSC supported the ex-vivo expansion of UCB HSC when compared with MSC expanded in serum containing media. Additionally, umbilical cord matrix (UCM) and adipose tissue (AT), which are alternative sources for MSCs, were also explored as possible tissues for establishing stromal feeder layers.

Chapter V tackles a critical parameter in *ex-vivo* expansion HSCs, which is the cytokine cocktail used to supplement the expansion medium. Previously at SCBL, an FC-CD experimental design was followed to optimize the cytokine concentration in QBSF-60 medium. However, high degradation of glutamine, high levels of megakaryocytic differentiation and low expansion in the absence of stroma, lead to the necessity of using other HSC expansion medium. StemSpan SFEM II is a defined serum-free media which can be supplemented with several different cytokine cocktails to achieve different outcomes, with high levels of expansion. Specifically, to unveil the role of stromal feeder layers on cytokine cocktails, a face-centred cube design (FC-CD) of experiments was performed to access the optimal cytokine concentration in the presence and absence of stroma, for the expansion of CD34⁺ cells using this media.

II. Introduction

II.1 Brief History

Hematopoietic Stem Cells (HSCs) are the most extensively studied cells in stem cell biology and medicine. The earliest evidence of a cell responsible for the generation of blood cells, from embryogenesis to adulthood, dates back to 1945. Experiments with adult cattle fraternal twins (*i.e.* originated from two different zygotes, but sharing the same placenta) found that individuals had blood cells with different origins, that origin being their twin, suggesting that cells interchanged during embryonic/fetal development were able to persist and continuously provide a source of blood cells different from those of the host throughout the life of an individual.⁴ The years that followed saw a boom in hematopoietic studies, such as the Nobel prize-winning studies of Medawar on acquired immune tolerance upon hematopoietic cell infusions in fetal and neonatal mice,⁵ and the birth of hematopoietic cell transplantation to revert radiation-driven hematopoietic failure^{6,7}. In 1961, seminal work by Till and McCulloch showed that: i) hematopoiesis could be studied as a quantitative science; ii) clonal hematopoietic cells in the bone marrow could give rise to mixed myeloerythroid progeny (*i.e.* granulocytes, macrophages, erythrocytes, megakaryocytes); iii) the cells responsible for that progeny could self-renew; iv) cells from the lymphoid system (*i.e.* Thymus, lymph nodes and spleen) had a common link with myeloerythroid cells.⁸⁻¹² These results ultimately suggested the existence of a common cell that could give rise to all cell types present in the blood system.

II.2. Bone Marrow Niche

The hematopoietic stem cell niche commonly refers to the pairing of hematopoietic, mesenchymal, and vascular cell populations that regulate HSC self-renewal, differentiation, and proliferation. The first suggestion that a given biologic microenvironment could influence HSCs fate appeared in 1970. Wolf and Trentin placed an explant of irradiated bone marrow stroma into the spleen of irradiated, and marrow-injected mice, where myelomonocytic colonies appeared in the ectopic marrow, while the surrounding spleen tissue contained mainly erythroid colonies. Most interestingly, at the spleen-marrow interface, individual colonies were simultaneously myelomonocytic on the bone side and erythroid on the spleen side.¹³

II.2.1 Endosteal Region

In adults, HSCs and their primitive progeny are located within the Bone Marrow (BM), contiguously to the endosteal surface of trabecular bone (**Figure 1**)¹⁴.

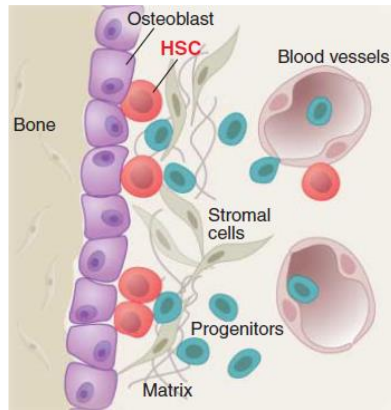


Figure 1 - Schematic diagram of hematopoietic and niche cellular components in the bone marrow. Moore & Lemischka. Stem cells and their niches. Science 311, 1880–1885 (2006).

Manipulation of osteoblast numbers correlates with HSC counts in the bone marrow, indicating that osteoblast cells play a critical role in the maintenance of the bone marrow niche. For instance, increased numbers of N-cadherin⁺ CD45⁻ spindle-shaped osteoblasts (SNO) lead to higher HSC numbers, without changes in the committed progenitor populations. Consistently, deletion of osteoblast cells in transgenic mice caused the loss of lymphoid, erythroid, and myeloid progenitors in the bone marrow followed by HSC depletion. During these events, peripheral HSCs increase, and active extramedullary hematopoiesis takes place in the spleen and liver.¹⁵ This not only demonstrates SNOs critical role in the bone marrow niche, but also constitutes evidence that other HSC niches exist.

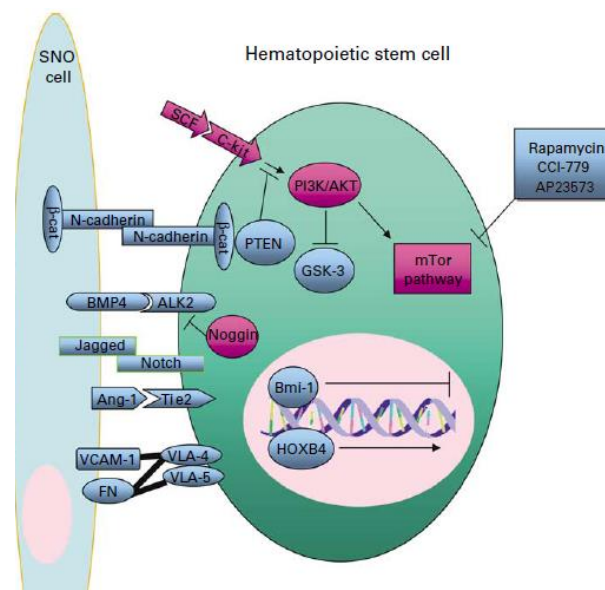


Figure 2 - SNO-HSC signalling in the bone marrow endosteal niche. Purple: Promotes stem cell differentiation; **Blue:** Maintains HSC immaturity. Hofmeister et al. Ex-vivo expansion of umbilical cord blood stem cells for transplantation: growing knowledge from the hematopoietic niche. Bone Marrow Transplant. 39, 11–23 (2007).

Osteoblasts have been proposed to support HSC function by forming direct interactions via N-cadherin-mediated adhesion (**Figure 2**),^{16,17} although this idea has been highly controversial. Functional studies using conditional knockout of N-cadherin (*Cdh2*) in hematopoietic and stromal cells¹⁸ and osteoblasts¹⁹ have not revealed any change in HSC numbers, although overexpression of N-cadherin has been reported to alter HSC numbers.²⁰ Activated osteoblasts can produce osteopontin, which limits HSC expansion,²¹ as well as angiopoietin-1 and thrombopoietin, which bind the Tie2 and MPL receptors, respectively, and contribute to HSC quiescence.^{22–24}

II.2.2 Perivascular Regions and Mesenchymal Stem/Progenitor Cells

Although it has been suggested that the endosteal region is enriched in HSCs, their distribution may not be as narrow as initially suggested.²⁵ After transplantation in irradiated mice, HSCs preferentially home to the endosteal surfaces of the trabecular bone region, but randomly distribute in non-irradiated recipients.^{26,27} HSCs undergo expansion after bone marrow damage in the endosteal region where osteoblasts and blood vessels are in close proximity.^{26,27} Lethal irradiation is known to disrupt the sinusoidal network, which may account for the relocalization of HSCs to the endosteum.²⁸ Since the endosteum is vascularized with arteriolar vessels that are more resistant to genotoxic insults, it is likely that vascular niches differentially contribute to bone marrow regeneration.

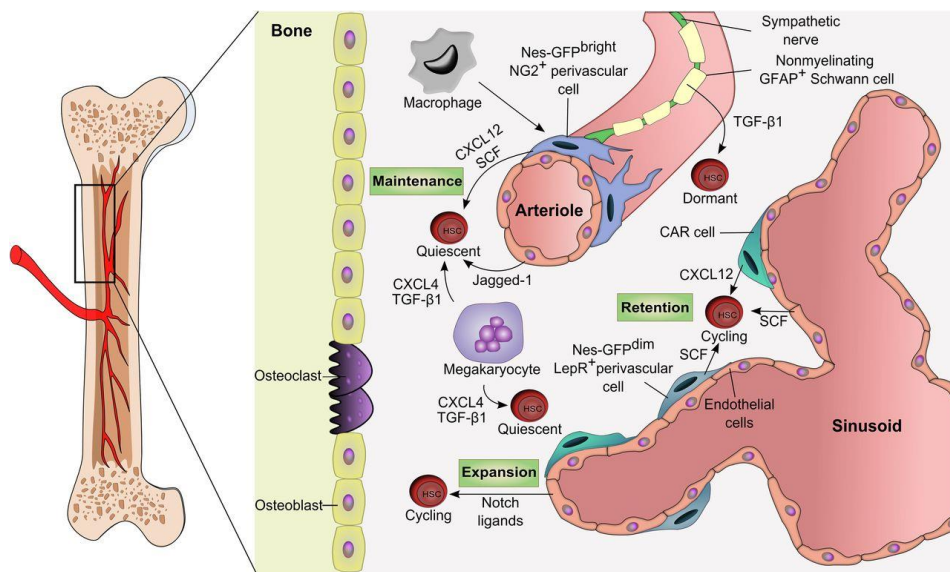


Figure 3 - The adult bone marrow HSC niche. Dormant HSCs are found around arterioles where factors such as CXCL12 and SCF secreted by perivascular, endothelial, Schwann, and sympathetic neuronal cells promote their maintenance. Less quiescent or activated HSCs are located near sinusoidal niches which are likely diverse in their influence for self-renewal, proliferation, and differentiation. Hematopoietic cells such as macrophages or megakaryocytes are examples of HSC-derived progeny that can feed back to the niche to influence HSC migration or proliferation. GFAP, glial fibrillary acidic protein; TGF-β1, transforming growth factor beta-1. **Boulais, P. E. & Frenette, P. S. Making sense of hematopoietic stem cell niches. Blood 125, 2621–2629 (2015).**

The bone marrow vasculature is heterogeneous in its expression of molecules that are thought to facilitate cell homing, such as E-selectin and SDF-1 (also known as CXCL12)²⁹. Regarding vascularization, several studies suggest that microenvironments neighbouring blood vessels may constitute an HSC niche. In fact, HSC were reported to be near sinusoidal blood vessels,³⁰ and

to be generated in vascular areas during embryonic development^{31–33}. Most interestingly, extramedullary hematopoiesis occurs in perivascular areas upon hematopoietic stress³⁴.

Secondly, endothelial cells from the bone marrow express factors that promote hematopoiesis, such as granulocyte colony-stimulating factor (G-CSF), granulocyte–macrophage colony-stimulating factor (GM-CSF), macrophage colony-stimulating factor (M-CSF), stem cell factor (SCF; also known as KIT ligand), interleukin-6 (IL-6) and FMS-related tyrosine kinase 3 ligand (FLT3L; also known as FLK2 ligand).³⁵ Additionally, endothelial cells were shown to express the adhesion molecules E-selectin, P-selectin, vascular cell adhesion molecule 1 (VCAM1) and intercellular adhesion molecule 1 (ICAM1)³⁶, and were found to enable the transit of HSCs and immune cells between the bone marrow and the periphery.³⁷

Mesenchymal stem/stromal cell (MSCs) activity was described decades ago but the lack of unique cell surface markers and the disparity between lineage tracing models and isolation methods have hampered their characterization. MSCs wrap around blood vessels and adrenergic nerve fibres, both in the central and endosteal bone marrow regions, and they express several proteins that regulate HSC maintenance, including SDF-1 (CXCL12), angiopoietin 1 and SCF.²⁹

Perivascular CD146⁺ CD45⁻ MSCs provide structural support and interact directly with HSCs.³⁸ A subpopulation of CD146⁺ bone marrow cells is characterized by the expression of the cytoplasmic filament protein nestin in mice, which allows the prospective identification of perivascular MSCs which are significantly associated with HSCs. These cells are able to form clonal spheres that can self-renew, multi-differentiate at the clonal level into the major mesenchymal lineages, and generate hematopoietic activity *in vivo* upon serial transplantation³⁹. In humans, a sub-population of PDGFR α ⁺ CD51⁺ cells represent a subset of CD146⁺ cells expressing nestin, which can also be cultured as non-adherent mesenspheres that significantly expand multipotent hematopoietic progenitors able to engraft immunodeficient mice⁴⁰. Deletion of nestin⁺ MSCs leads to a 50% reduction in bone marrow HSC numbers with a proportional increase in the spleen HSCs, suggesting that nestin⁺ MSC are responsible for retaining HSCs in the bone marrow niche.³⁹ CXCL12-abundant reticular (CAR) cells are a MSC subpopulation.⁴¹ CAR cells are scattered throughout the bone marrow, secrete factors that support hematopoiesis, and are located adjacent to a substantial proportion of phenotypically defined HSCs²⁹. The deletion of CAR cells in the adult mouse lead to a decrease in HSC numbers and an increase in HSC quiescence⁴². As the aforementioned nestin⁺ MSCs also express high levels of CXCL12, nestin⁺ MSCs may represent a functional subtype of CAR cells that are found in the perivascular location, but are hypothesized to be participants in HSC regulation^{29,39}.

II.2.4 Oxygen Gradient and Functional Zones

Data suggests that although osteoblasts are determinant for maintaining the bone marrow niche, they do not directly contribute to HSC maintenance. Examples of this are the selective deletion of critical niche factors in osteoblasts, and recent imaging studies of the bone marrow, that did not reveal a significant association between osteoblasts and HSCs.^{43,44} However, one proposed view of the endosteal niche is that was that it might provide a hypoxic environment for maintaining HSCs in a quiescent state whereas the vascular niche allows HSCs to proliferate and differentiate in an environment in which oxygen is more available.⁴⁵

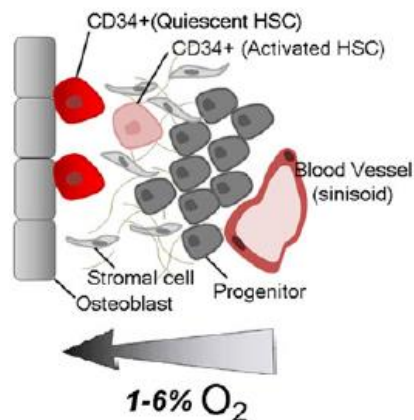


Figure 4 - Oxygen gradient within the bone marrow niche. Mohyeldin et al. Oxygen in stem cell biology: a critical component of the stem cell niche. *Cell Stem Cell* 7, 150–161 (2010).

Several stromal cells and progenitor cells physically reside between the HSCs and the closest blood vessel, hence, it was postulated that the bone marrow was relatively hypoxic when compared to other tissues, as these cells competed for the already scarce nutrient and oxygen supply (**Figure 4**)⁴⁶. Mathematical models based on animal data supported this hypothesis and predicted oxygen tensions to be as low as 1%.⁴⁷ However, it is now widely accepted that gradients of oxygen of 1% in hypoxic niches up to 6% in the sinusoidal cavity exist within the human bone marrow.⁴⁸

Expectedly, low oxygen tensions in stem cell niches offer a selective advantage, avoiding the generation of reactive oxygen species (ROS) typical of aerobic metabolism, which can damage DNA.⁴⁹ By residing in low oxygen tension tissues, HSCs maintain slow-cycling proliferation rates while avoiding the oxidative stress associated with more well-oxygenated tissue. In fact, mouse embryonic fibroblasts accumulate more mutations and senesce faster when cultured under 20% O₂ when compared to culture under 3% O₂.⁵⁰ Additionally, hypoxia has been shown to activate molecular pathways in multiple stem cell systems that appear to regulate Oct4 and Notch signalling, two important regulators of “stemness”.⁵¹ Furthermore, small oxygen tensions variations were shown to modulate proliferation in human Embryonic Stem Cells (hESC),⁵² suggesting that oxygen gradients is also one of the factors controlling proliferation and quiescence in stem cell niches. For example, it has been observed that HSCs present in the hypoxic niche express higher levels of Notch signalling⁵³, telomerase and cell-cycle inhibitor p21, than cells closer to the vasculature.⁵⁴ Most interestingly, CD34⁺ cultured in 0.1% O₂ were found to revert to

a G0 quiescent state.⁵⁵ Consistently, the most slowly cycling hematopoietic cells are found in the hypoxic zones close to bone surface and distant from capillaries,^{56,57} highlighting the importance of hypoxic niches in HSC proliferation arrest. In fact, HSCs in aged mice are localized farther from the endosteum than in young mice, with the central marrow zone favouring proliferation, supporting the existence of two functionally distinct areas in the bone marrow⁵⁸. This is consistent with the increasing number but decreasing function of aged HSCs.⁵⁹

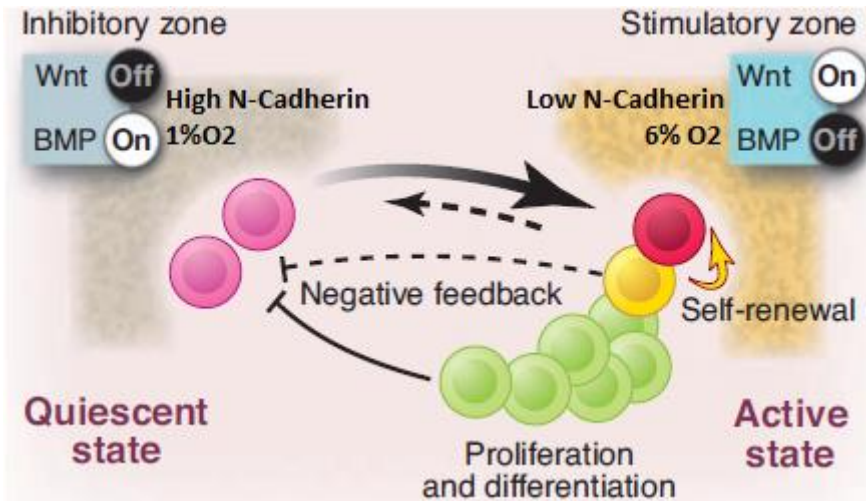


Figure 5 – Simplified scheme of HSC distribution in the bone marrow. Adapted from: Li et al. Coexistence of Quiescent and Active Adult Stem Cells in Mammals. *Science* 327, 542–545 (2010).

The endosteal niche comprises the most primitive HSCs, with superior long-term reconstitution potential (LT-HSC). However, LT-HSCs cycle only once every 145 days on average, thus not being enough to solely generate billions of blood cells.⁶⁰ Live-tracking of HSCs showed the existence of hematopoietic cell subsets localized to distinct locations according to the stage of differentiation, with long-term reconstituting quiescent HSCs associated to endosteal areas, and more mitotically active HSCs located closer to the vascular regions of the bone marrow.²⁶ In fact, studies suggest that N-cadherin expression is not necessary for bone marrow niche function and HSC maintenance¹⁸, but rather for distinguishing between reserved/quiescent (higher N-Cadherin levels) cells from active/primed (lower N-Cadherin levels).⁶¹ Coexistence of quiescent and active stem cells in the bone marrow may explain these observations, with active HSCs supporting the daily production of blood cells, whereas reserved/quiescent HSCs function as a backup, to replenish active stem cells depletion upon hematopoiesis (**Figure 5**).^{60–62}

II.3. Human Hematopoietic Lineages

The hematopoietic system supplies our body with >100 billion mature blood cells every day that carry out functions such as oxygen transport, immunity, and tissue remodelling. HSCs, located at the top of the hematopoietic hierarchy, are responsible for replenishing our pool of blood cells throughout life.⁴⁵ Only 1 in 106 cells in human BM is a transplantable HSC.⁶³ Thus, one must purify HSCs from the bulk of committed cells. Mouse HSCs were first isolated as a lineage-negative (Lin⁻), c-Kit⁺, Sca-1⁺ (LSK) population^{64,65}. However, mouse studies do not allow

straightforward comparison with human HSCs. In fact, human HSCs express FLT3 receptor,⁶⁶ while mouse cells do not, and mouse HSCs express CD150 while human cells do not.⁶⁷

CD34 marks human HSCs as well as more differentiated progenitors (*i.e.* all multipotent stem cells with gradually decreasing levels of self-renewal). Firstly, CD90 (Thy1) was identified as a stem cell marker.⁶⁸ Thus, CD34⁺CD90⁺ define a small cell population with multi-lineage capacity.⁶⁹ Further studies introduced CD45RA and CD38 as markers of more differentiated progenitors, negatively enriched for HSCs⁷⁰⁻⁷². Thus, human HSCs have been defined as CD34⁺CD38⁻CD90⁺CD45RA⁻ Lin⁻ (**Figure 6**).⁷³ Lin⁻ refers to the negative selection by a cocktail containing cell surface markers (e.g. CD2, CD3, CD11b, CD14, CD15, CD16, CD19, CD56, CD123, among others) for all terminally differentiated populations (B cell; T cell; NK; dendritic cell, monocyte, granulocyte, megakaryocyte, and erythrocyte). However, not all stem cells are covered by these combinations that, nonetheless, have become popular. In fact, even in humans, there are HSCs that are CD34⁻/CD38⁻. The use of the CD133 marker was one step ahead in HSC study as both CD34⁺ and CD34⁻ HSCs were CD133⁺.⁷⁴

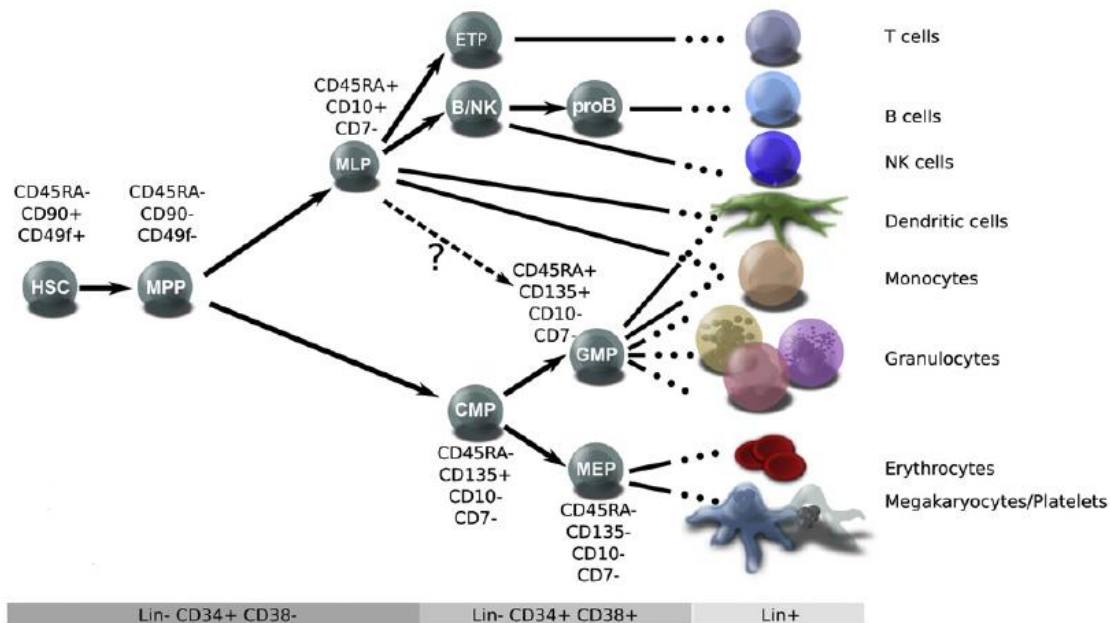


Figure 6 – Classical human hematopoiesis lineages model. HSC: Hematopoietic Stem Cell; MPP: Multipotent Progenitor; MLP: Multi-Lymphoid Progenitor; CMP: Common Myeloid Progenitor; GMP: Granulocyte-Monocyte Progenitor; MEP: Megakaryocyte-Erythroid Progenitor; **Adapted From:** Doulatov et al. Hematopoiesis: A Human Perspective. Cell Stem Cell 10, 120–136 (2012).

II.4. In vitro assays

A major challenge in hematopoiesis is to conceive assays that give information to experimental studies and clinical hematology. Thus, specific assays were developed with the objective of studying two basic parameters: cell proliferation (measured by the number of cells produced) and differentiation potential (estimated by the number of different lineages represented in its progeny).⁷⁵

Colony forming unit in culture (CFU-C) assays are short-term, semi-solid colony assays, which identify and quantify lineage-restricted progenitors in well-standardized conditions. The assay immobilizes the progenitor cells (*i.e.* erythroid, granulocytic, macrophage and megakaryocytic), which supports the three-dimensional growth of the hematopoietic colonies while preventing migration of the cells so that they remain within a colony. Each type of colony has specific characteristics (*i.e.* composition, size, color, and disposition) that allow identification of the differentiation potential of the culture.

CFU-GEMM (Colony-forming unit-granulocyte, erythroid, macrophage, megakaryocyte), also described as CFU-Mix, is characterized by colony containing both erythroid (hemoglobinized) cells and 20 or more non-erythroid (not hemoglobinized) cells (**Figure 7**). Typically, this has erythroid cells in the centre and non-erythroid cells on the periphery. This is relatively infrequent in most cell samples, but tends to be higher in umbilical cord blood and (mobilized) peripheral blood samples than in bone marrow.

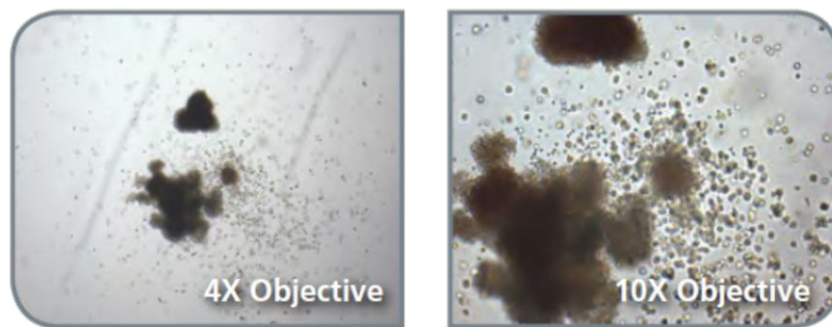


Figure 7 - CFU-GEMM colonies.

CFU-GM (Colony-forming unit-granulocyte, macrophage) is characterized by a colony containing more than 20 granulocytes and/or macrophages. It does not appear red or brown (*i.e.* cells are not hemoglobinized). Individual cells can usually be distinguished, in particular at the edge of the colony (**Figure 8**). Large colonies may have one or more dense dark cores. They are generally larger in umbilical cord blood samples than in bone marrow or (mobilized) peripheral blood.

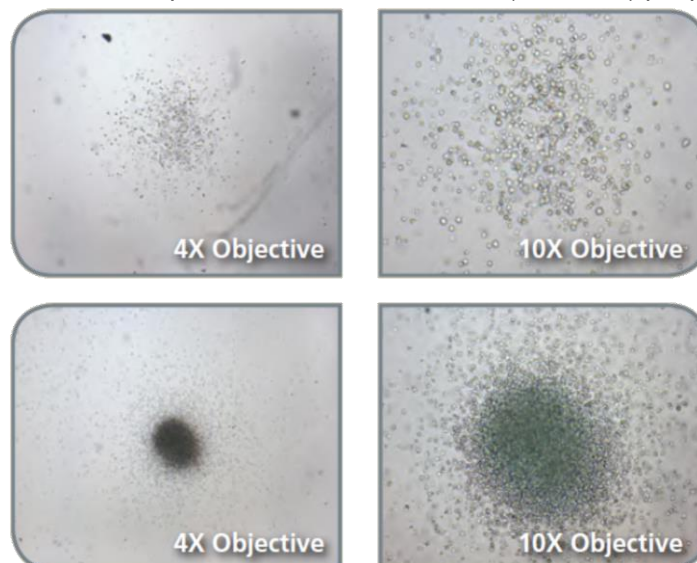


Figure 8 - CFU-GM Colonies. Normal (top) and Large (Bottom) colonies

BFU-E (Burst-forming unit-erythroid) is a colony containing more than 200 erythroblasts in single or multiple clusters. It appears red or brown as the cells are hemoglobinized, but is difficult to distinguish individual cells within each cluster (**Figure 9**). These are generally larger and have more clusters in umbilical cord blood than in bone marrow or (mobilized) peripheral blood

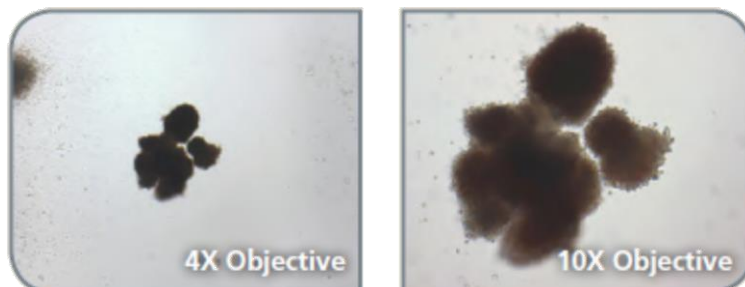


Figure 9 - BFU-E colonies

The Cobblestone-Area Forming Cells (CAFC) is an assay in which a stromal feeder cell layer is first allowed to grow to confluency, and then a cell suspension of HSC is seeded on top. Due to reproducibility issues, defined stromal cell lines are used for this purpose, such as immortalized murine stromal cell lines (*i.e.* MS-5). Primitive cells present in the inoculated cell sample will migrate through the stromal layer and form groups of tightly packed cells. At specific time points after initiation of the assay, individual wells are microscopically screened for the presence or absence of “cobblestone areas,” which are defined as colonies of five or more small cells that grow underneath the stromal layer (**Figure 10**).

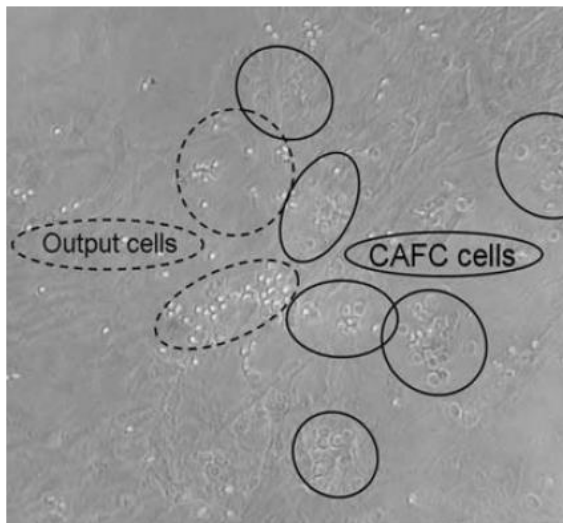


Figure 10 – CAFC colony assay. Cobblestone areas are shown (straight-lined circles) as well as two areas with output (phase bright) cells shown in dashed circles. **Adapted from:** van Os et al. In vitro assays for cobblestone area-forming cells, LTC-IC, and CFU-C. *Methods Mol. Biol.* Clifton NJ 430, 143–157 (2008).

The one-step CAFC provides a straightforward visual screening, but the assay must be performed at limiting dilutions to avoid overlap of cobblestone areas; besides, it gives no information on the heterogeneity or long-term multipotency of individual CAFC. Although standardized short-term and long-term colony assays easily quantify lineage-committed myeloid precursors, identification of true primitive stem cells which have the long-term ability to repopulate all blood lineages still depends on *in vivo* transplantation assays into an irradiated recipient^{75,76}.

II.5. HSC Transplantation.

The entire hematopoietic system can be repopulated following infusion of HSCs, meaning their transplantation can be used to treat/cure a range of hematological diseases. The use of Bone marrow HSCs for human transplantation dates back to the 1950s⁷⁷ but other sources have many characteristics which make them well suited for clinical use as well. Nowadays, more than 30.000 patients with hematological malignancies every year receive high-dose chemotherapy followed by HSC transplantation from Bone marrow, G-CSF mobilized Peripheral Blood (mPB), and Umbilical Cord Blood (UCB).^{73,78}

HSC transplantation faces two major immunological challenges: i) The recipient's immune system may reject the transplant, which leads to graft failure; ii) The occurrence of graft-versus-host disease (GvHD), in which T-lymphocytes within the graft attack the recipient's skin, liver, and gastrointestinal tract, causing damage that, if left unchecked, can be fatal.^{79,80} Although large improvements were made over the years in the understanding of the human major histocompatibility complex (HLA), which reduced the risks of both graft rejection and GvHD, GvHD still poses a serious problem for a well-matched donor and recipient, unless specific immunosuppressive agents to block T lymphocyte proliferation are administered.^{81,82} Curiously, preclinical and clinical data revealed that allogeneic HSC transplantation had also graft-versus-tumour (GvT) effect, in which donor lymphocytes present in the graft recognize and kill the host's tumour cells.^{83,84} Consistently, patients who developed GvHD were less likely to suffer cancer relapse⁸⁵⁻⁸⁷, highlighting a link between GvHD and GvT. Thus, strategies to reduce GvHD incidence (*i.e.* T-lymphocyte depletion and HSC immune selection) end up reducing the GvT effect of infused marrow cells, and may increase the patient's risk of relapse of malignant diseases.⁸⁸⁻⁹¹ Given the serious risks/side effects associated with conventional HSC transplantation, and its limitations, this therapy is restricted to mostly young patients who are in good medical condition, as opposed to patients ranging from 65 to 70 years, to whom most hematological disorders are diagnosed.

II.5.1 Mobilized Peripheral Blood.

Initially, the only HSC source available was bone marrow, which was harvested from the pelvis or sternum under general anesthesia. Eventually, increasing evidence grew that the absolute number of HSCs present within the transplant were proportional to the robustness of hematopoietic engraftment, and increasing doses of HSC significantly lowered mortality from infectious complications post-transplant.⁹² This realization led to the search for means of increasing the number of HSCs that could be harvested for transplantation. Eventually, human hematopoietic cytokine G-CSF was shown to mobilize primitive HSC with long-term repopulating ability into the peripheral blood with relatively high efficiency.⁹³ Ultimately, this demonstrated that mPB was a viable source for HSC transplantation. In comparison with bone marrow harvesting, mPB provides a non-invasive, HSC-enriched source, leading to the gradual replacement of bone marrow with mPB in the clinical setting over the past years, accounting for ~75% of HSC

transplants from unrelated adult donors⁹² and ~99% of autologous HSC transplants⁹⁴. Several multi-centre randomized trials have collectively shown that although engraftment/reconstitution is often faster and more robust with mPB than with bone marrow, it is also associated with a significantly higher rate of chronic and acute GvHD, but with no significant improvement in survival.^{135,140–143} Nevertheless, specific characteristics of the patients may dictate which source of the HSC graft is best.⁹² Patients with higher risk of graft failure/rejection may benefit from the use of mPB, given its ability to mediate more robust engraftment^{95–98}, whereas more immunosuppressed patients with lower graft rejection probability may prefer bone marrow transplantation, due to its lower GvHD incidence.

II.5.2 Umbilical Cord Blood.

Umbilical Cord Blood was first used in clinical practice, in 1988 in a 5-year old patient with severe aplastic anemia.^{99,100} The first signs of engraftment appeared after 22 days with no GVHD signs, and more than 20 years after the UCB transplant, the patient remains healthy with complete long-term haematological and immunological donor reconstitution.^{99,101} These encouraging results suggested that: i) a single cord contained enough HSC to reconstitute haematopoiesis; ii) UCB could safely be collected at birth; and iii) UCB HSC could be cryopreserved and thawed without negatively affecting repopulating ability.

Since then, an increase in allogeneic UCB transplantation has been observed. In fact, UCB transplantations surpassed the number of bone marrow transplants in 2009.¹⁰² Much of this success is due to the creation of worldwide network of cord blood banks, allowing the collection, cryopreservation, and distribution of over 600,000 UCB.¹⁰³ Many advantageous characteristics turn UCB an ideal HSC source for transplantation⁷⁸: i) Increased availability of banked samples – UCB is donated, quality-tested and banked in advance, turning it ideal in acute settings and abolishing the long delay inherent to the use of bone marrow; ii) Immaturity of the immune cells present in UCB is far less likely to cause GvHD than bone marrow or mPB; iii) Contrary to bone marrow and mPB, perfect HLA-matching is not necessary between donor and recipient for a UCB transplant to be successful; iv) UCB is less likely to transmit viruses when compared to bone marrow or mPB;

The maximum degree of HLA disparity that will still allow engraftment has yet to be determined, but in contrast with HLA-mismatched bone marrow transplantation, even unrelated 1 or 2 antigen mismatched UCB transplants result in an acceptable grade of acute GvHD.¹⁰⁴ Ultimately, the continuous birth of children and non-invasive harvesting allows easier worldwide banking, which combined with less strict HLA-matching increases the patient's chance of finding a suitable donor. This is especially critical in the case of ethnic minority groups, which are less likely to find a suitable BM donor.

However, UCB transplantation also poses some drawbacks, such as higher rates of engraftment failure due to low volume collection, and delayed engraftment of neutrophils and platelets (time to neutrophil recovery is a major indicator of post-transplant mortality¹⁰⁵), which lengthen hospital

stays and increases the risk of serious complications.¹⁰² A single UCB unit has sufficient cells ($2-5 \times 10^6$ CD34+) to repopulate new-borns or small children, but not larger weight adolescents and adults (optimal dose $>2 \times 10^5$ CD34+/kg), limiting the use of UCB to paediatric cases.^{102,106} Multiple UCB unit transplantation into the same recipient provides a straightforward increase in cell dose, making the use of two UCB grafts a standard practice for adult patients, leading to less engraftment failure rates when compared to single UCB transplant recipients.¹⁰⁷ However, it does not increase the speed of engraftment compared with the recipients of single UCB unit transplantation, or that observed for other graft sources.^{108,109}

Although this approach allows for a more effective engraftment, some studies have suggested that multiple cord blood unit transplantation is associated with increased GvHD, while simultaneously having an increased cost compared to the use of a single UCB unit.¹⁰² Interestingly, when multiple UCB units are transplanted, both contribute to initial recovery, but only HSCs from a single UCB unit are able to dominate hematopoiesis and ultimately produce long-term durable hematopoietic engraftment, with the cells from the other UCB unit being lost long-term.^{109,110}

II.6. Ex-vivo expansion of HSCs.

One can enhance the engrafting capability of a UCB unit by *ex-vivo* expansion, accomplishing not only increased cell numbers with haematopoietic reconstitution potential, but also providing a selective expansion of short-term engrafting HSCs.

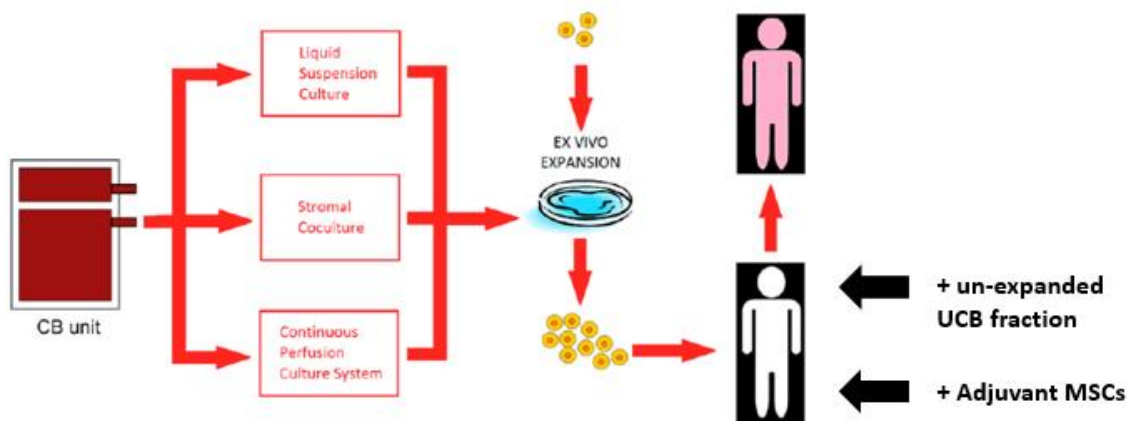


Figure 11 - Schematic of ex vivo expansion techniques for cord blood transplantation. Adapted From: Munoz, J. et al. Concise Review: Umbilical Cord Blood Transplantation: Past, Present, and Future. *Stem Cells Transl. Med.* 3, 1435–1443 (2014).

If one takes into account that neutrophil recovery depends on early-engrafting cells, and not LT-HSCs, the ability to expand these progenitors becomes critical.⁷³ Expansion of UCB units can augment the numbers of colony-forming unit–granulocyte-macrophages (CFU-GMs), which are higher in UCB compared with mPB or BM.^{100,111} Moreover, the proliferative ability of UCB CD34⁺CD38⁻ is higher than their BM counterparts.^{112,113} However, even though *ex vivo* expansion leads to earlier initial hematopoietic recovery, it ends up with later graft failure, due to the loss of

long-term repopulating activity.¹¹⁴ *Ex-vivo* expanded grafts provide a clinical advantage nonetheless, especially in combination with 'un-manipulated' fractions of the same cell source unit, where the former would provide faster initial hematopoietic reconstitution, and the latter long-term sustainable hematopoiesis.¹¹⁵

Many procedures have been attempted to expand the HSCs pool, by a rational combination of many factors such as initial stem/progenitor cell enrichments and oxygen tension,¹¹⁶ culture duration¹¹⁷, cytokine cocktails¹¹⁸, blocking in vitro differentiation of early progenitor cells¹¹⁹ and co-culture with stromal feeder layers.^{1,120,121} **Table 1** presents a selection of the some results, reported in the literature until 2013, on the *ex vivo* expansion of both mononuclear cells (MNCs) and CD34⁺-enriched UCB cultures, under liquid suspension or co-culture conditions, as well as presence/absence of serum in media compositions.¹¹⁵

Table 1 - Summary of the main results focusing on UCB expansion under static conditions, either on liquid suspension cultures or in the presence of mesenchymal stem/stromal cells feeder layers. **From:** Andrade, P. Z., Santos *et al.* Stem cell bioengineering strategies to widen the therapeutic applications of hematopoietic stem/progenitor cells from umbilical cord blood: *J. Tissue Eng. Regen. Med.* 9, 988–1003 (2015).

Expansion system	Cytokines/other molecules	Serum	Days in culture	Fold expansion TNC	Fold expansion CD34 ⁺	Reference
<i>Liquid suspension</i>						
	SCF, TPO, G-CSF	No	10	56	4	(Shpall <i>et al.</i> , 2002)
	SCF, Flt-3L; IL-6; TPO; TEPA	10% FCS	21	219	6	(de Lima <i>et al.</i> , 2008)
	Notch ligand δ -1; SCF; Flt-3L, IL-6; TPO; IL-3	No	16	660	160	(Delaney <i>et al.</i> , 2010)
	IL-6, TPO, SCF, SR-1, Flt-3L	No	7	51	24	(Boitano <i>et al.</i> , 2010)
	SCF, Flt-3L, TPO, Angpt5	No	10	220	n.a.	(Zhang <i>et al.</i> , 2008)
	SCF, Flt-3L, TPO, IL-3	No	10	300	12	(Zhang <i>et al.</i> , 2006)
	SCF, TPO, Flt-3L, IL-3, G-CSF, GM-CSF and IL-6	No	7	n.a.	66	(Yao <i>et al.</i> , 2006)
	SCF, Flt-3L, MGDF, IL-3	30% FBS	9	n.a.	2.5	(Araki <i>et al.</i> , 2006)
	SCF, Flt-3L, MGDF, IL-3, 5-AzaD, TSA	30% FBS	9	n.a.	5	(Araki <i>et al.</i> , 2006)
	IL-6, TPO, SCF, Flt-3L	10% FBS	21	n.a.	9.5	(Gunetti <i>et al.</i> , 2008)
	SCF, TPO, Garcinol	No	7	n.a.	7.4 (CD34 ⁺ CD38 ⁻ cells)	(Nishino <i>et al.</i> , 2011)
	SCF, TPO, Flt-3L	No	14	34	8.9	(Du <i>et al.</i> , 2012)
	SCF, Flt-3L, TPO, G-CSF	No	14	400	80	(Duchez <i>et al.</i> , 2012)
	SCF, Flt-3L, TPO, IL-6 (10% O ₂)	No	8	n.a.	20	(Tursky <i>et al.</i> , 2012)
<i>Stromal co-culture</i>						
BM MSC	SCF, TPO, Flt-3L	No	7	25	15	(Andrade <i>et al.</i> , 2010)
BM MSC	SCF, TPO, G-CSF	20% FBS	14	12	12	(Robinson <i>et al.</i> , 2006)
BM MSC	SCF, Flt-3L, bFGF, UIF	No	26	241	35	(da Silva <i>et al.</i> , 2005)
BM MSC	SCF, Flt-3L, bFGF, UIF	No	18	280	35	(da Silva <i>et al.</i> , 2010)
BM MSC	SCF, IL-3, G-CSF	No	12	21	21.4	(Madkaikar <i>et al.</i> , 2007)
BM MSC	SCF, Flt-3L, TPO, IL-3	No	10	500	50	(Zhang <i>et al.</i> , 2006)
PMSC	SCF, TPO, Flt-3L, TPO	No	14	99	13	(Luan <i>et al.</i> ,)
BM MSC	SCF, TPO, bFGF	No	7	n.a.	35	(Walenda <i>et al.</i> , 2011)

SCF, stem cell factor; TPO, thrombopoietin; G-CSF, granulocyte colony-stimulating factor; Flt-3L, Fms-like tyrosine kinase-3 ligand; TEPA, tetraethylenepentamine; IL, interleukin; Angpt5, angiopoietin-5; MGDF, megakaryocyte growth and development factor; 5-azaD, 5-aza-2'-deoxycytidine; TSA, trichostatin A; bFGF, basic fibroblast growth factor; SR-1, stem reginin 1; FBS, fetal bovine serum; FCS, fetal calf serum; TNC, total nucleated cells; PMSC, placental-derived MSCs.

Most traditional cytokine/supplement combinations rely on early-acting cytokines SCF and Flt-3L, and some also on TPO and members of the interleukin (IL) family. A summary of the most-used cytokines/molecules in *ex vivo* expansion culture systems targeting HSCs amplification and their proposed functions is presented in **Table 2**.

Table 2 - Summary of cytokines and other molecules used in human hematopoietic stem/progenitor cell culture ex-vivo with their reported functions. **From:** Andrade, P. Z., Santos *et al.* Stem cell bioengineering strategies to widen the therapeutic applications of hematopoietic stem/progenitor cells from umbilical cord blood: J. Tissue Eng. Regen. Med. 9, 988–1003 (2015).

Cytokine/molecule	Reported function
Stem cell factor (SCF)	Growth factor for HSC progenitor cell expansion; synergizes with Flt-3L
Fms-like tyrosine kinase-3 ligand (Flt-3L)	Potentiates the effects of other cytokines (including SCF); promotes survival of HSCs
Thrombopoietin (TPO)	Stimulator of megakaryocytopoiesis; survival and proliferation of HSCs
Granulocyte CSF (G-CSF)	Mobilization of HSCs to peripheral blood; HSCs expansion
Interleukin 3 (IL-3)	Together with IL-6, promotes proliferation of HSCs
Interleukin 6 (IL-6)	Together with IL-3, promotes proliferation of HSCs
Interleukin 10 (IL-10)	Helps proliferation of HSCs
Interleukin 11 (IL-11)	Shortens the G ₀ period of the cell cycle of HSCs
Jagged-1	Regulates HSC self-renewal through Notch system
Platelet-derived growth factor (PDGF)	Mitogen for connective tissue cells
δ -1	Enhance self-renewal through Notch system
Stem regenin-1 (SR1)	Antagonist of aryl hydrocarbon receptor; prevents differentiation of HSCs
Angiopoietin-5 (Angpt-5)	Unknown; cytokine produced by mouse fetal liver cells, which support the <i>ex vivo</i> expansion of mouse HSCs

When comparing liquid-suspension cultures with stromal co-culture, it is to notice that CD34⁺ expansion is higher in the latter (**Table 1**). Furthermore, although cytokine leads to an increase in Total nucleated cells (TNCs) after UCB expansion, the rapidity of engraftment did not improve in clinical trials relying solely on cytokines.¹²² Rather than long-term HSC, this is probably due to the expansion of early acting multipotent progenitors (MPPs) and cytokine-induced differentiation of more committed progenitors (CD34⁺ CD38⁻ or CD34⁺ Lin⁻) into cells of committed lineage (CD34⁺ Lin⁺) that have poor BM homing capabilities.^{114,123} Furthermore, intercellular signalling between cells from distinct lineages and stages of differentiation,^{124–126} or within the same lineage¹²⁷, is able to disturb stem/progenitor cell expansion. This inhibition can be done through competition for cytokines and nutrients, or by secreting factors that alter the HSC cell cycle rate and promote differentiation and/or apoptosis.^{128–130} In fact, several mature progenitors express factors such as transforming growth factor- β (TGF β), tumour necrosis factor- α (TNF α), interleukin-3 (IL-3), macrophage inflammatory protein-1 α (MIP-1 α) and monocyte chemoattractant protein-1 (MCP-1)¹²⁵, all of which inhibit HSC expansion. Therefore, methods must be devised to selectively expand cells that possess better bone marrow homing capabilities, and to block the differentiation of HPCs into more committed progeny (i.e. TEPA^{131,132,133}; Notch Signalling^{134,135}; NAM^{136,137,138}; SR1¹³⁹).

II.5.1 Stromal feeder layers

In adults, HSCs and their primitive progeny are located within the bone marrow, contiguously to the endosteal surface of trabecular bone, and interactions of vascular/stromal cells with HSCs are known to be of great importance for their maintenance, thus making BM MSCs cells ideal to mimic their natural niche when culturing HSCs *in vitro*. Consistently, it was reported that adherent stromal feeder layers are able to promote *ex vivo* expansion/maintenance of human HSCs cultured on top. This system also preserves the ability of expanded UCB cells to engraft in an *in vivo* model. However, it is still not know if these positive effects are solely due to soluble factors^{140,141}, or if direct cell-cell contact is required¹⁴². Nonetheless, direct contact of haematopoietic cells with stromal cells has been associated with an improvement in stem/progenitor cell expansion.^{1,142} Increased numbers of more lineage-committed cells¹⁴³, and

CD7⁺ early lymphoid progenitors were also reported in these type of cultures.^{1,144} Distinct co-culture systems have been tested for the expansion of HSCs. Although most of them use bone marrow mesenchymal stem/stromal cells (MSC)-derived as feeder layers, some systems use different stromal sources, different isolation protocols of stromal cells, and diverse cytokine combinations (**Table 1**). Consequently, divergent results have been reported and thus the role of stroma in hematopoietic cell co-cultures remains a very controversial issue.¹

There are several well-defined sources for MSCs in the body besides the bone marrow (BM) such as adipose tissue¹⁴⁵, lung¹⁴⁶, liver¹⁴⁷, umbilical cord matrix (*i.e.* Wharton's jelly; UCM)¹⁴⁸, synovium tissue¹⁴⁹, amniotic fluid¹⁵⁰, fetal blood¹⁵¹, dental pulp¹⁵², and skeletal muscle¹⁵³. The most primitive MSC population can be obtained from fetal tissues such as the umbilical cord matrix, the Wharton's jelly¹⁵⁴ and UCB¹⁴⁸.

Of these, the richest source of MSCs in adults is the adipose tissue (AT), which is easily accessible and a well-characterized methodology is available for the isolation of cells from this source. As it is estimated, about 500 times more AT-MSCs can be isolated from fat tissue than from the same amount of BM.¹⁵⁵ The UCM is also a fruitful MSC source, as Wharton's jelly contains mainly primitive MSC, which increases their potential in therapeutic applications¹⁵⁴, furthermore, it is collected alongside UCB, allowing for quick harvesting of both components of the co-culture expansion system, from the same donor (UCB-HSCs and UCM-MSCs). These studies raise the question if BM-MSCs are equivalent to AT-MSCs and UCM-MSCs, or if they are divergent from them. In terms of availability, UCM-MSCs would have all the advantages referred for UCB, while AT MSCs would benefit from the abundance of adipose tissue collection around the world (*e.g.* Liposuction surgeries), which in combination with the high yield of isolation protocols provides a fast, cost-effective source of MSCs. Efforts are being made in the direction of using human origin, clinical-grade MSCs as feeder layers, prepared under good manufacturing practice (GMP)-compliant conditions, to overcome possible contamination risks from compounds of animal origin (*e.g.* Fetal bovine serum). Additionally, other MSCs sources are also being explored to serve as feeder layers in co-culture systems.

III. Materials and Methods.

III.1. Human Samples.

Bone marrow aspirates, Umbilical Cord, and Adipose tissue samples were obtained from IPO Lisboa, Hospital São Francisco Xavier, and Clínica de Todos-Os-Santos, respectively. All the samples were obtained after informed consent of the donors, and their harvesting and collection performed in accordance with the protocols of the respective institutions.

III.1.1. Processing Umbilical Cord Blood.

Low-density mononuclear cells (MNCs) were isolated from Umbilical cord blood (UCB) samples by Ficoll density gradient centrifugation, followed by a red blood cell lysis with NH₄Cl (10 minutes at room temperature). The lysis was stopped by adding fetal bovine serum (FBS, Hyclone). MNCs were quickly stored at -80°C in cell culture freezing medium (Recovery™; GIBCO® Life Technologies™, 50 x 10⁶ cells/vial). The samples were banked in liquid nitrogen at -180°C the day after.

III.1.2. Purification of CD34⁺-enriched cells.

To obtain a suspension of purified Hematopoietic Stem and Progenitor Cells (HSCs), UCB MNCs were picked from the cryopreserved samples and thawed in Dulbecco's Modified Eagle's Medium (DMEM, GIBCO® Life Technologies™) with 20% FBS supplemented with DNase I (10µg/mL) to avoid clump formation. A maximum of 250 x 10⁶ cells (5 vials) were thawed per 50 mL of thawing medium. UCB MNCs were then enriched for CD34⁺ cells through magnetic activated cell sorting (MACS®, Miltenyi Biotec and EasySep®, StemCell Technologies™), following manufacturer's instructions.

III.2. Cell Counting.

To perform routine cell counting, cell samples were centrifuged at 349 g for 7 minutes, the supernatant discarded, the sample resuspended (V_{res}) and counted in a Neubauer chamber with trypan blue solution. The total number of cells in the resuspended sample was determined by dividing the count by the number of squares counted, times the dilution factor in trypan blue solution (DF), times V_{res} , times 10 000 (**Equation 1**).

Equation 1

$$Total\ Cells\ in\ suspension = \frac{\#count}{\#squares\ counted} \times DF \times V_{res} \times 10000$$

III.3. MSC cell culture.

III.3.1. Thawing.

Frozen MSC samples were thawed in DMEM 20% FBS or StemGro® hMSC Medium (Corning®) in case xeno-free conditions were required, counted and plated as mentioned in the following sections.

III.3.1. *Ex-vivo* expansion in static conditions.

Adherent cultures of MSCs were plated with a cell density between 3×10^3 cells/cm² and 6×10^3 cells/cm², in polystyrene T-Flasks or flat bottom multiwell-plates (Corning®).

Culture Media: To grow MSCs, serum-containing (SC) or xeno-free (XF) media can be used. The SC medium consists in low-glucose DMEM supplemented with 10% (v/v) Fetal Bovine Serum, MSC qualified (FBS, Life Technologies™). MSCs expanded in DMEM 10%FBS will be hereinafter referred to as SC MSCs. The XF medium used was either StemPro® MSC SFM (Life Technologies), supplemented with GlutaMax™ (Life Technologies™), or DMEM supplemented with 5% xeno-free Human Platelet Lysate (HPL) (BSSub™-XF, AventaCell BioMedical Co., Ltd.). MSCs expanded in StemPro® and BSSub™-XF will be hereinafter referred to as XF MSCs and HPL-XF MSCs, respectively. 1% (v/v) of antibiotic was added to all culture media to avoid contaminations. In the specific case of XF MSCs expansion, a pre-coating with CELLstart™ (Invitrogen®, Carlsbad, CA) is needed before plating the cells (1 hour at 37°C, 5% CO₂). CELLstart™ is a fully-defined, xenogeneic-free humanized substrate for stem cell culture, produced under cGMP¹⁵⁶, and compensates for the lack of adhesion molecules in StemPro®, which are necessary for the MSCs to be cultured in an adherent fashion.

Passaging: If a given MSC population is to be maintained in culture for long periods, adherent MSCs must be harvested upon reaching 70%-80% confluence from the recipient with proteolytic enzymes, and re-plated into a new recipient. The media in which cells are cultured are determinant in the choice of which enzyme solutions to use. Accutase® (Sigma) was used in the case of SC MSCs, while TrypLE™ Select CTS™ (1X) was used for XF and HPL-XF MSCs. Washing media was added in a 1:3 proportion to dilute the enzymatic agent, DMEM+10% FBS (HyClone™) for SC MSCs and StemGro® hMSC Medium (Corning®) for XF MSCs.

III.4. HSC/MSC Expansion Systems.

A HSC/MSC co-culture system was used to expand fresh CD34⁺ cells.

III.4.1. Establishment of MSC-derived feeder layers.

To establish a MSC-derived stromal feeder layer capable of supporting HSC expansion, 95-100% and 60-70% confluent BM MSCs and AT/UCM MSC, respectively, had their growth inactivated by replacing the culture media with DMEM-10%FBS, supplemented with mitomycin C (0.5 µg/mL), for 2.5 hours, at 37°C, 5% CO₂.

III.4.2. HSC expansion media.

Two expansion media were used. i) Quality Biological Serum-Free medium (QBSF-60; Quality Biological, Inc.), supplemented with a specific cytokine cocktail, hereinafter referred as Z9: SCF (60 ng/ml), Flt-3L (55 ng/ml), TPO (50ng/ml) and bFGF (5 ng/ml); ii) StemSpan™ SFEM II (Stem Cell Technologies™) + Z9.

III.4.3. Expansion of CD34⁺-enriched cells in Static conditions.

Suspensions of CD34⁺-enriched cells were cultured (30-50 x 10³ cells/mL) on top of a previously inactivated human MSC-derived feeder layer, for 7 days without media change, at 37°C, 5%CO₂. CD34⁺-enriched cells were also cultured in the absence of a stromal feeder layer (noStr) as a control condition.

III.5. *In vitro* assays.

Fresh CD34⁺-cells (day-0) were harvested for CAFCs assay (2 x 10³ cells per condition), for CFU-C assay (1 x 10³ cells per condition), and for Flow Cytometry analysis. At the end of the co-culture (day-7), the number of total nucleated cells (TNC) after expansion was determined, harvested for CAFCs assay (2 x 10³ cells per condition), for CFU-C assay (5 x 10³ cells per condition), and for Flow Cytometry analysis.

III.5.1. Proliferative analysis

Total hematopoietic expansion is evaluated by assessing the fold-increase in total cell number. This is calculated by dividing the number of cells at the end of the culture period (day-7) by the number of cells at the beginning of the culture (day-0).

III.5.2. Phenotypic analysis

Both fresh CD34⁺-enriched cells and expanded CD34⁺-enriched cells were analysed by flow cytometry (FACScalibur, Becton Dickinson), using a panel of monoclonal antibodies (FITC-, or PE-conjugated) against: CD90 for HSCs; CD34 and CD133 for stem/progenitor cells; CD41 for megakaryocyte lineage, and CD14 for monocytic lineage; CD15 and CD33 for myeloid lineage; CD7 for early lymphoid cells. A minimum of 3 x 10⁴ cells/tube were incubated with these monoclonal antibodies for 15 min in the dark at room temperature. Cells were washed afterwards with PBS and fixed with 1% paraformaldehyde (Sigma). Appropriate isotype controls were also prepared for every experiment to exclude the possibility of non-specific binding of antibodies to Fc receptors. A minimum of 10 000 events was collected for each sample. Analysis was performed using FlowJo software.

III.5.3. Clonogenic Potential assay

Colony forming unit in culture (CFU-C) assays are short-term, semi-solid colony assays. Three different scores were attributed to the colonies according to their composition, size, and color:

Colony-forming unit–granulocyte macrophage (CFU–GM), colony-forming unit–granulocyte, erythroid, macrophage, megakaryocyte (CFU-Mix) and burst forming unit–erythroid (BFU–E).¹⁵⁷

Both fresh (day-0) and expanded (day-7) UCB CD34⁺-enriched cells are analysed to evaluate their clonogenic potential. Fold-increase in clonogenic potential from day-0 to day-7 is measured for each of the three scores. The clonogenic assays are performed by plating 1×10^3 fresh cells at day-0, and 5×10^3 expanded cells at day-7, in MethoCult GF H4434 (Stem Cell Technologies). The assay is done on 4-well plates with 2cm^2 each. Three of the wells were loaded with the cell sample, the fourth was loaded with purified water to provide a steady source of humidity throughout the assay. The clonogenic cultures were maintained at 37°C and 5% CO₂. After 14 days, the colonies were counted and categorized. Total CFU numbers were calculated by dividing the number of counted colonies for day-0 or day-7, by the number of cells plated for day-0 or day-7, and this value then multiplied by the total number of cells (TNC) in culture for the day of harvest (day-0 or day-7). **(Equation 2)**

Equation 2

$$\text{TotalCFU/CAFCs at day } X = \frac{\text{\#CFU/CAFC count}}{\text{\#Cells plated at day } X} \times \text{\#TNC at day } X$$

***IV. Hematopoietic supportive capacity of different
mesenchymal stem/stromal cell populations***

IV.1 Background

Efforts are being made towards the use of human origin, clinical-grade MSCs to support HSCs – either in the form of feeder layer-assisted expansion^{1,120}, or co-transplantation to improve engraftment¹⁵⁸ – prepared under good manufacturing practice (GMP)-compliant conditions, to overcome possible contamination risks from compounds of animal origin such as Fetal Bovine Serum (FBS), and obviate animal welfare concerns. At SCBL, although a serum-free MSCs/HSCs co-culture expansion system¹ was successfully established, the MSC-derived feeder layers are still established using serum-supplemented medium (DMEM 10%FBS). To prepare MSCs under GMP-compliant conditions is the next step regarding their usage in clinical practice. In this study, two xeno-free alternatives to FBS were tested for their ability to expand BM MSCs, with the objective of establishing a stromal feeder layer capable of supporting hematopoietic expansion of UCB HSCs. Additionally, alternative sources of MSCs – adipose tissue (AT) and umbilical cord matrix (UCM) were tested.

IV.2 Establishment of xenogeneic (xeno)-free bone marrow (BM) MSC-derived feeder layers for HSC expansion

- StemPro® MSC SFM (Life Technologies™)

StemPro® MSC SFM XenoFree (StemPro) has been developed for the expansion of human MSCs under completely serum-free and xeno-free conditions. Using this medium, human MSCs can be expanded for multiple passages while maintaining their multipotent phenotype (i.e. ability to differentiate into osteogenic, chondrogenic and adipogenic lineages). Furthermore, StemPro is cGMP compliant which allows for traceability and manufacturing reliability.¹⁵⁹

In this study, BM MSCs were expanded in static conditions, in StemPro (XF MSCs, **Figure 12a**) or serum-supplemented (SS MSCs, **Figure 12b**) medium.

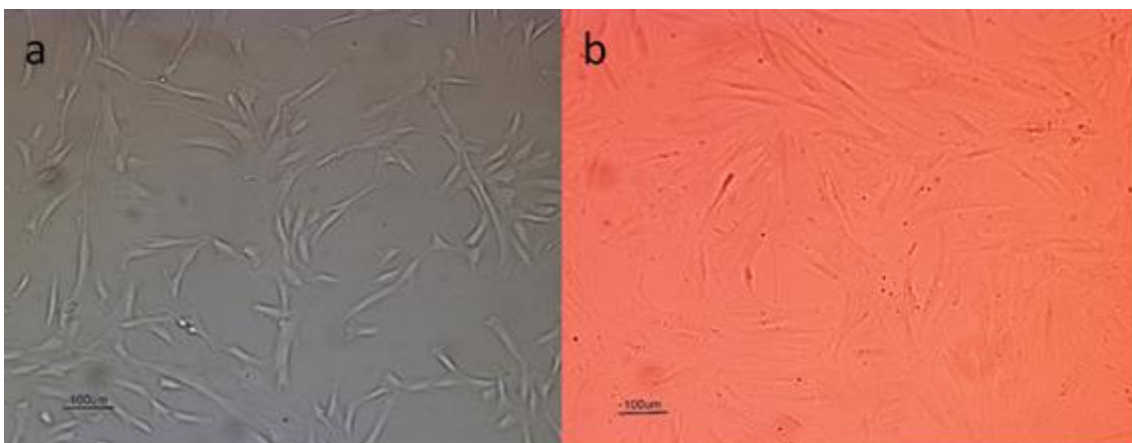


Figure 12 – Plastic adherent BM MSC cell culture, expanded in **a)** StemPro – XF MSCs **b)** DMEM 10% FBS – SS MSCs

Even when isolated from the same donor, the XF and SC MSC populations display visible differences early on. For instance, XF MSCs display a faster growth than SS MSCs, but are significantly smaller than the latter. Considering that changing the expansion media alters MSCs

size and cell division kinetics, differences may also be observed on the hematopoietic supportive capacity of each population. Before initiating MSC/HSC co-cultures, the stromal feeder layer have to be treated with mitomycin-C. Thus, we decided to evaluate how the XF MSC-derived feeder layer responded to mitomycin-C treatment plus 7 days of culture in HSC expansion medium.

With the current system, to derive stromal feeder layers capable of supporting HSC expansion, 95-100% confluent BM MSCs must have its growth inactivated by replacing the culture media with DMEM-10%FBS + 0.5 µg/mL mitomycin-C. After the treatment step with mitomycin, MSCs will not spend resources on growth metabolism, but rather on the metabolism responsible for supporting HSCs expansion in culture.

However, using the same approach with BM MSCs expanded in StemPro did not allow for a viable feeder layer (**Figure 13**).

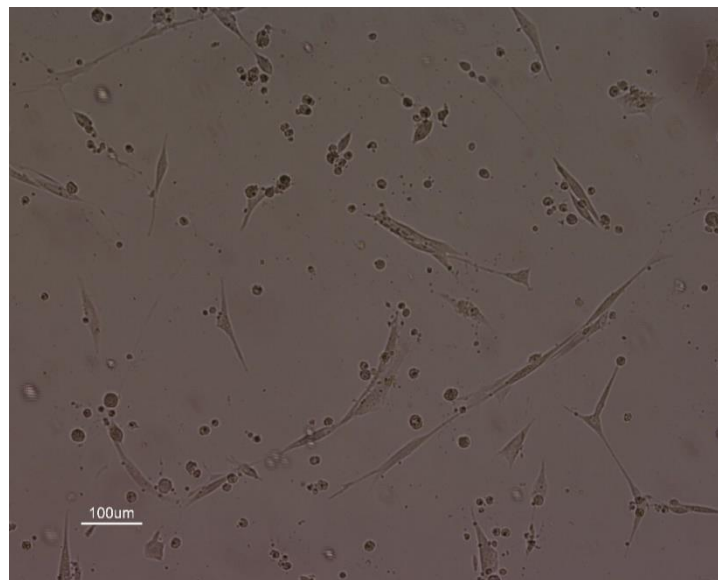


Figure 13 – Representative image of a senescent XF MSC-derived feeder layer

This occurrence impaired the possibility of establishing a MSC/HSC co-culture expansion system and it was hypothesized that XF MSCs may differ from SS MSCs in terms of sensibility to mitomycin-C treatment. Thus, an array of mitomycin-C concentrations was tested to treat XF MSCs. In this way, confluent XF MSCs were treated with either 0.5, 5, or 50 µg.mL⁻¹ of mitomycin-C and cultured in QBSF+Z9 expansion media for seven days. Furthermore, with the goal of maintaining a fully GMP-compliant inactivation protocol, mitomycin-C was also diluted in StemPro medium, as opposed to the standard serum-supplemented medium. SS MSC-derived feeder layers were included in the test as viability controls as no senescence episodes were observed in these cultures.

In Table 3 is represented the number of cells obtained and their viability after the mitomycin-C treatment step and 7 days of culture in QBSF+Z9. XF MSC-derived feeder layers treated with 50 µg/mL mitomycin C diluted either in StemPro or DMEM+10% FBS medium entered senescence after 7 days, with very few cells remaining adherent to the well (**Table 3**).

Table 3 - Number of cells measured at day 0 (D0) and day 7 (D7), and viability at day 7, of XF and SS MSCs inactivated in different media and mitomycin-C concentration.

	Mitomycin C	Media	#Cells D0	#Cells D7	Viability D7
SS MSC	–	No treatment		5.78E+04	93%
SS MSC	0.5 ug.mL ⁻¹	DMEM 10%FBS	1.67E+04	2.00E+04	90%
XF MSC	–	No treatment		–	0%
XF MSC	5 ug.mL ⁻¹	DMEM 10%FBS		3.44E+04	73%
XF MSC	5 ug.mL ⁻¹	StemPro® MSC XFM	6,93E+04	–	0%
XF MSC	0.5 ug.mL ⁻¹	DMEM 10%FBS		6.28E+04	76%
XF MSC	0.5 ug.mL ⁻¹	StemPro® MSC XFM		–	0%

Regarding the controls, both maintained cell viability values around 90%, but the non-treated sample had an increase in cell numbers, whereas the treated sample did only slightly, indicating a successful growth inactivation of the feeder layer. (**Table 4, Figure 14a**). Regarding the XF MSCs-derived feeder layers, only the culture whose mitomycin-C treatment step was performed using 0.5 ug.mL⁻¹ of mitomycin-C diluted in DMEM 10%FBS had its number of cells maintained from day 0 to day 7. (**Figure 14b**). The best result yielded a 76% of feeder layer viability, which is sub-optimal when compared with our current system, which is always above 90%. (**Table 3**)

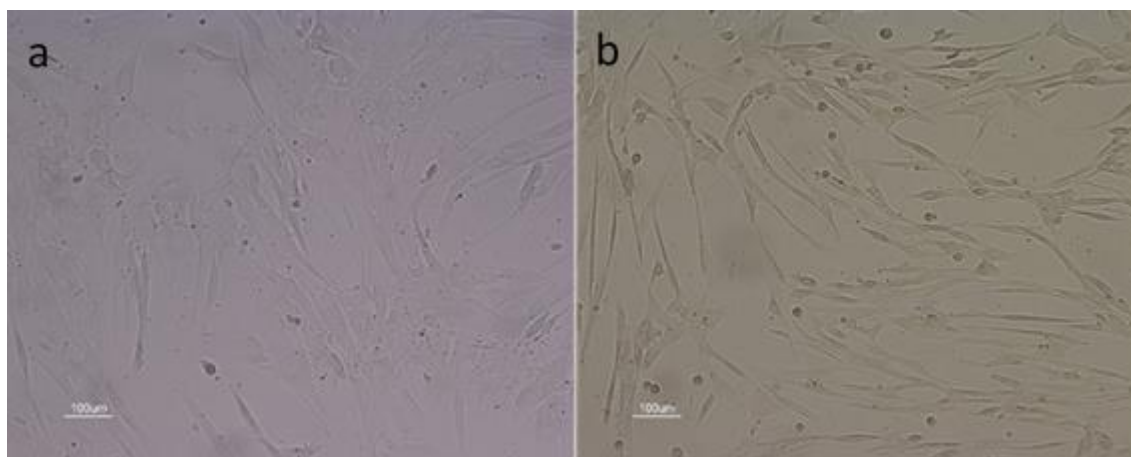


Figure 14 – Comparison of BM MSC feeder layers expanded either in DMEM 10%FBS treated with 0.5 ug.mL⁻¹ of mitomycin-C (**a**) or in StemPro® MSC SFM XenoFree treated with 0.5 ug.mL⁻¹ of mitomycin-C (**b**).

Feeder-layer senescence is a serious hurdle to the establishment of a functional HSC/MSC co-culture system, as it does not allow for the MSCs to support HSCs growth. Most importantly, feeder layer death and detachment ends up contaminating the final cellular product, the expanded HSCs, with cellular debris that need to be removed prior to transplantation. Because of the mentioned limitations, GIBCO® StemPro® MSC SFM (Life Technologies™) does not seem to be a viable alternative to establish MSC-derived feeder layers. This may be due to lack of sufficient adhesion molecules to withstand 7 days in a confluent state. In fact, the need for a pre-coating

with CELLstart™ for the expansion of XF MSCs and the exacerbated senescence when using StemPro® in the inactivation protocol (**Table 3**) support this hypothesis.

- Human Platelet Lysate (HPL) – BSSub™-XF (AventaCell BioMedical Co. Ltd.)

Although the GMP-compliant isolation and expansion of MSCs relies on the commercialization of chemically defined xeno-free culture media, their exact composition is not fully disclosed. The scientific community is looking for alternatives in this regard that allow safe, efficient and cost-effective cell expansion and production in cell therapy and regenerative medicine research.

Human platelet lysate (HPL) arises as a potential candidate to successfully replace FBS in cell culture medium. Through a high throughput proteomic array analysis, FGF/EGF, TGF- β /BMP and VEGF/PDGF were found to be highly represented in HPL.¹⁶⁰ HPL-supplemented medium has been used with a variety of cells of primary origin and established cell lines with non-xenogeneic formulation, due to absence of bovine or other animal-derived proteins.¹⁶¹ In collaboration with AventaCell BioMedical Co., Ltd., the use of BSSub™-XF (hereinafter referred to as HPL-XF)-supplemented medium (DMEM 5%HPL) was exploited for the establishment of MSC XF-derived feeder layers capable of supporting HSC expansion. As in the case StemPro, we wanted to see how MSCs cultivated in DMEM 5%HPL reacted to the treatment step with mitomycin-C. For what was observed in culture, BM MSCs grow faster when cultured with HPL-supplemented medium when compared with FBS-supplemented medium.

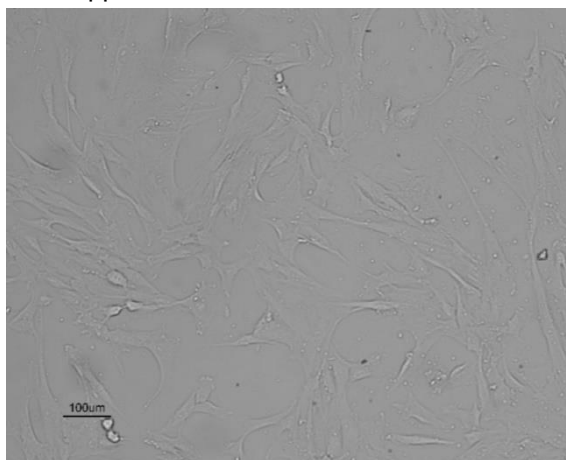


Figure 15 - BM MSCs expanded in DMEM 5%HPL-XF prior to mitomycin-C treatment

To account for the higher proliferative potential, 60-70% confluent BM MSCs (**Figure 15**) were treated with 5 $\mu\text{g}\cdot\text{mL}^{-1}$ of mitomycin-C and maintained in HSC expansion medium supplemented with bFGF (this growth factor is part of the cytokine cocktail to assure the maintenance of the stromal feeder layers in the absence of serum.¹²⁰) for 7 days (**Figure 16**). Their total number of cells and viability were assessed (**Figure 17**). These results were compared with non-treated samples.

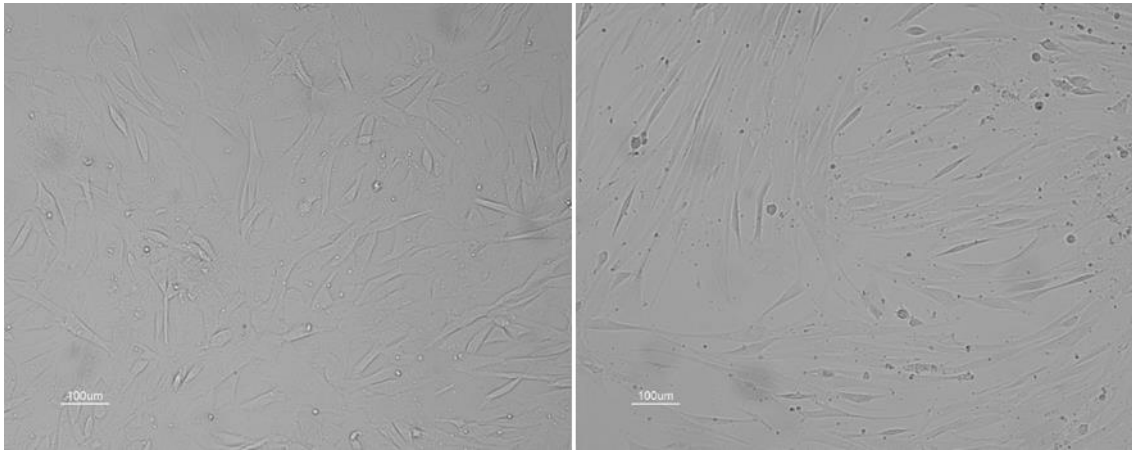


Figure 16 - BM MSC feeder layers expanded in DMEM 5%HPL-XF: a) BM MSC at day-7, without mitomycin-C treatment; **b)** BM MSC at day-7, 0.5 µg mitomycin-c treatment.

Additionally, since the growth-inactivation step can be done up to 48h before starting MSC/HSC co-cultures it was hypothesized that additional 48h in the presence of MSC expansion medium would give time for the cells to recover after the harsh inactivation step. Therefore, an additional condition was performed, with mitomycin-C treated cultures left in DMEM 5%HPL-XF for 48h after mitomycin-C growth inactivation, before starting the 7-day culture in StemSpan + bFGF.

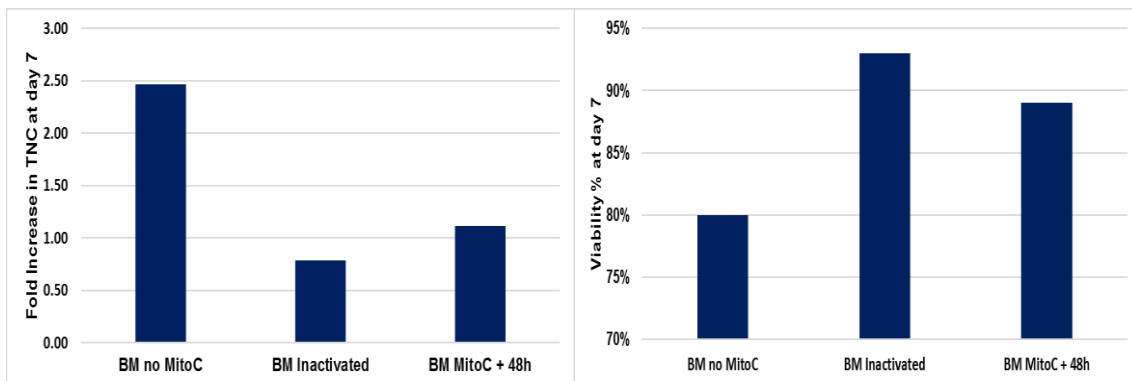


Figure 17 – DMEM 5%HPL-XF expanded BM MSCs stromal layers: Fold increase in total number of cells (Left) and Viability measurement (Right) after 7 days in co-culture media, for non-treated samples (BM no MitoC), 5 µg.mL⁻¹ treated samples (BM Inactivated), and treated samples left for 48h in HPL prior to 7-day culture (BM MitoC + 48h). (n=3)

The non-inactivated BM MSCs continued growing throughout the seven days in culture, with a 2.5-fold increase in total number of cells (**Figure 17**). Inversely, mitomycin-c treated MSC cultures did not divide any further throughout the 7 days in culture (**Figure 17**). However, although not multiplying, the viability of the inactivated cultures was not compromised and it was even superior to the non-inactivated cultures (**Figure 17**). Inactivated cell cultures left in MSC expansion medium for 48h also had their growth arrested, but had lower viability percentages (**Figure 17**). Contrarily to StemPro®, BM MSCs expanded in DMEM 5%HPL-XF seem to behave similarly to BM MSCs expanded in DMEM 10%FBS regarding feeder layer establishment, with >90% viability and growth arrest after mitomycin-C treatment and 7 days in culture in HSC/MSC co-culture media (**Figure 17**).

After establishing viable BM MSCs feeder layer in DMEM 5%HPL-XF, the next step was to evaluate their hematopoietic supportive capacity, when compared with SS MSC- derived feeder layers. A pool of UCB donor (n=2; 3×10^4 CD34⁺/mL) was expanded in StemSpan + Z9 in co-culture with single donor of BM MSCs expanded either in DMEM 5%HPL-XF or DMEM 10%FBS, and compared with cultures absent of stroma (noSTR). After 7 days, the fold increase in total number of cells and their clonogenic potential (see III.5.3) was assessed (Figure 18).

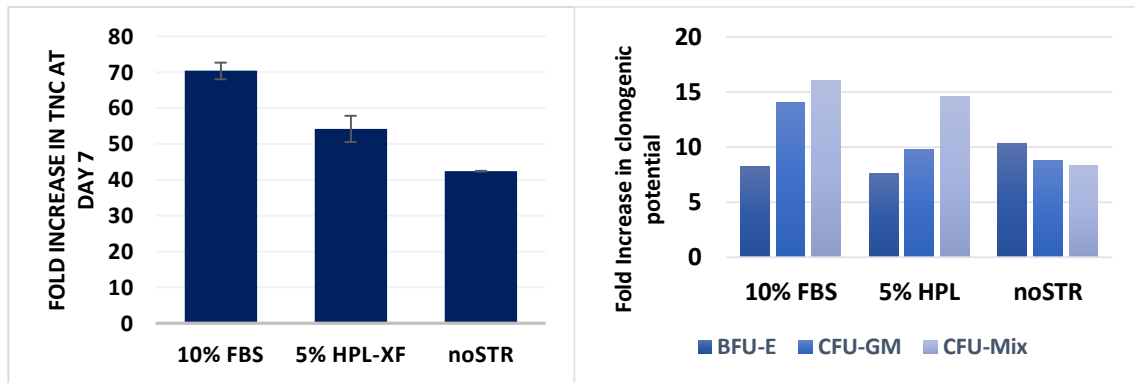


Figure 18 - Side-by-side comparison of the ex-vivo hematopoietic supportive capacity of BM MSC feeder layers expanded either in DMEM 10% FBS or DMEM 5% HPL-XF, and in the absence of stroma (noSTR): Outputs measured as fold increase in total nucleated cells (TNC, results presented as Mean \pm SEM; n=3), and clonogenic potential as measured by Burst forming units – erythroid (BFU-E), Colony forming units – granulocyte monocyte (CFU-GM), and Colony forming units – mix (CFU-Mix).

Additionally, the content of the different hematopoietic subpopulations was assessed at day 0 (Figure 19) and day 7 (Figure 20), and fold their increase calculated (Figure 21).

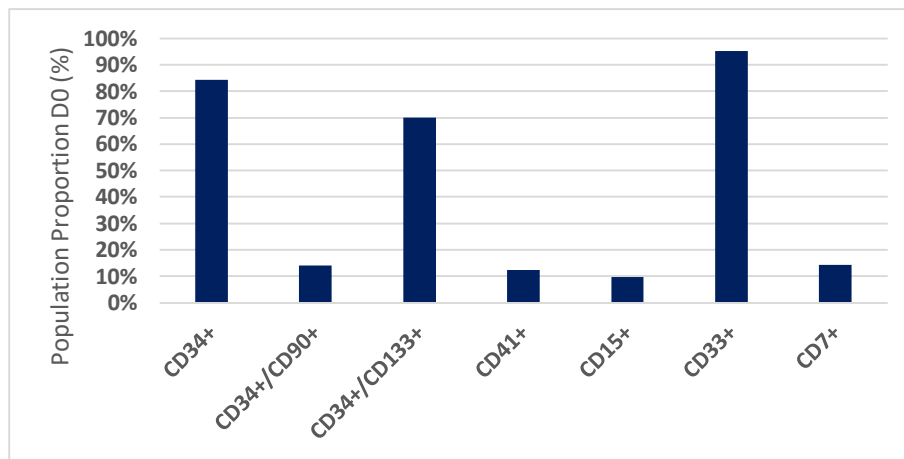


Figure 19 - Content of hematopoietic subpopulations for fresh CD34+-enriched UCB sample (day 0).

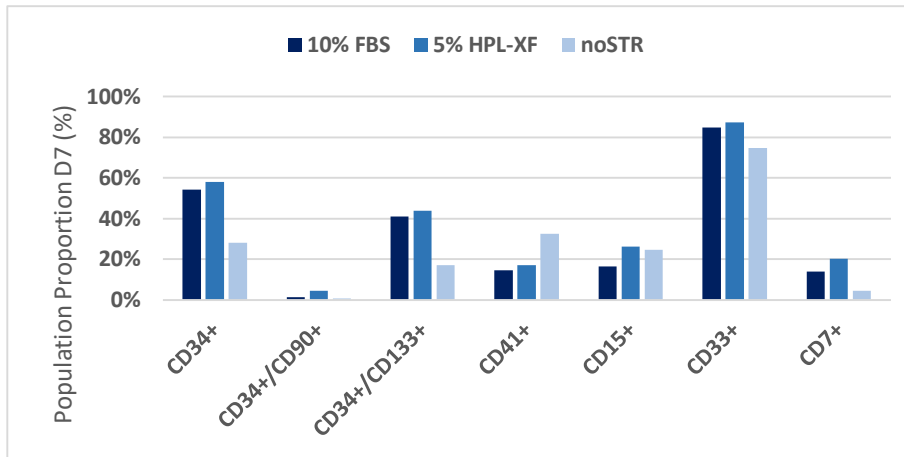


Figure 20 – Proportion of hematopoietic subpopulations for expanded CD34+-enriched UCB samples (day 7), in co-culture with BM MSC expanded feeder layers in DMEM 10%FBS, DMEM 5% HPL or in the absence of stroma (noSTR).

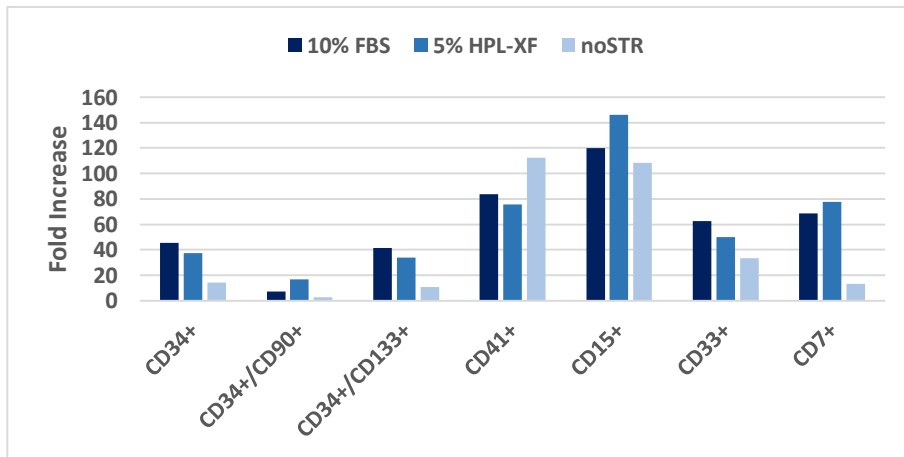


Figure 21 – Fold increase in hematopoietic subpopulations for expanded CD34+-enriched UCB samples (day 7 relative to day 0), in co-culture with BM MSC expanded feeder layers in DMEM 10%FBS, DMEM 5% HPL or in the absence of stroma (noSTR).

Although not being able to reach as higher fold increase in TNC when compared with DMEM 10% FBS, this condition still improved the ex-vivo expansion of UCB HSCs when compared with the no stroma condition (**Figure 18a**). Together with the similar clonogenic potential (**Figure 18b**) and hematopoietic proportions (**Figure 20**) when compared to 10% FBS, supplementing DMEM with 5% HPL-XF seems to provide an efficient xeno-free alternative to our current system, which is based on DMEM 10%FBS-expanded MSCs. Additionally, its content in CD34+ cells was higher than the 10%FBS condition (**Figure 20**). Of notice, even though it had lower fold increase in TNC, 5%HPL-XF condition still achieved higher numbers of CD15 and CD7 populations than 10% FBS (**Figure 21**). Further studies with more BM MSCs donors should take this data into account, because CD15 is expressed in mature neutrophils¹⁶², whose number is a critical parameter in UCB transplantation, which usually suffers from delayed engraftment of neutrophils and platelets.¹⁰⁵ On the other hand, CD7 surface marker is expressed on the earliest, immature thymocytes that express neither CD4 nor CD8. Because of their immaturity, in principle, this does not increase the chance of GvHD. However, it is also expressed on mature T cells, which, if

present, will cause GvHD upon transplantation. Thus, further studies should account for this possibility.

IV.3 Establishment of xenogeneic (xeno)-free feeder layers from alternative MSC sources for HSC expansion

Taking a step further, BSSub™-XF-supplemented medium was also used to expand UCM MSCs and AT MSCs, with the objective of establishing MSC-derived feeder layers from alternative sources. Even though they are both usually regarded as biological waste, adipose tissue was found to provide an alternative HSC niche to the bone marrow¹⁶³ and about 500 times more MSCs can be isolated from fat tissue than from the same amount of BM.¹⁵⁵ On the other hand, primitive MSCs present in UCM increases its potential in therapeutic applications¹⁵⁴. Furthermore, UCM is collected alongside UCB, allowing for quick harvesting of both components of the co-culture expansion system, from the same donor (UCB-HSCs and UCM-MSCs). Thus, is of great interest to study both these sources on their capability of supporting hematopoiesis. Although BM is the most common source of MSCs, umbilical cords and lipoaspirates are routinely discarded after birth and lipoaspirations, respectively, in clinics and hospitals, making these easily accessible and non-invasive sources of MSCs, obviating ethical concerns.

Therefore, it was hypothesised if MSCs from other sources had hematopoietic supportive capacity, such as BM MSCs. To accomplish that, UCM MSCs and AT MSCs, expanded in HPL-XF-supplemented medium, were tested as possible feeder layers.

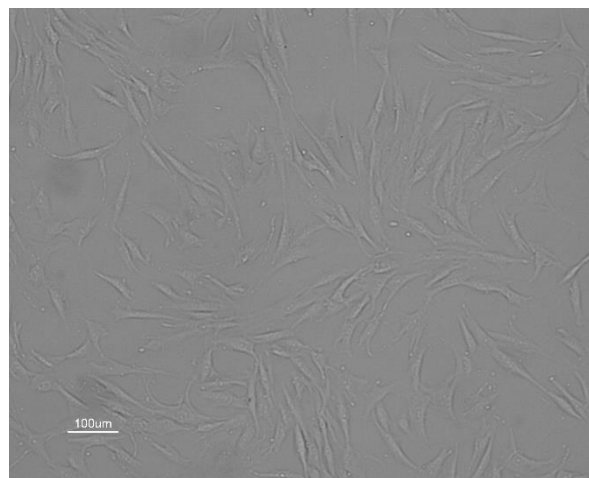


Figure 22 – 60-70% Confluent AT MSCs expanded in DMEM 5%HPL-XF prior to inactivation

To see if mitomycin-C was able to inactivate the growth of AT MSCs expanded in DMEM 5%HPL-XF, 60-70% confluent AT MSCs (**Figure 22**), were treated with either 0.5, 5, or 50 ug.mL⁻¹ of mitomycin-C, maintained in StemSpan + bFGF co-culture media for 7 days (**Figure 23**).

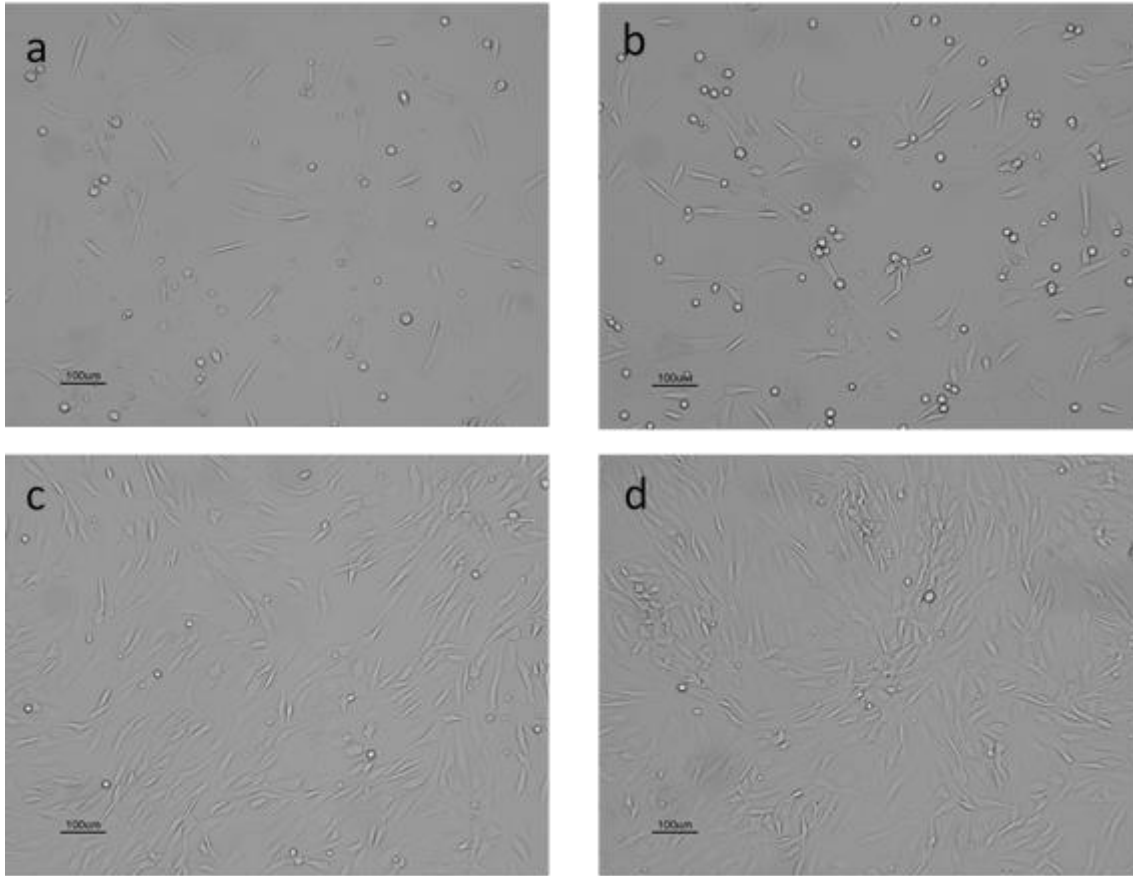


Figure 23 – DMEM 5%HPL-XF expanded AT MSC-derived feeder layers at day 7: A) 50 $\mu\text{g.mL}^{-1}$ Mitomycin-C treatment; B) 5 $\mu\text{g.mL}^{-1}$ Mitomycin-C treatment; C) 0.5 $\mu\text{g.mL}^{-1}$ Mitomycin-C treatment; D) Without Mitomycin-C treatment.

Their total number of cells and viability was assessed (**Figure 24**), and results compared with non-inactivated samples.

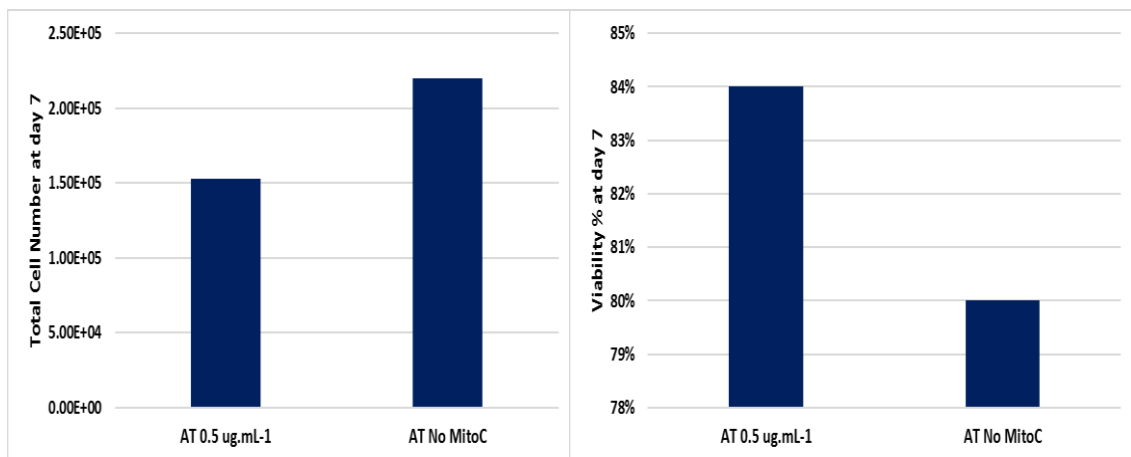


Figure 24 - DMEM 5%HPL-XF expanded AT MSCs stromal layers: Fold increase in total number of cells and Viability % measurement after 7 days in co-culture media, for non-treated samples (AT no MitoC), and 5 $\mu\text{g.mL}^{-1}$ treated samples (AT 5 $\mu\text{g.mL}^{-1}$)

Only the cultures that had been treated with 0.5 $\mu\text{g.mL}^{-1}$ of mitomycin-C were able to maintain a feeder-layer throughout the 7 days of culture (**Figure 23c**), without senescence and surface detachment (**Figure 23a,b**). Expectedly, non-inactivated feeder layers (**Figure 23d**) showed

some overgrowth (**Figure 24a**) comparatively to the 0.5 $\mu\text{g.mL}^{-1}$ mitomycin-C treated samples, but the latter had higher viability at the end of the culture (**Figure 24b**).

The same experimental procedure was followed to see if mitomycin-C was able to inactivate the growth of UCM MSCs expanded in DMEM 5%HPL-XF. Thus, 60-70% confluent UCM MSCs (**Figure 25**), were treated with either 0.5, 5, or 50 $\mu\text{g.mL}^{-1}$ of mitomycin-C, and maintained in StemSpan + bFGF co-culture media for 7 days (**Figure 26**)

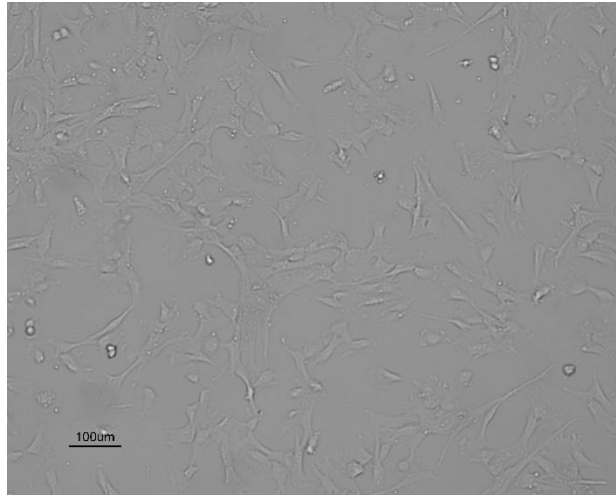


Figure 25 – 60-70% confluent UCM MSC expanded in DMEM 5%HPL-XF prior to mitomycin treatment.

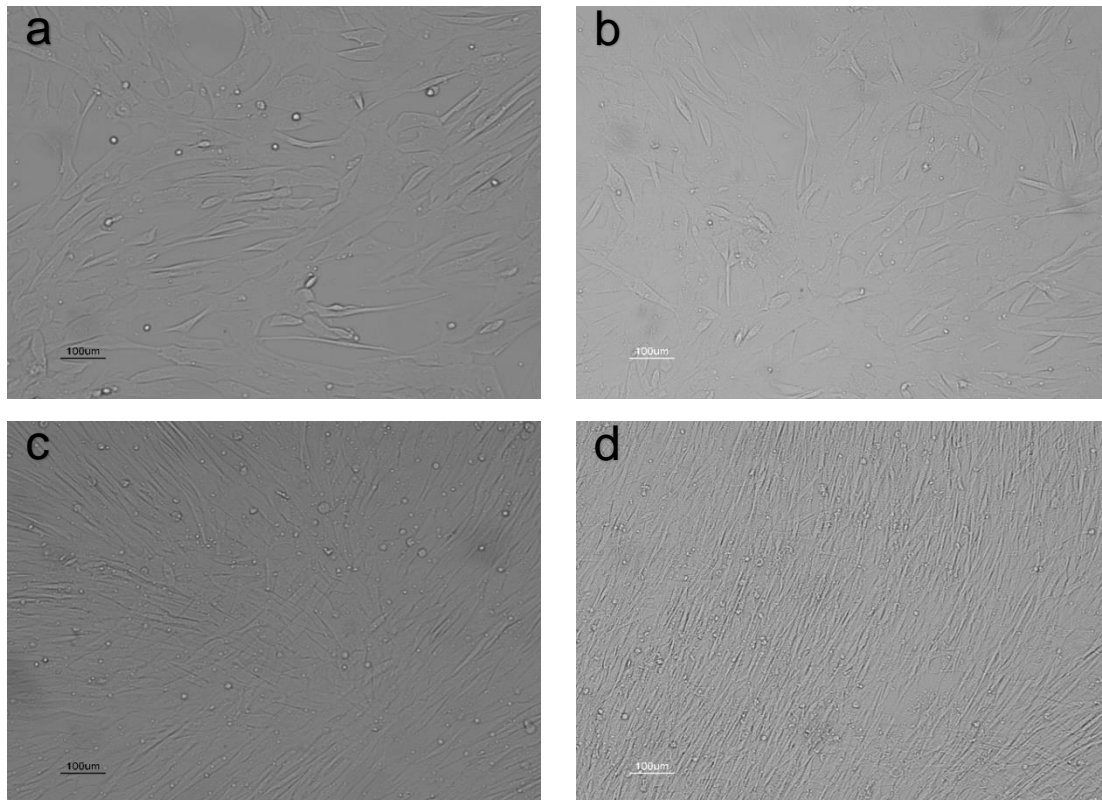


Figure 26 - DMEM 5%HPL-XF expanded UCM MSC-derived feeder layers at day 7: a) 50 $\mu\text{g.mL}^{-1}$ mitomycin-c treatment; b) 5 $\mu\text{g.mL}^{-1}$ mitomycin-c treatment; c) 0.5 $\mu\text{g.mL}^{-1}$ mitomycin-c treatment; d) Without mitomycin-c treatment;

The non-inactivated MSCs did not show any growth arrest after seven days in culture (**Figure 26d**). Since 0.5 $\mu\text{g.mL}^{-1}$ mitomycin-C treatment did not allow for effective growth arrest (**Figure 26c**), a concentration of 5 $\mu\text{g.mL}^{-1}$ mitomycin-C was chosen to assure a effective growth inactivation (**Figure 26b**).

To evaluate that this was an appropriate concentration to use, the total number of cells and viability was accessed throughout the 7 days of the culture for 5 $\mu\text{g.mL}^{-1}$ mitomycin-C-treated cultures (**Table S1**), rather than only at the end of the 7 days in culture (**Figure 27**). These results were compared with non-treated samples. As with BM MSCs, an additional condition was performed, with mitomycin-C treated cultures left in DMEM 5%HPL-XF for 48h after mitomycin-C growth inactivation, before starting the 7-day culture in StemSpan + bFGF.

The non-treated UCM MSCs had their number increase throughout the seven days in culture. Inversely, UCM MSCs of the treated cultures did not divide any further throughout the 7 days in culture (**Figure 27**). However, although not multiplying, the viability of the inactivated cultures was not compromised and was superior to that of the non-treated cultures (**Figure 27**).

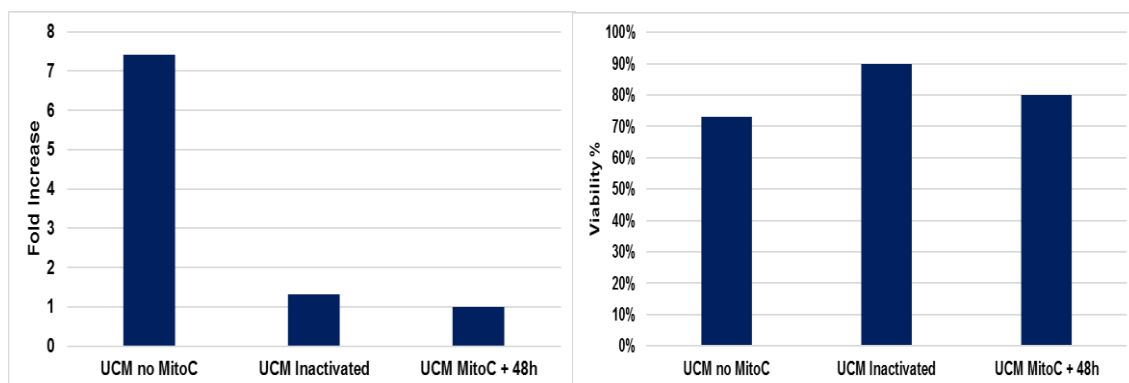


Figure 27 - DMEM 5%HPL-XF expanded UCM MSCs stromal layers, inactivated with 5 $\mu\text{g.mL}^{-1}$ mitomycin-c: a) Fold increase in total number of cells and b) Viability measurement after 7 days in co-culture media, for non-inactivated samples (UCM no MitoC), 5 $\mu\text{g.mL}^{-1}$ inactivated samples (UCM StemSpan), and inactivated samples left for 48h in HPL prior to 7-day culture (BM HPL 48h)

Similarly to BM MSC-derived feeder layers, UCM MSC-derived feeder layers can be left in MSC expansion media after mitomycin-C inactivation without compromising growth arrest but with lower viability percentages (**Figure 27**).

Both AT and UCM sources were shown to be capable of establishing feeder layers, with efficient growth arrest and high viabilities at the end of the culture (**Figure 24 and 27**). Contrarily to BM MSCs, AT and UCM MSCs experience a boom in their proliferation upon contact, rapidly growing on top of each other, with an apparent lack of mitomycin-C sensibility, ending up in feeder-layer overgrowth, which is detrimental for the HSC/MSC co-culture. Viable MSC-derived feeder layers were only achieved when inactivating 60-70% confluent populations (**Figure 22 and 25**), rather than the usual 90-100% confluence for BM MSCs expanded with DMEM 10%FBS. Additionally for UCM MSCs, mitomycin-C concentration was increased from 0.5 $\mu\text{g.mL}^{-1}$ to 5 $\mu\text{g.mL}^{-1}$.

To the author's knowledge, even though several MSC sources have already been expanded with HPL,¹⁶⁴ or with other serum-free alternatives¹⁶⁵, this is the first study that shows that is feasible to perform HSC/MSC co-culture without using any compounds from animal origin in all steps of the process, using BM MSCs to support the expansion of HSCs in a fully xeno-free fashion. Still, some studies have already been performed on the characteristics of MSCs from AT and UCM sources, such proliferation and differentiation potential,^{164,166} and immunomodulatory activity¹⁶⁷⁻¹⁶⁹, but none of them reported the derivation of stromal feeder-layer from alternative sources of MSCs with the objective of supporting HSCs' expansion in a fully xeno-free fashion. Further studies should include a side-by-side comparison of BM, AT, and UCM sources for their ability to support *ex-vivo* expansion of UCB HSCs, bone marrow homing capabilities of the expanded cells, as well as short-term and long-term engraftment studies in an *in vivo* model.

V. Systematic delineation of optimal cytokine concentrations through a two-level face-centered cube design (FC-CD).

V.1 Background and Experimental Design

Design of Experiments (DoE) relies on polynomial models (transfer functions) for mathematical and statistical descriptions of the relation between process factors (X 's) and process responses (Y 's) (**Equation 3**).

Equation 3

$$Y = f(X) + e$$

Where $f(X)$ is the actual DoE model, which quantifies the cause and effect relationships between factors and responses, and e value represents the residuals, variation of Y not described by the model. Represents the random variation inherent to the process. DoE quantifies how large the random variation is¹⁷⁰. For example, if one considers a hypothetical response Y , depending on two factors X_1 and X_2 , there will be three levels of hierarchy on the $f(X)$ polynomial (**Figure 28**):

- Linear terms (main effects): Response surface is represented as a plain in the multidimensional space. Good statistical support with few runs.
- Interaction terms: Higher level of complexity, adds an interaction effect between factors X_1 and X_2 .
- Quadratic terms: Full complexity of the model, allows for second degree curvature, by adding X_1^2 and X_2^2 . Can either describe a maximum, a minimum, or a plateau on the process responses.

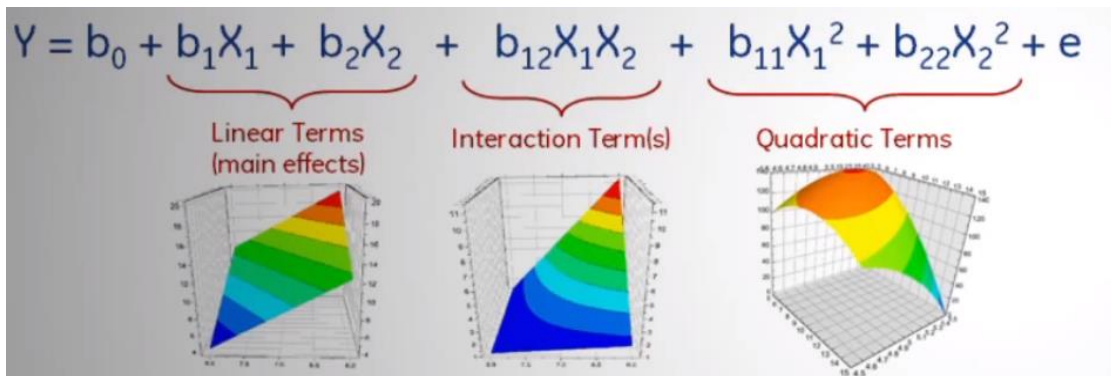


Figure 28 – Representation of the hierarchy levels in the polynomial: **Adapted from:** gelifesciences. Understanding Design of Experiments (DoE) in Protein Purification.

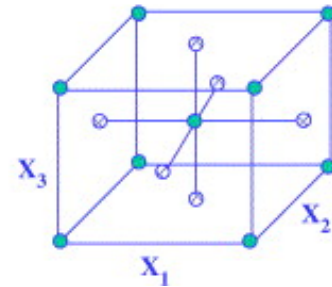
With that, DoE allows for a systematic way of changing process inputs and analysing the resulting process outputs in order to quantify the cause and effect relationship between them, as well as the random variability of the process in a minimum number of runs. Previously at our laboratory, a cytokine cocktail was successfully optimized using an experimental design approach, for the *ex vivo* expansion of UCB HSC in co-culture with human BM MSC-derived feeder layers in a serum-free culture medium (QBSF) supplemented with SCF, Flt-3, TPO and bFGF for 7 days¹¹⁸. However, high degradation rates in glutamine, high levels of megakaryocytic differentiation¹⁷¹ and low expansion in the absence of stroma, lead to the necessity of using other expansion medium. In the last years, new media have been developed for the expansion of HSCs, such as StemSpan

SFEM II from Stem Cell Technologies, that can efficiently support the expansion of HSCs without the presence of a stromal feeder layer.¹⁷² StemSpan SFEM II is a defined serum-free media which can be supplemented with several different cytokine cocktails to achieve different outcomes. Specifically, to unveil the role of stromal feeder layers on cytokine cocktails, a face-centred cube design (FC-CD) of experiments was performed to access the optimal cytokine concentration for StemSpan SFEM II, and explore the differences in terms of cytokine concentrations in the presence and absence of a stromal feeder layer, for the expansion of CD34⁺ cells. SCF, FLT3-L and TPO are among the most widely used cytokines for expanding CD34⁺ cells (**Table 1,2**). HSCs throughout all stages of development of the individual express the same levels of the receptor for SCF (c-KIT).¹⁷³ The stromal cells that surround HSCs are a component of the stem cell niche, and they release several ligands, including SCF, which increases HSCs survival *in vitro*. Furthermore, SCF has been shown to increase adhesion and thus may play a large role in ensuring that HSCs remain correctly placed in the niche.¹⁷⁴ FLT3 is a receptor tyrosine kinase with homology to c-Kit and widely expressed on HSCs and progenitors. Injection of its ligand (FLT3-L) *in vivo* increases the number of early myeloid and lymphoid progenitors but not committed T cell or B cell precursors, and its crucial for dendritic cells development.¹⁷⁵ However, it was shown that short-term but not long-term HSCs express FLT3.^{176,177} Additionally, FLT3-L induces adhesion of hematopoietic cells to stromal cells via (VLA)-4- and VLA-5-dependent mechanisms¹⁷⁸. Finally, TPO is the cytokine that regulates megakaryocyte production, and also HSC quiescence in the bone marrow. The expression pattern of MPL (TPO receptor) provides clues to the dual functions of TPO, with MPL expressed predominantly on megakaryocytes, platelets, hemangioblasts and hematopoietic stem cells.¹⁷⁹ Long-term HSCs, which are MPL⁺, are closely associated with TPO-producing osteoblasts in the niche.²⁴ TPO stimulates the expression of Tie2 on HSCs, which is the receptor for angiopoietin-1 (Ang-1), and helps keep HSCs adhered to the osteoblastic niche.²² This suggests that TPO is actively involved in maintaining the association of HSCs with the niche.

Thus, a two-level face-centered cube design (FC-CD) was performed in order to optimize the concentrations of 3 factors in StemSpan SFEM II, either in the presence or absence of a stromal feeder layer: SCF, Flt-3L, and TPO, tested either at 0 ng.mL⁻¹ (low level, -1) or 100 ng.mL⁻¹ (high level, +1) (**Table 4**). An additional factor, bFGF, was kept at a constant concentration (5 ng.mL⁻¹), since this growth factor assures the maintenance of the stromal feeder layers in the absence of serum.¹²⁰ The experimental design was composed by 17 runs: 8 factorial points, 6 axial points, 3 replicated center points (which provide an estimation of the experimental error). As the experimental design is replicated at the central point, it is possible to estimate the random measurement variability (commonly designated by pure error) for each response variable. Thus, it is possible to divide the residual variation of experiments into two portions, one which accounts for the unreliability of the response variables measurement (random or pure error), and another which accounts for all remaining variability that cannot be explained by the factors and interactions present in the model neither by random error (lack of fit).

Table 3 - Design matrix for the optimization of the cytokine cocktail, and cube representation of the design used in the present studies: SCF, Flt-3L, TPO were tested either at 0 ng mL⁻¹ (low level, -1) or 100 ng mL⁻¹ (high level, +1), respectively. Mid level (0) = 50 ng mL⁻¹.

Runs	SCF	FLT-3L	TPO
11	0	-1	0
2	-1	-1	+1
12	0	+1	0
14	0	0	+1
4	-1	+1	+1
16 (C)	0	0	0
13	0	0	-1
6	+1	-1	+1
7	+1	+1	-1
17 (C)	0	0	0
15 (C)	0	0	0
8	+1	+1	+1
1	-1	-1	-1
5	+1	-1	-1
9	-1	0	0
3	-1	+1	-1
10	+1	0	0



One can obtain a second order model by fitting the experimental data to **Equation 3**, generating **Equation 4**.

Equation 4

$$y = \beta_1(X_1) + \beta_2(X_2) + \beta_3(X_3) + \beta_{1,2}(X_{1,2}) + \beta_{1,3}(X_{1,3}) + \beta_{2,3}(X_{2,3}) + \beta_{1,1}(X_1)^2 + \beta_{2,2}(X_2)^2 + \beta_{3,3}(X_3)^2 + e$$

where y is the response measured (i.e. in this case fold increase in TNC, CD34⁺ cells, BFU-E, CFU-GM, CFU-Mix), β_i the regression coefficients corresponding to the main effects, $\beta_{i,j}$ the coefficients for the second order interactions and $\beta_{i,i}$ the quadratic coefficients. To determine the regression coefficients, a sequential backward elimination procedure was followed, where the least significant terms ($p > 0.05$) of the **Equation 4**, in each step, were eliminated and absorbed into the error.

V.2. No Stroma model

A pool of UCB HSC (two donors, 3×10^4 cells.mL⁻¹) was cultured on StemSpan for 7 days, using the cytokine cocktails presented in **Table 4**. At the end of the culture, the results were as presented in **Table 5**.

Table 4 – Results for each response variable in the no stroma model, after 7 days in culture measured as fold increase in: Total nucleated cells (TNC), CD34⁺, BFU-E, CFU-GM and CFU-mix.

Runs	FI TNC	FI CD34 ⁺	FI BFU-E	FI CFU-GM	FI CFU-Mix
11	31.2	35.0	27.0	59.5	60.7
2	9.1	35.3	9.9	13.8	16.4
12	34.0	42.4	40.3	28.8	38.6
14	35.6	43.0	22.8	44.0	61.6
4	15.4	35.9	18.8	20.5	21.2
16 (C)	32.7	26.2	80.2	2.6	40.4
13	5.6	49.6	1.2	1.7	1.7
6	26.9	29.8	20.2	26.9	38.1
7	6.7	37.9	1.0	12.9	6.3
17 (C)	36.6	42.1	23.7	62.4	57.7
15 (C)	31.7	41.8	49.7	12.7	29.1
8	47.0	36.8	89.7	38.7	53.8
1	0.7	84.1	0.04	0.5	0.11
5	2.4	51.8	3.36	2.4	2.8
9	14.0	43.9	35.79	11.7	24.3
3	1.77	50.1	1.60	1.8	2.9
10	43.3	47.8	39.28	67.2	72.6

Using a Pareto chart of the effects, one can determine the magnitude and the importance of a given factor on the process outputs. The chart displays the absolute value of the effects and draws a reference line on the chart according to the p-value selected, which in this case was $p=0.05$. Any effect that extends beyond this reference line is potentially important. As presented on **Figure 29**, only the TNC response variable returned at least one statistically significant effect.

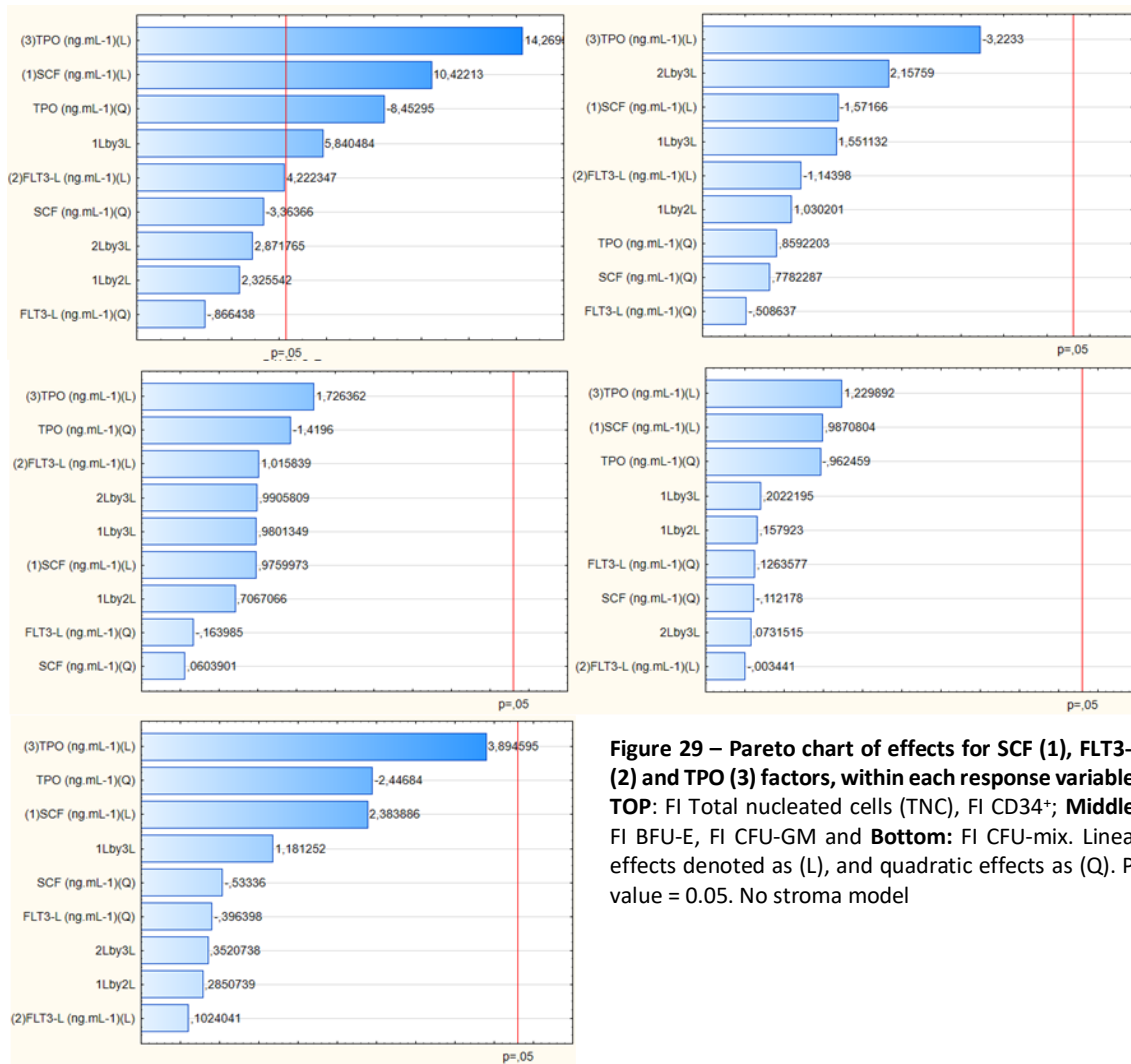


Figure 29 – Pareto chart of effects for SCF (1), FLT3-L (2) and TPO (3) factors, within each response variable: TOP: FI Total nucleated cells (TNC), FI CD34+; Middle: FI BFU-E, FI CFU-GM and Bottom: FI CFU-mix. Linear effects denoted as (L), and quadratic effects as (Q). P-value = 0.05. No stroma model

Following the sequential backward elimination procedure for the FI TNC variable, the three least significant terms were eliminated pooled into the error, and a new Pareto chart was plotted (**Figure 30**). Although FLT3-L linear effect and SCF quadratic effect terms being below the drawn line, their p-values were close enough to 0.05 to be considered important. In fact, the model had R_2 value of 0,94, which means that this specific model fits well to the experimental data, as indicated by the non-significance of the Lack of Fit test (**Figure 30**).

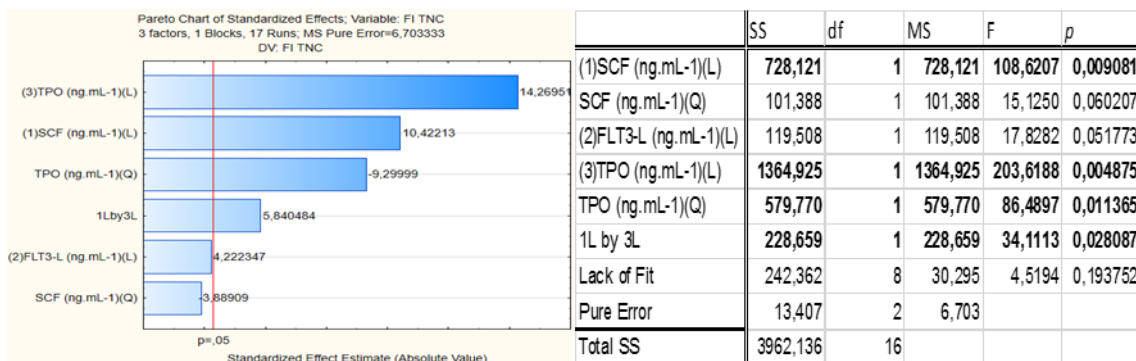


Figure 30 – Adjusted Pareto Chart (left) and ANOVA table (right) for FI TNC response variable. No stroma model

Additionally, it is necessary to confirm whether there is a trend or systematic variations when analysing residual variation, or if it only possesses random variation. As shown in **Figure 31**, data is normally distributed, indicating that whatever this model cannot predict is most likely random variation following a normal distribution.

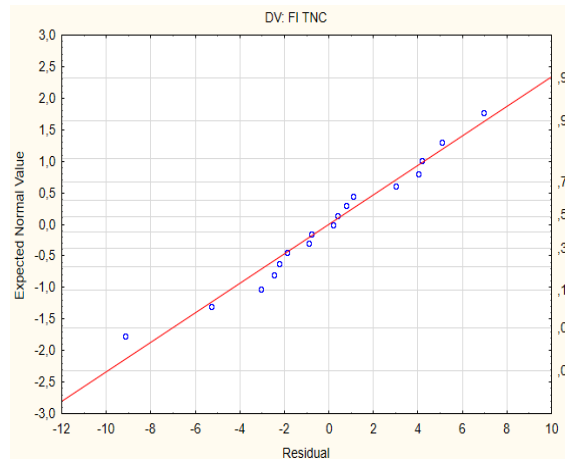


Figure 31 – Normal probability plot of residuals, for the FI TNC response variable of no stroma model

Fitted response surface plots were used with the purpose of interpreting the model. Two factors are plotted against each other, and generate a graph of the polynomial predictions from the function obtained from fitting the regression coefficients (**Figure 32**) to **Equation 4**.

	Regress. Coeff
Mean/Interc.	-4,36694
(1)SCF (ng.mL-1)(L)	0,29517
SCF (ng.mL-1)(Q)	-0,00231
(2)FLT3-L (ng.mL-1)(L)	0,06914
(3)TPO (ng.mL-1)(L)	0,68017
TPO (ng.mL-1)(Q)	-0,00553
1L by 3L	0,00214

Figure 32 – Regression coefficients for the FI TNC response variable of no stroma model.

As shown in **Figure 33**, the optimal cytokine concentration to maximize TNC FI, was around 70-90 ng/mL for TPO and 80-120 ng/mL for SCF. However, this was only accomplished due to the presence of the Quadratic Effect for SCF in the model (p value = 0.06). Otherwise, the maximum concentration for SCF would be predicted to be out of the range of the model (**Figure 33**).

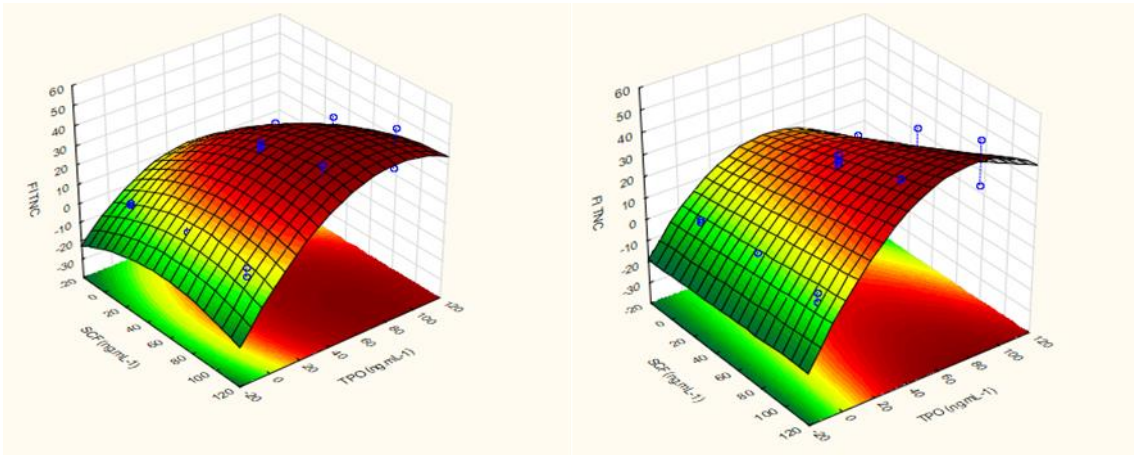


Figure 33 - Fitted response surface plot for SCF and TPO with (left) or without (Right) the quadratic effect for SCF, for the no stroma model

Similarly, FLT3-L maximum concentration was out of the range on this model. Lack of significance of the quadratic term (**Figure 29**) means that the maximum concentration tested also maximizes the expansion of hematopoietic stem/progenitor cells. SCF and TPO maintained the same maximum values when plotted against FLT3-L (**Figure 34**).

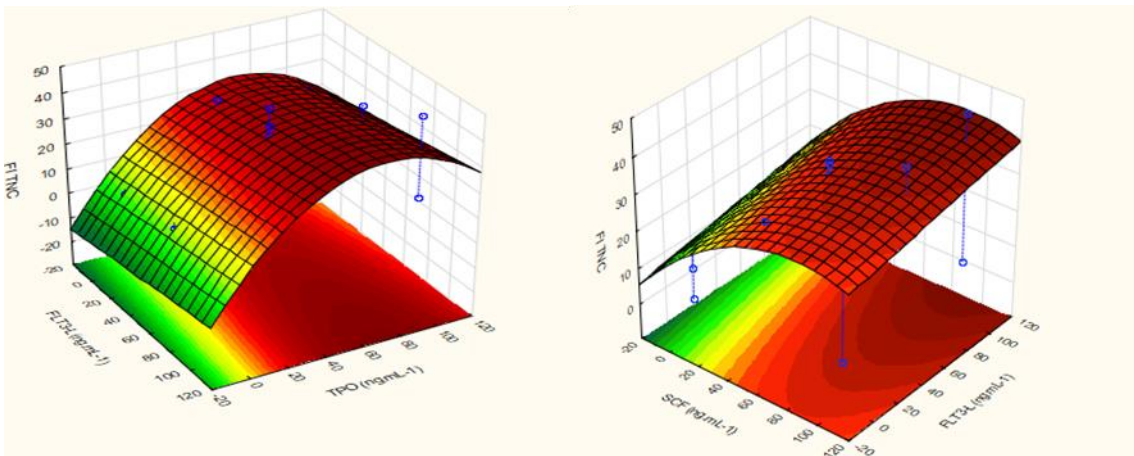


Figure 34 - Fitted response surface plot for FLT3-L and TPO (left) and SCF and FLT3-L (Right) for the no stroma model

V.3. Stroma model

The same pool of UCB HSC used in the no stroma model (3×10^4 cells.mL⁻¹) was cultured on top of a confluent pool of BM MSC-derived stromal feeder layer, for 7 days on StemSpan, using the cytokine cocktails presented in **Table 2**, according to a two-level Face Centered Cube Design. At the end of the culture, the results were as presented in **Table 7**.

Table 6 - Results for each response variable in the no stroma model, after 7 days in culture measured as fold increase in: Total nucleated cells (TNC), CD34⁺, BFU-E, CFU-GM and CFU-mix.

Runs	FI TNC	FI CD34+	FI BFU-E	FI CFU-GM	FI CFU-Mix
11	46.2	17.3	35.1	49.1	71.4
2	12.3	10.0	24.4	12.7	15.1
12	55.6	29.6	53.5	49.8	66.3
14	62.7	36.4	59.2	78.3	79.2
4	25.3	15.2	8.4	25.1	32.4
16 (C)	55.3	30.7	118.9	40.9	68.9
13	32.4	19.7	20.4	21.0	27.9
6	50.2	25.4	54.9	56.5	81.9
7	52.7	27.7	55.6	36.2	100.7
17 (C)	36.7	14.8	52.3	30.2	29.6
15 (C)	54.4	22.4	78.6	31.2	48.7
8	66.0	27.6	77.0	59.8	106.5
1	0.9	0.8	0.1	0.3	1.2
5	11.8	5.7	8.9	9.0	17.2
9	25.1	9.9	20.9	27.7	38.8
3	4.7	2.2	1.3	6.0	5.8
10	66.2	26.0	58.9	81.4	101.1

Of notice, the 17th run, which consists in one of the replicated center points, had a less than expected fold increase in total nucleated cells, when compared with the other runs and center points (**Table 7**). Expectedly, because replicated center points measure the unreliability of the measurement response variables, having the 17th run inserted into the model resulted in absence of statistical significance for all but one factor (**Figure 35**). This indicates that differences in the process outputs were a result of random variability and not due to the influence of different factor concentrations. Additionally, in a similar fashion to the no stroma model in **VI.3 (Figure 29)**, only the FI TNC response output retrieved at least one statistically significant effect for the stroma model. Thus, a second analysis was performed, without the 17th run. Expectedly, this improved the statistical significance of the model (**Figure 35**), with all but two factors being significant, for the FI TNC response variable.

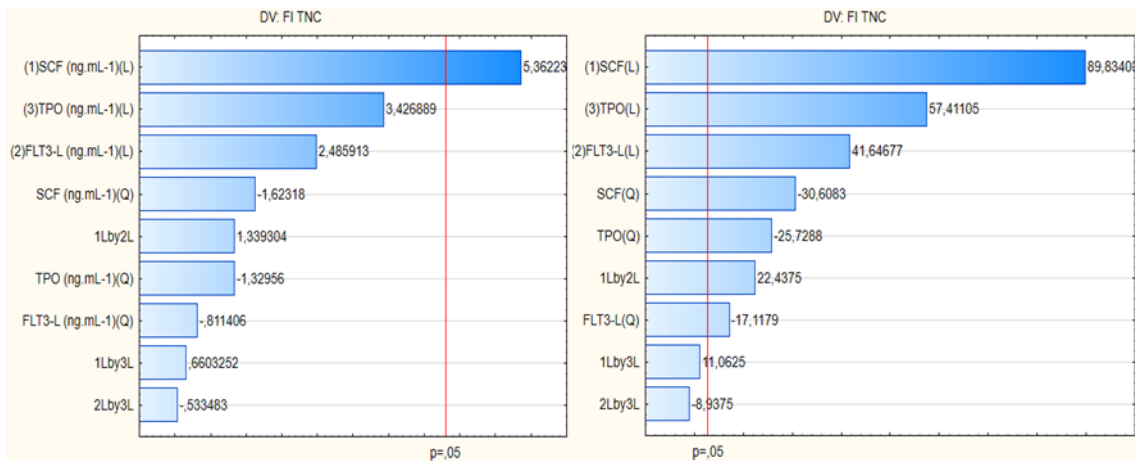


Figure 35 – Pareto chart of effects for the FI TNC response variable. Before (left) and After (right) adjustment. Stroma model.

Although the interaction effects of SCF by TPO (1Lby3L), and FLT3-L by TPO (2Lby3L) were below the drawn line, their p-values were close enough to 0.05 to be considered important. In fact, the model had R_2 value of 0,97, which means that this specific model fits well to the experimental data, as indicated by the non-significance of the Lack of Fit test (**Figure 36**).

	SS	df	MS	F	p
(1)SCF (ng.mL-1)(L)	3188,209	1	3188,209	8070,153	0,007086
SCF (ng.mL-1)(Q)	370,121	1	370,121	936,869	0,020792
(2)FLT3-L (ng.mL-1)(L)	685,216	1	685,216	1734,453	0,015283
FLT3-L (ng.mL-1)(Q)	115,762	1	115,762	293,022	0,037148
(3)TPO (ng.mL-1)(L)	1302,135	1	1302,135	3296,028	0,011088
TPO (ng.mL-1)(Q)	261,519	1	261,519	661,971	0,024731
1L by 2L	198,890	1	198,890	503,441	0,028354
1L by 3L	48,347	1	48,347	122,379	0,057392
2L by 3L	31,557	1	31,557	79,879	0,070935
Lack of Fit	243,511	5	48,702	123,278	0,068268
Pure Error	0,395	1	0,395		
Total SS	7680,203	15			

Figure 36 – ANOVA table for the FI TNC response variable after adjustment, for the stroma model. Stroma model

Additionally, it necessary to confirm whether there is a trend or systematic variations when analysing residual variation, or if it only possesses random variation. As shown in **Figure 37**, data

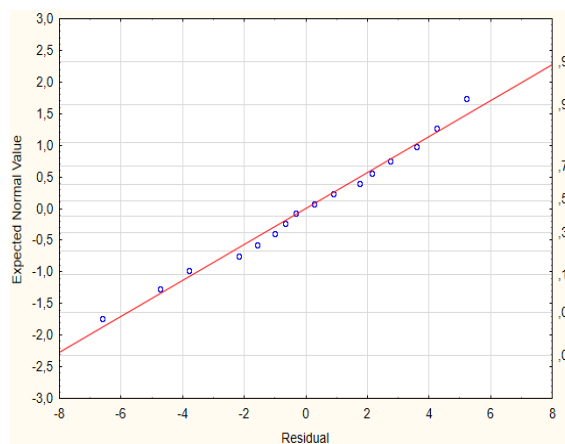


Figure 37 – Normal probability plot of residuals, for the FI TNC response variable for the stroma model. Stroma model

is normally distributed, indicated that whatever this model cannot predict is most likely random variation following a normal distribution

Fitted response surface plots were used with the purpose of interpreting the model. Two factors are plotted against each other, and generate a graph of the polynomial predictions from the function obtained from fitting the regression coefficients (**Figure 38**) to **Equation 4**.

	Regress. Coeff
Mean/Interc.	-3,88113
(1)SCF (ng.mL-1)(L)	0,68217
SCF (ng.mL-1)(Q)	-0,00474
(2)FLT3-L (ng.mL-1)(L)	0,37061
FLT3-L (ng.mL-1)(Q)	-0,00265
(3)TPO (ng.mL-1)(L)	0,61717
TPO (ng.mL-1)(Q)	-0,00398
1L by 2L	0,00199
1L by 3L	0,00098
2L by 3L	-0,00079

Figure 38 – Regression coefficients for the FI TNC response variable for the stroma model.

As shown in **Figure 39**, the predicted optimal cytokine concentration to maximize TNC FI, was around 80-110 ng/mL for both SCF and FLT3-L (TPO fixed at 80 ng.mL⁻¹).

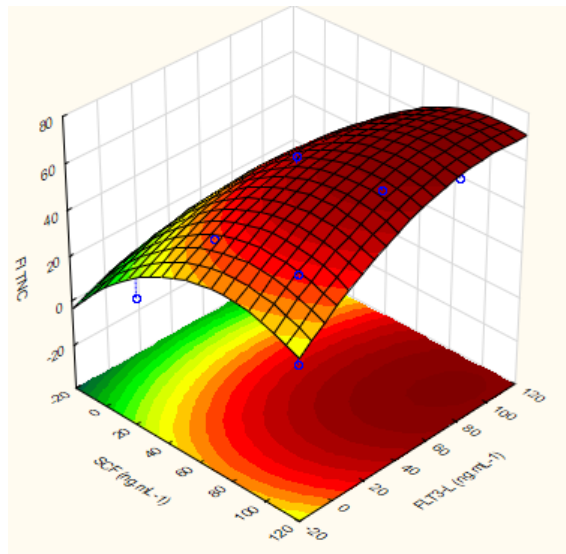


Figure 39 - Fitted response surface plot for SCF and Flt3-L for the stroma model

Taking that into account, SCF and TPO were plotted against each other with different fixed values of FLT3-L, either 50 ng/mL or 100 ng/mL (**Figure 40**). At 50 ng/mL, TPO optimal values ranged from 55 to 110 ng/mL, and SCF from 70 to 120 ng/mL (**Figure 40**). Consistently with the optimum values calculated for FLT3-L, the higher FLT3-L concentration enables to pinpoint the maximum value of SCF and TPO more accurately. Thus, when fixing FLT3-L concentration to 100 ng/mL, TPO was predicted to range from 70 to 90 ng/mL, and SCF from 90 to 110 ng/mL.

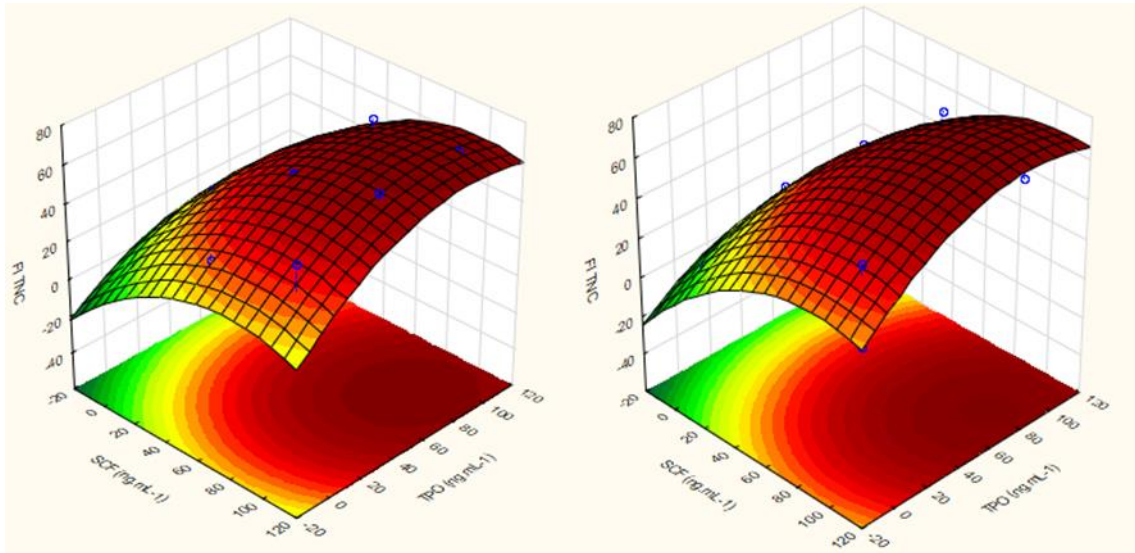


Figure 40 - Fitted response surface plot for SCF and TPO, with FLT3-L fixed at 50ng.mL (left) or at 100 ng.mL (right) for the stroma model

Similarly, when plotting FLT3-L against TPO, SCF was fixed at 100 ng/mL. Hence, FLT3-L optimal concentration was predicted to range from 80 to 110 ng/mL once again, as well as TPO, with a predicted range of 70-90 ng/mL (**Figure 41**).

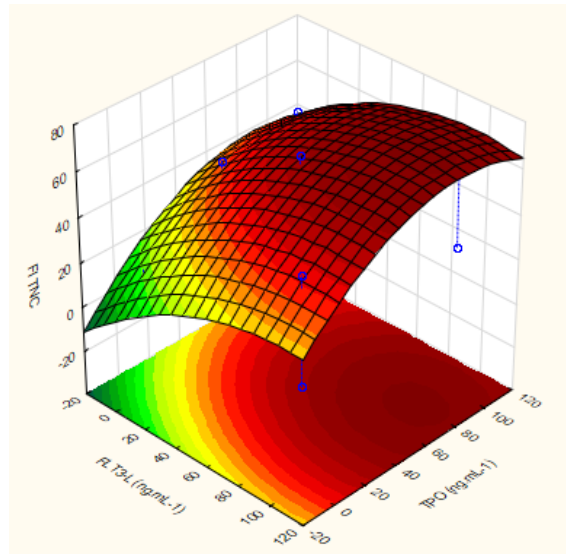


Figure 41 - Fitted response surface plot for FLT3-L and TPO for the stroma model

V.4. Discussion

Several *ex vivo* culture systems have been used with different rates of success by testing different cytokine cocktails in stroma-containing or stroma-free cultures with serum or serum-free conditions (**Table 1**). Indeed, many cytokine combinations tested include SCF, Flt-3L and TPO, which are presumed to promote extensive cell self-renewal and to limit levels of apoptosis.^{2,3} Previously at SCBL, a cytokine cocktail was successfully optimized for the *ex vivo* expansion of UCB HSC in a serum-free culture system using human BM MSC-derived feeder layers, supplemented with SCF, Flt-3, TPO, using an experimental design approach.¹¹⁸ In the present study, an attempt was made to optimize the concentration of these factors in StemSpan SFEM II, either in the presence or not of a stromal feeder layer, through a two-level face-centred cube design (FC-CD) of experiments. Both stroma and no stroma models only retrieved significant values for the FI TNC response variable (**Figure 29 and 36**). Regarding the optimal cytokine concentrations predicted by the fitted response surface plots to maximize FI TNC response variable, TPO had a straightforward analysis, with a predicted concentration of 70-90 ng.mL⁻¹ for both models. Of notice, on the previous study in QBSF-60, this cytokine had been predicted to have its optimum value outside of the range tested at the time by our group, as the maximum concentration tested (50 ng.mL⁻¹) also maximized the expansion.¹¹⁸ On the other hand, SCF optimal concentration is not independent of the presence of stroma, expectedly, since SCF is known to be secreted by MSCs.⁴⁵ Expectedly, SCF optimal value for FI TNC maximization for the no stroma model had an higher optimum values (**Figure 33**, 80-120ng.mL⁻¹) than for the stroma model (**Figure 39**, 90-110 ng.mL⁻¹). Similarly, the stroma model was predicted to have lower optimum concentrations of FLT3-L (**Figure 41**) than the no stroma model (**Figure 34**). In fact, for the no stroma model, since FLT3-L had a positive main effect (in the absence of a significant second order term), the maximum concentration tested also maximizes the expansion of cells in culture, raising the question whether the optimum value for this cytokine should be located outside of the range tested. Altogether, to capture the optimum cytokine concentrations to maximize the fold increase in TNC, both models seem to need a readjustment in the maximum levels of the factors being tested, since SCF and FLT3-L were either predicted to be located near (**Figure 33, 39, 41**) or beyond (**Figure 34**) the maximum concentrations tested, for the FI TNC response variable. Concerning the remaining response variables, which were all non-significant, the model assumed that differences in the process outputs were a result of random variability and not due to the influence of different factor concentrations. Replicates of the experiments (i.e. more biological samples) should be done to gather more information until obtaining statistically significant values. Additionally, it would be interesting to analyse CD34⁺CD38⁻CD90⁺CD45RA⁻ surface markers to analyse HSC expansion. Each new measurement should be taken under consistent experimental conditions, but replicates will be done in different days. To account for this, one must introduce data into the model as blocks, which are categorical variables that explain variation in the response variable not caused by the factors, but due to incidental differences between days. This would minimize bias and variance of the error because of nuisance factors.¹⁸⁰ After accounting for these drawbacks and obtaining statistically significant data, one can begin to

validate the results, by testing the new cytokine cocktails against our previous cocktail (Z9) and compare the obtained the results with the predicted values.

VI. Conclusions and Future Trends

Since their identification, HSC have been the focus of intensive research, and have proven to be invaluable and lifesaving in the treatment of hematologic malignancies. Cord blood transplantation as a source of stem cells has the potential to fill the gap of a growing population of patients who do not have a fully matched donor but need allogeneic hematopoietic stem cell transplantation. For that, advances must be made on the ex-vivo expansion of these cells, as to allow for adults to receive this type of transplants.

Results of traditional methods of UCB ex-vivo expansion solely using cytokines were disappointing. On the other hand, expanding UCB HSCs in co-culture with MSCs led to an increase in graft content and improved engraftment, highlighting the importance of optimizing the cocktail cytokines in the presence of stroma. However, MSCs are still today retrospectively isolated from primary human BM samples based on their high adherence to plastic. This leads to highly heterogeneous populations, which leads to reproducibility issues if one wants to translate the HSC/MS into clinical practice. This heterogeneity of the MSC population can be one of the causes compromising the maintenance of the most primitive HSC with long-term multilineage engraftment capacity. To address this issue, future studies should rely on specific surface marker selection of MSC populations¹⁸¹. Furthermore, alternative MSCs sources such as AT and UCM are still to be studied on their capability to expand UCB cells effectively and improve engraftment in *in vivo* studies. Other methods use HSC-differentiation blockers, such as nicotinamide analogues, copper chelators, inducing constitutive *Notch* signalling, or an aryl hydrocarbon receptor antagonist (StemReginin1).¹¹⁹ Many of these methods lead to substantial expansions of total nucleated cells and CD34⁺ cells, and significantly improved time to neutrophil or platelet engraftment in patients transplanted with the expanded products, when compared to the recipients of unmanipulated UCB transplantation.¹¹⁹ Thus, it would be of great interest to combine some of the aforementioned approaches, and perform *in vivo* transplantation assays, which can undoubtedly demonstrate the cells ability to repopulate all blood lineages, constituting the ultimate proof of HSC activity.⁷⁶ On that topic, an efficient approach to enhance engraftment focuses on increasing the homing capacity of UCB cells to the bone marrow, through modulation of membrane lipid rafts, modulation of homing molecules, enhancing metabolic response to homing stimuli, or bioavailability enhancement of chemottractants.¹⁸² Finally, after weighing all options, performing these approaches in a bioreactor culture system should be taken into account, as to surpass cell productivity limitations and limited monitoring typical of static cell culture.

VII. Supplementary Figures

Timepoint		UCM (No Inact)	UCM SS	UCM (48h)
Pre-Inact	Viab (%)		94%	
	TNC		3,33E+04	
D0	Viab (%)		76%	
	TNC		2,44E+04	
HPL (24H)	Viab (%)			88%
	TNC			3,92E+04
HPL (48H)	Viab (%)			83%
	TNC			4,89E+04
D1	Viab (%)	87%	84%	85%
	TNC	8,33E+04	2,89E+04	3,78E+04
D2	Viab (%)	89%	90%	87%
	TNC	1,96E+05	2,89E+04	2,78E+04
D3	Viab (%)	91%	78%	75%
	TNC	2,64E+05	2,78E+04	2,28E+04
D4	Viab (%)		89%	90%
	TNC		6,89E+04	4,22E+04
D5	Viab (%)	87%	87%	89%
	TNC	3,46E+05	3,78E+04	1,89E+04
D6	Viab (%)	80%	87%	86%
	TNC	1,87E+05	2,61E+04	2,80E+04
D7	Viab (%)	73%	90%	80%
	TNC	1,81E+05	3,22E+04	2,44E+04

VIII. References

1. da Silva, C. L. *et al.* Dynamic cell-cell interactions between cord blood haematopoietic progenitors and the cellular niche are essential for the expansion of CD34+, CD34+CD38- and early lymphoid CD7+ cells. *J. Tissue Eng. Regen. Med.* **4**, 149–158 (2010).
2. Levac, K., Karanu, F. & Bhatia, M. Identification of growth factor conditions that reduce ex vivo cord blood progenitor expansion but do not alter human repopulating cell function in vivo. *Haematologica* **90**, 166–172 (2005).
3. Murray, L. J. *et al.* Thrombopoietin, flt3, and kit ligands together suppress apoptosis of human mobilized CD34+ cells and recruit primitive CD34+ Thy-1+ cells into rapid division. *Exp. Hematol.* **27**, 1019–1028 (1999).
4. Owen, R. D. IMMUNOGENETIC CONSEQUENCES OF VASCULAR ANASTOMOSES BETWEEN BOVINE TWINS. *Science* **102**, 400–401 (1945).
5. Billingham, R. E., Brent, L. & Medawar, P. B. Actively acquired tolerance of foreign cells. *Nature* **172**, 603–606 (1953).
6. Weissman, I. L. & Shizuru, J. A. The origins of the identification and isolation of hematopoietic stem cells, and their capability to induce donor-specific transplantation tolerance and treat autoimmune diseases. *Blood* **112**, 3543–3553 (2008).
7. Ho, A. D., Haas, R. & Champlin, R. E. *Hematopoietic Stem Cell Transplantation*. (CRC Press, 2000).
8. Till, J. E. & McCulloch, E. A. A direct measurement of the radiation sensitivity of normal mouse bone marrow cells. *Radiat. Res.* **14**, 213–222 (1961).
9. Becker, A. J., McCulloch, E. A. & Till, J. E. Pillars article: Cytological demonstration of the clonal nature of spleen colonies derived from transplanted mouse marrow cells. *Nature*. 1963. 197:452-454. *J. Immunol. Baltim. Md 1950* **192**, 4945–4947 (2014).
10. Siminovitch, L., McCulloch, E. A. & Till, J. E. THE DISTRIBUTION OF COLONY-FORMING CELLS AMONG SPLEEN COLONIES. *J. Cell. Physiol.* **62**, 327–336 (1963).
11. Wu, A. M., Till, J. E., Siminovitch, L. & McCulloch, E. A. A cytological study of the capacity for differentiation of normal hemopoietic colony-forming cells. *J. Cell. Physiol.* **69**, 177–184 (1967).
12. Wu, A. M., Till, J. E., Siminovitch, L. & McCulloch, E. A. CYTOLOGICAL EVIDENCE FOR A RELATIONSHIP BETWEEN NORMAL HEMATOPOIETIC COLONY-FORMING CELLS AND CELLS OF THE LYMPHOID SYSTEM. *J. Exp. Med.* **127**, 455–464 (1968).
13. Wolf, N. S. & Trentin, J. J. Differential proliferation of erythroid and granuloid spleen colonies following sublethal irradiation of the bone marrow donor. *J. Cell. Physiol.* **75**, 225–229 (1970).
14. Taichman, R. S. Blood and bone: two tissues whose fates are intertwined to create the hematopoietic stem-cell niche. *Blood* **105**, 2631–2639 (2005).
15. Visnjic, D. *et al.* Hematopoiesis is severely altered in mice with an induced osteoblast deficiency. *Blood* **103**, 3258–3264 (2004).
16. Zhang, J. *et al.* Identification of the haematopoietic stem cell niche and control of the niche size. *Nature* **425**, 836–841 (2003).
17. Hofmeister, C. C., Zhang, J., Knight, K. L., Le, P. & Stiff, P. J. Ex vivo expansion of umbilical cord blood stem cells for transplantation: growing knowledge from the hematopoietic niche. *Bone Marrow Transplant.* **39**, 11–23 (2007).
18. Kiel, M. J., Acar, M., Radice, G. L. & Morrison, S. J. Hematopoietic stem cells do not depend on N-cadherin to regulate their maintenance. *Cell Stem Cell* **4**, 170–179 (2009).
19. Bromberg, O. *et al.* Osteoblastic N-cadherin is not required for microenvironmental support and regulation of hematopoietic stem and progenitor cells. *Blood* **120**, 303–313 (2012).
20. Hosokawa, K. *et al.* Cadherin-Based Adhesion Is a Potential Target for Niche Manipulation to Protect Hematopoietic Stem Cells in Adult Bone Marrow. *Cell Stem Cell* **6**, 194–198 (2010).
21. Stier, S. *et al.* Osteopontin is a hematopoietic stem cell niche component that negatively regulates stem cell pool size. *J. Exp. Med.* **201**, 1781–1791 (2005).
22. Arai, F. *et al.* Tie2/angiopoietin-1 signaling regulates hematopoietic stem cell quiescence in the bone marrow niche. *Cell* **118**, 149–161 (2004).
23. Qian, H. *et al.* Critical Role of Thrombopoietin in Maintaining Adult Quiescent Hematopoietic Stem Cells. *Cell Stem Cell* **1**, 671–684 (2007).
24. Yoshihara, H. *et al.* Thrombopoietin/MPL signaling regulates hematopoietic stem cell quiescence and interaction with the osteoblastic niche. *Cell Stem Cell* **1**, 685–697 (2007).
25. Mendelson, A. & Frenette, P. S. Hematopoietic stem cell niche maintenance during homeostasis and regeneration. *Nat. Med.* **20**, 833–846 (2014).
26. Lo Celso, C. *et al.* Live-animal tracking of individual haematopoietic stem/progenitor cells in their niche. *Nature* **457**, 92–96 (2009).
27. Xie, Y. *et al.* Detection of functional haematopoietic stem cell niche using real-time imaging. *Nature* **457**, 97–101 (2009).
28. Hooper, A. T. *et al.* Engraftment and Reconstitution of Hematopoiesis Is Dependent on VEGFR2-Mediated

- Regeneration of Sinusoidal Endothelial Cells. *Cell Stem Cell* **4**, 263–274 (2009).
29. Mercier, F. E., Ragu, C. & Scadden, D. T. The bone marrow at the crossroads of blood and immunity. *Nat. Rev. Immunol.* **12**, 49–60 (2011).
 30. Kiel, M. J. *et al.* SLAM family receptors distinguish hematopoietic stem and progenitor cells and reveal endothelial niches for stem cells. *Cell* **121**, 1109–1121 (2005).
 31. North, T. E. *et al.* Hematopoietic stem cell development is dependent on blood flow. *Cell* **137**, 736–748 (2009).
 32. Lancrin, C. *et al.* Blood cell generation from the hemangioblast. *J. Mol. Med. Berl. Ger.* **88**, 167–172 (2010).
 33. Adamo, L. *et al.* Biomechanical forces promote embryonic haematopoiesis. *Nature* **459**, 1131–1135 (2009).
 34. O'Malley, D. P. Benign extramedullary myeloid proliferations. *Mod. Pathol. Off. J. U. S. Can. Acad. Pathol. Inc* **20**, 405–415 (2007).
 35. Rafii, S., Mohle, R., Shapiro, F., Frey, B. M. & Moore, M. A. Regulation of hematopoiesis by microvascular endothelium. *Leuk. Lymphoma* **27**, 375–386 (1997).
 36. Mazo, I. B. *et al.* Hematopoietic progenitor cell rolling in bone marrow microvessels: parallel contributions by endothelial selectins and vascular cell adhesion molecule 1. *J. Exp. Med.* **188**, 465–474 (1998).
 37. Sipkins, D. A. *et al.* In vivo imaging of specialized bone marrow endothelial microdomains for tumour engraftment. *Nature* **435**, 969–973 (2005).
 38. Sacchetti, B. *et al.* Self-renewing osteoprogenitors in bone marrow sinusoids can organize a hematopoietic microenvironment. *Cell* **131**, 324–336 (2007).
 39. Méndez-Ferrer, S. *et al.* Mesenchymal and haematopoietic stem cells form a unique bone marrow niche. *Nature* **466**, 829–834 (2010).
 40. Frenette, P. S., Pinho, S., Lucas, D. & Scheiermann, C. Mesenchymal Stem Cell: Keystone of the Hematopoietic Stem Cell Niche and a Stepping-Stone for Regenerative Medicine. *Annu. Rev. Immunol.* **31**, 285–316 (2013).
 41. Sugiyama, T., Kohara, H., Noda, M. & Nagasawa, T. Maintenance of the hematopoietic stem cell pool by CXCL12-CXCR4 chemokine signaling in bone marrow stromal cell niches. *Immunity* **25**, 977–988 (2006).
 42. Omatsu, Y. *et al.* The essential functions of adipo-osteogenic progenitors as the hematopoietic stem and progenitor cell niche. *Immunity* **33**, 387–399 (2010).
 43. Nombela-Arrieta, C. *et al.* Quantitative imaging of haematopoietic stem and progenitor cell localization and hypoxic status in the bone marrow microenvironment. *Nat. Cell Biol.* **15**, 533–543 (2013).
 44. Kunisaki, Y. *et al.* Arteriolar niches maintain haematopoietic stem cell quiescence. *Nature* **502**, 637–643 (2013).
 45. Boulais, P. E. & Frenette, P. S. Making sense of hematopoietic stem cell niches. *Blood* **125**, 2621–2629 (2015).
 46. Mohyeldin, A., Garzón-Muvdi, T. & Quiñones-Hinojosa, A. Oxygen in stem cell biology: a critical component of the stem cell niche. *Cell Stem Cell* **7**, 150–161 (2010).
 47. Chow, D. C., Wenning, L. A., Miller, W. M. & Papoutsakis, E. T. Modeling pO₂ distributions in the bone marrow hematopoietic compartment. II. Modified Kroghian models. *Biophys. J.* **81**, 685–696 (2001).
 48. Eliasson, P. & Jönsson, J.-I. The hematopoietic stem cell niche: Low in oxygen but a nice place to be. *J. Cell. Physiol.* **222**, 17–22 (2010).
 49. Cipolleschi, M. G., Dello Sbarba, P. & Olivetto, M. The role of hypoxia in the maintenance of hematopoietic stem cells. *Blood* **82**, 2031–2037 (1993).
 50. Busuttil, R. A., Rubio, M., Dollé, M. E. T., Campisi, J. & Vijg, J. Oxygen accelerates the accumulation of mutations during the senescence and immortalization of murine cells in culture. *Aging Cell* **2**, 287–294 (2003).
 51. Simon, M. C. & Keith, B. The role of oxygen availability in embryonic development and stem cell function. *Nat. Rev. Mol. Cell Biol.* **9**, 285–296 (2008).
 52. Ezashi, T., Das, P. & Roberts, R. M. Low O₂ tensions and the prevention of differentiation of hES cells. *Proc. Natl. Acad. Sci. U. S. A.* **102**, 4783–4788 (2005).
 53. Gustafsson, M. V. *et al.* Hypoxia requires notch signaling to maintain the undifferentiated cell state. *Dev. Cell* **9**, 617–628 (2005).
 54. Jang, Y.-Y. & Sharkis, S. J. A low level of reactive oxygen species selects for primitive hematopoietic stem cells that may reside in the low-oxygenic niche. *Blood* **110**, 3056–3063 (2007).
 55. Hermitte, F., Brunet de la Grange, P., Belloc, F., Praloran, V. & Ivanovic, Z. Very low O₂ concentration (0.1%) favors G₀ return of dividing CD34+ cells. *Stem Cells Dayt. Ohio* **24**, 65–73 (2006).
 56. Parmar, K., Mauch, P., Vergilio, J.-A., Sackstein, R. & Down, J. D. Distribution of hematopoietic stem cells in the bone marrow according to regional hypoxia. *Proc. Natl. Acad. Sci. U. S. A.* **104**, 5431–5436 (2007).
 57. Kubota, Y., Takubo, K. & Suda, T. Bone marrow long label-retaining cells reside in the sinusoidal hypoxic niche. *Biochem. Biophys. Res. Commun.* **366**, 335–339 (2008).
 58. Köhler, A. *et al.* Altered cellular dynamics and endosteal location of aged early hematopoietic progenitor cells revealed by

- time-lapse intravital imaging in long bones. *Blood* **114**, 290–298 (2009).
59. Chambers, S. M. *et al.* Aging hematopoietic stem cells decline in function and exhibit epigenetic dysregulation. *PLoS Biol.* **5**, e201 (2007).
 60. Wilson, A. *et al.* Hematopoietic stem cells reversibly switch from dormancy to self-renewal during homeostasis and repair. *Cell* **135**, 1118–1129 (2008).
 61. Haug, J. S. *et al.* N-cadherin expression level distinguishes reserved versus primed states of hematopoietic stem cells. *Cell Stem Cell* **2**, 367–379 (2008).
 62. Li, L. & Clevers, H. Coexistence of Quiescent and Active Adult Stem Cells in Mammals. *Science* **327**, 542–545 (2010).
 63. Wang, J. C., Doedens, M. & Dick, J. E. Primitive human hematopoietic cells are enriched in cord blood compared with adult bone marrow or mobilized peripheral blood as measured by the quantitative in vivo SCID-repopulating cell assay. *Blood* **89**, 3919–3924 (1997).
 64. Ikuta, K. & Weissman, I. L. Evidence that hematopoietic stem cells express mouse c-kit but do not depend on steel factor for their generation. *Proc. Natl. Acad. Sci. U. S. A.* **89**, 1502–1506 (1992).
 65. Spangrude, G. J., Heimfeld, S. & Weissman, I. L. Purification and characterization of mouse hematopoietic stem cells. *Science* **241**, 58–62 (1988).
 66. Sitnicka, E. *et al.* Human CD34+ hematopoietic stem cells capable of multilineage engrafting NOD/SCID mice express flt3: distinct flt3 and c-kit expression and response patterns on mouse and candidate human hematopoietic stem cells. *Blood* **102**, 881–886 (2003).
 67. Larochelle, A. *et al.* Human and rhesus macaque hematopoietic stem cells cannot be purified based only on SLAM family markers. *Blood* **117**, 1550–1554 (2011).
 68. Baum, C. M., Weissman, I. L., Tsukamoto, A. S., Buckle, A. M. & Peault, B. Isolation of a candidate human hematopoietic stem-cell population. *Proc. Natl. Acad. Sci. U. S. A.* **89**, 2804–2808 (1992).
 69. Murray, L. *et al.* Enrichment of human hematopoietic stem cell activity in the CD34+Thy-1+Lin- subpopulation from mobilized peripheral blood. *Blood* **85**, 368–378 (1995).
 70. Bhatia, M., Wang, J. C., Kapp, U., Bonnet, D. & Dick, J. E. Purification of primitive human hematopoietic cells capable of repopulating immune-deficient mice. *Proc. Natl. Acad. Sci. U. S. A.* **94**, 5320–5325 (1997).
 71. Conneally, E., Cashman, J., Petzer, A. & Eaves, C. Expansion in vitro of transplantable human cord blood stem cells demonstrated using a quantitative assay of their lympho-myeloid repopulating activity in nonobese diabetic-scid/scid mice. *Proc. Natl. Acad. Sci. U. S. A.* **94**, 9836–9841 (1997).
 72. Lansdorp, P. M., Sutherland, H. J. & Eaves, C. J. Selective expression of CD45 isoforms on functional subpopulations of CD34+ hemopoietic cells from human bone marrow. *J. Exp. Med.* **172**, 363–366 (1990).
 73. Doulatov, S., Notta, F., Laurenti, E. & Dick, J. E. Hematopoiesis: A Human Perspective. *Cell Stem Cell* **10**, 120–136 (2012).
 74. Guo, Y., Lübbert, M. & Engelhardt, M. CD34- Hematopoietic Stem Cells: Current Concepts and Controversies. *STEM CELLS* **21**, 15–20 (2003).
 75. Coulombel, L. Identification of hematopoietic stem/progenitor cells: strength and drawbacks of functional assays. *Oncogene* **23**, 7210–7222 (2004).
 76. van Os, R. P., Dethmers-Ausema, B. & de Haan, G. In vitro assays for cobblestone area-forming cells, LTC-IC, and CFU-C. *Methods Mol. Biol. Clifton NJ* **430**, 143–157 (2008).
 77. Thomas, E. D., Lochte, H. L., Lu, W. C. & Ferrebee, J. W. Intravenous Infusion of Bone Marrow in Patients Receiving Radiation and Chemotherapy. *N. Engl. J. Med.* **257**, 491–496 (1957).
 78. Porada, C. D., Atala, A. J. & Almeida-Porada, G. The hematopoietic system in the context of regenerative medicine. *Methods* (2015). doi:10.1016/j.ymeth.2015.08.015
 79. Barriga, F., Ramírez, P., Wietstruck, A. & Rojas, N. Hematopoietic stem cell transplantation: clinical use and perspectives. *Biol. Res.* **45**, 307–316 (2012).
 80. Patel, S. A. & Rameshwar, P. Stem Cell Transplantation for Hematological Malignancies: Prospects for Personalized Medicine and Co-therapy with Mesenchymal Stem Cells. *Curr. Pharmacogenomics Pers. Med.* **9**, 229–239 (2011).
 81. Choi, S. W., Levine, J. E. & Ferrara, J. L. M. Pathogenesis and Management of Graft-versus-Host Disease. *Immunol. Allergy Clin. North Am.* **30**, 75–101 (2010).
 82. Storb, R. *et al.* Methotrexate and Cyclosporine Compared with Cyclosporine Alone for Prophylaxis of Acute Graft versus Host Disease after Marrow Transplantation for Leukemia. *N. Engl. J. Med.* **314**, 729–735 (1986).
 83. Barnes, D. W. & Loutit, J. F. Treatment of murine leukaemia with x-rays and homologous bone marrow. II. *Br. J. Haematol.* **3**, 241–252 (1957).
 84. Barnes, D. W., Corp, M. J., Loutit, J. F. & Neal, F. E. Treatment of murine leukaemia with X rays and homologous bone marrow; preliminary communication. *Br. Med. J.* **2**, 626–627 (1956).
 85. Sullivan, K. M. *et al.* Influence of acute and chronic graft-versus-host disease on relapse and survival after bone marrow transplantation from HLA-identical siblings as treatment of acute and chronic leukemia. *Blood* **73**, 1720–1728 (1989).

86. Weiden, P. L. *et al.* Antileukemic effect of graft-versus-host disease in human recipients of allogeneic-marrow grafts. *N. Engl. J. Med.* **300**, 1068–1073 (1979).
87. Weiden, P. L., Sullivan, K. M., Flournoy, N., Storb, R. & Thomas, E. D. Antileukemic effect of chronic graft-versus-host disease: contribution to improved survival after allogeneic marrow transplantation. *N. Engl. J. Med.* **304**, 1529–1533 (1981).
88. Shizuru, J. A., Negrin, R. S. & Weissman, I. L. Hematopoietic stem and progenitor cells: clinical and preclinical regeneration of the hematolymphoid system. *Annu. Rev. Med.* **56**, 509–538 (2005).
89. Aversa, F. *et al.* Treatment of high-risk acute leukemia with T-cell-depleted stem cells from related donors with one fully mismatched HLA haplotype. *N. Engl. J. Med.* **339**, 1186–1193 (1998).
90. Aversa, F. *et al.* Improved outcome with T-cell-depleted bone marrow transplantation for acute leukemia. *J. Clin. Oncol. Off. J. Am. Soc. Clin. Oncol.* **17**, 1545–1550 (1999).
91. Papadopoulos, E. B. *et al.* T-cell-depleted allogeneic bone marrow transplantation as postremission therapy for acute myelogenous leukemia: freedom from relapse in the absence of graft-versus-host disease. *Blood* **91**, 1083–1090 (1998).
92. Anasetti, C. *et al.* Peripheral-blood stem cells versus bone marrow from unrelated donors. *N. Engl. J. Med.* **367**, 1487–1496 (2012).
93. Drize, N., Chertkov, J. & Zander, A. Hematopoietic progenitor cell mobilization into the peripheral blood of mice using a combination of recombinant rat stem cell factor (rrSCF) and recombinant human granulocyte colony-stimulating factor (rhG-CSF). *Exp. Hematol.* **23**, 1180–1186 (1995).
94. Jantunen, E. & Varmavuori, V. Plerixafor for mobilization of blood stem cells in autologous transplantation: an update. *Expert Opin. Biol. Ther.* **14**, 851–861 (2014).
95. Petersdorf, E. W. *et al.* Major-histocompatibility-complex class I alleles and antigens in hematopoietic-cell transplantation. *N. Engl. J. Med.* **345**, 1794–1800 (2001).
96. Sierra, J. *et al.* Transplantation of marrow cells from unrelated donors for treatment of high-risk acute leukemia: the effect of leukemic burden, donor HLA-matching, and marrow cell dose. *Blood* **89**, 4226–4235 (1997).
97. Spellman, S. *et al.* The detection of donor-directed, HLA-specific alloantibodies in recipients of unrelated hematopoietic cell transplantation is predictive of graft failure. *Blood* **115**, 2704–2708 (2010).
98. Guardiola, P. *et al.* Retrospective comparison of bone marrow and granulocyte colony-stimulating factor-mobilized peripheral blood progenitor cells for allogeneic stem cell transplantation using HLA identical sibling donors in myelodysplastic syndromes. *Blood* **99**, 4370–4378 (2002).
99. Gluckman, E. *et al.* Hematopoietic reconstitution in a patient with Fanconi's anemia by means of umbilical-cord blood from an HLA-identical sibling. *N. Engl. J. Med.* **321**, 1174–1178 (1989).
100. Broxmeyer, H. E. *et al.* Human umbilical cord blood as a potential source of transplantable hematopoietic stem/progenitor cells. *Proc. Natl. Acad. Sci. U. S. A.* **86**, 3828–3832 (1989).
101. Gluckman, E. *et al.* Transplantation of umbilical cord blood in Fanconi's anemia. *Nouv. Rev. Fr. Hématologie* **32**, 423–425 (1990).
102. Broxmeyer, H. E. in *StemBook* (Harvard Stem Cell Institute, 2008).
103. Ballen, K. K., Gluckman, E. & Broxmeyer, H. E. Umbilical cord blood transplantation: the first 25 years and beyond. *Blood* **122**, 491–498 (2013).
104. Garderet, L. *et al.* The umbilical cord blood alphabeta T-cell repertoire: characteristics of a polyclonal and naive but completely formed repertoire. *Blood* **91**, 340–346 (1998).
105. Brunstein, C. G. & Wagner, J. E. Umbilical cord blood transplantation and banking. *Annu. Rev. Med.* **57**, 403–417 (2006).
106. Gluckman, E. *et al.* Milestones in umbilical cord blood transplantation. *Br. J. Haematol.* **154**, 441–447 (2011).
107. De Lima, M. *et al.* Double-chimaerism after transplantation of two human leucocyte antigen mismatched, unrelated cord blood units. *Br. J. Haematol.* **119**, 773–776 (2002).
108. Barker, J. N., Scaradavou, A. & Stevens, C. E. Combined effect of total nucleated cell dose and HLA match on transplantation outcome in 1061 cord blood recipients with hematologic malignancies. *Blood* **115**, 1843–1849 (2010).
109. Barker, J. N. *et al.* Transplantation of 2 partially HLA-matched umbilical cord blood units to enhance engraftment in adults with hematologic malignancy. *Blood* **105**, 1343–1347 (2005).
110. Lister, J. *et al.* Multiple unit HLA-unmatched sex-mismatched umbilical cord blood transplantation for advanced hematological malignancy. *Stem Cells Dev.* **16**, 177–186 (2007).
111. Broxmeyer, H. E. *et al.* Human umbilical cord blood: A clinically useful source of transplantable hematopoietic stem/progenitor cells. *Int. J. Cell Cloning* **8**, 76–91 (1990).
112. Cardoso, A. A. *et al.* Release from quiescence of CD34+ CD38- human umbilical cord blood cells reveals their potentiality to engraft adults. *Proc. Natl. Acad. Sci.* **90**, 8707–8711 (1993).
113. Mayani, H. *et al.* Kinetics of Hematopoiesis in Dexter‐Type Long‐Term Cultures

- Established from Human Umbilical Cord Blood Cells. *Stem Cells* **16**, 127–135 (1998).
114. McNiece, I. K., Almeida-Porada, G., Shpall, E. J. & Zanjani, E. Ex vivo expanded cord blood cells provide rapid engraftment in fetal sheep but lack long-term engraftment potential. *Exp. Hematol.* **30**, 612–616 (2002).
 115. Andrade, P. Z., Santos, F. dos, Cabral, J. M. S. & da Silva, C. L. Stem cell bioengineering strategies to widen the therapeutic applications of haematopoietic stem/progenitor cells from umbilical cord blood: Stem cell bioengineering strategies to widen UCB clinical applications. *J. Tissue Eng. Regen. Med.* **9**, 988–1003 (2015).
 116. Andrade, P. Z., da Silva, C. L., dos Santos, F., Almeida-Porada, G. & Cabral, J. M. S. Initial CD34+ cell-enrichment of cord blood determines hematopoietic stem/progenitor cell yield upon Ex vivo expansion. *J. Cell. Biochem.* **112**, 1822–1831 (2011).
 117. Douay, L. Experimental culture conditions are critical for ex vivo expansion of hematopoietic cells. *J. Hematother. Stem Cell Res.* **10**, 341–346 (2001).
 118. Andrade, P. Z., dos Santos, F., Almeida-Porada, G., da Silva, C. L. & S Cabral, J. M. S. Systematic delineation of optimal cytokine concentrations to expand hematopoietic stem/progenitor cells in co-culture with mesenchymal stem cells. *Mol. Biosyst.* **6**, 1207–1215 (2010).
 119. Mehta, R. S. *et al.* Novel Techniques for Ex Vivo Expansion of Cord Blood: Clinical Trials. *Front. Med.* **2**, (2015).
 120. da Silva, C. L. *et al.* A human stromal-based serum-free culture system supports the ex vivo expansion/maintenance of bone marrow and cord blood hematopoietic stem/progenitor cells. *Exp. Hematol.* **33**, 828–835 (2005).
 121. da Silva, C. L. *et al.* Differences amid bone marrow and cord blood hematopoietic stem/progenitor cell division kinetics. *J. Cell. Physiol.* **220**, 102–111 (2009).
 122. Jaroscak, J. *et al.* Augmentation of umbilical cord blood (UCB) transplantation with ex vivo-expanded UCB cells: results of a phase 1 trial using the AastromReplicell System. *Blood* **101**, 5061–5067 (2003).
 123. Williams, D. A. Ex vivo expansion of hematopoietic stem and progenitor cells--robbing Peter to pay Paul? *Blood* **81**, 3169–3172 (1993).
 124. Kirouac, D. C. & Zandstra, P. W. The systematic production of cells for cell therapies. *Cell Stem Cell* **3**, 369–381 (2008).
 125. Madlambayan, G. J. *et al.* Dynamic changes in cellular and microenvironmental composition can be controlled to elicit in vitro human hematopoietic stem cell expansion. *Exp. Hematol.* **33**, 1229–1239 (2005).
 126. Madlambayan, G. J. *et al.* Clinically relevant expansion of hematopoietic stem cells with conserved function in a single-use, closed-system bioprocess. *Biol. Blood Marrow Transplant. J. Am. Soc. Blood Marrow Transplant.* **12**, 1020–1030 (2006).
 127. Socolovsky, M. *et al.* Negative autoregulation by FAS mediates robust fetal erythropoiesis. *PLoS Biol.* **5**, e252 (2007).
 128. Cashman, J. D., Clark-Lewis, I., Eaves, A. C. & Eaves, C. J. Differentiation stage-specific regulation of primitive human hematopoietic progenitor cycling by exogenous and endogenous inhibitors in an in vivo model. *Blood* **94**, 3722–3729 (1999).
 129. Dao, M. A., Taylor, N. & Nolte, J. A. Reduction in levels of the cyclin-dependent kinase inhibitor p27(kip-1) coupled with transforming growth factor beta neutralization induces cell-cycle entry and increases retroviral transduction of primitive human hematopoietic cells. *Proc. Natl. Acad. Sci. U. S. A.* **95**, 13006–13011 (1998).
 130. Fortunel, N. *et al.* Specific dose-response effects of TGF-beta1 on developmentally distinct hematopoietic stem/progenitor cells from human umbilical cord blood. *Hematol. J. Off. J. Eur. Haematol. Assoc. EHA* **1**, 126–135 (2000).
 131. Peled, T. *et al.* Pre-clinical development of cord blood-derived progenitor cell graft expanded ex vivo with cytokines and the polyamine copper chelator tetraethylenepentamine. *Cytotherapy* **6**, 344–355 (2004).
 132. Peled, T., Landau, E., Prus, E., Treves, A. J. & Fibach, E. Cellular copper content modulates differentiation and self-renewal in cultures of cord blood-derived CD34+ cells. *Br. J. Haematol.* **116**, 655–661 (2002).
 133. Montesinos, P. *et al.* StemEx®(Copper Chelation Based) Ex Vivo Expanded Umbilical Cord Blood Stem Cell Transplantation (UCBT) Accelerates Engraftment and Improves 100 Day Survival In Myeloablated Patients Compared To a Registry Cohort Undergoing Double Unit UCBT: Results Of a Multicenter Study Of 101 Patients With Hematologic Malignancies. *Blood* **122**, 295–295 (2013).
 134. Varnum-Finney, B. *et al.* Pluripotent, cytokine-dependent, hematopoietic stem cells are immortalized by constitutive Notch1 signaling. *Nat. Med.* **6**, 1278–1281 (2000).
 135. Delaney, C. *et al.* Notch-mediated expansion of human cord blood progenitor cells capable of rapid myeloid reconstitution. *Nat. Med.* **16**, 232–236 (2010).
 136. Peled, T. *et al.* Nicotinamide, a SIRT1 inhibitor, inhibits differentiation and facilitates expansion of hematopoietic progenitor cells with enhanced bone marrow homing and engraftment. *Exp. Hematol.* **40**, 342–355.e1 (2012).
 137. Narala, S. R. *et al.* SIRT1 Acts as a Nutrient-sensitive Growth Suppressor and Its Loss Is Associated with Increased AMPK and Telomerase Activity. *Mol. Biol. Cell* **19**, 1210–1219 (2007).
 138. Horwitz, M. E. *et al.* Umbilical cord blood expansion with nicotinamide provides long-

- term multilineage engraftment. *J. Clin. Invest.* **124**, 3121–3128 (2014).
139. Wagner JE, Brunstein C, McKenna D, Sumstad D, Maahs S, Laughlin M, et al. StemRegenin-1 (SR1) expansion culture abrogates the engraftment barrier associated with umbilical cord blood transplantation (UCBT). *Blood* (2014) **124**:728.
 140. Oostendorp, R. A. J. et al. Long-term maintenance of hematopoietic stem cells does not require contact with embryo-derived stromal cells in cocultures. *Stem Cells Dayt. Ohio* **23**, 842–851 (2005).
 141. Lewis, I. D. et al. Umbilical cord blood cells capable of engrafting in primary, secondary, and tertiary xenogeneic hosts are preserved after ex vivo culture in a noncontact system. *Blood* **97**, 3441–3449 (2001).
 142. Cheng, X. et al. Human brain endothelial cells (HUBEC) promote SCID repopulating cell expansion through direct contact. *Growth Factors Chur Switz.* **25**, 141–150 (2007).
 143. Robinson, S. et al. Ex vivo expansion of umbilical cord blood. *Cytotherapy* **7**, 243–250 (2005).
 144. Frias, A. M. et al. Generation of functional natural killer and dendritic cells in a human stromal-based serum-free culture system designed for cord blood expansion. *Exp. Hematol.* **36**, 61–68 (2008).
 145. Zuk, P. A. et al. Multilineage cells from human adipose tissue: implications for cell-based therapies. *Tissue Eng.* **7**, 211–228 (2001).
 146. Fan, C. G. et al. Characterization and neural differentiation of fetal lung mesenchymal stem cells. *Cell Transplant.* **14**, 311–321 (2005).
 147. Campagnoli, C. et al. Identification of mesenchymal stem/progenitor cells in human first-trimester fetal blood, liver, and bone marrow. *Blood* **98**, 2396–2402 (2001).
 148. Érices, A., Conget, P. & Minguell, J. J. Mesenchymal progenitor cells in human umbilical cord blood. *Br. J. Haematol.* **109**, 235–242 (2000).
 149. De Bari, C., Dell’Accio, F., Tylzanowski, P. & Luyten, F. P. Multipotent mesenchymal stem cells from adult human synovial membrane. *Arthritis Rheum.* **44**, 1928–1942 (2001).
 150. In ’t Anker, P. S. et al. Amniotic fluid as a novel source of mesenchymal stem cells for therapeutic transplantation. *Blood* **102**, 1548–1549 (2003).
 151. Noort, W. A. et al. Mesenchymal stem cells promote engraftment of human umbilical cord blood-derived CD34(+) cells in NOD/SCID mice. *Exp. Hematol.* **30**, 870–878 (2002).
 152. Gronthos, S., Mankani, M., Brahimi, J., Robey, P. G. & Shi, S. Postnatal human dental pulp stem cells (DPSCs) in vitro and in vivo. *Proc. Natl. Acad. Sci. U. S. A.* **97**, 13625–13630 (2000).
 153. Williams, J. T., Southerland, S. S., Souza, J., Calcutt, A. F. & Cartledge, R. G. Cells isolated from adult human skeletal muscle capable of differentiating into multiple mesodermal phenotypes. *Am. Surg.* **65**, 22–26 (1999).
 154. Wang, H.-S. et al. Mesenchymal stem cells in the Wharton’s jelly of the human umbilical cord. *Stem Cells Dayt. Ohio* **22**, 1330–1337 (2004).
 155. Lindroos, B., Suuronen, R. & Miettinen, S. The potential of adipose stem cells in regenerative medicine. *Stem Cell Rev.* **7**, 269–291 (2011).
 156. CELLstart™ Xeno-Free Substrate for Stem Cell Culture. Available at: <http://www.thermofisher.com/pt/en/home/life-science/stem-cell-research/stem-cell-culture/stem-cell-research-misc/cellstart.html?CID=ta-lm-cellstart-CELLstart%E2%84%A2%20Xeno-Free%20Substrate%20for%20Stem%20Cell%20Culture>. (Accessed: 16th February 2016)
 157. Stem Cell Technologies. Identification of colonies from human hematopoietic progenitors. Available at: http://www.stemcell.com/~media/Technical%20Resources/C/O/E/F/B/wallchart_Human%20hematopoieticWEB.pdf?la=en.
 158. Le Blanc, K. et al. Transplantation of mesenchymal stem cells to enhance engraftment of hematopoietic stem cells. *Leukemia* **21**, 1733–1738 (2007).
 159. StemPro MSC SFM XenoFree - Thermo Fisher Scientific. Available at: <https://www.thermofisher.com/order/catalog/product/A1067501>. (Accessed: 22nd June 2016)
 160. Crespo-Diaz, R. et al. Platelet Lysate Consisting of a Natural Repair Proteome Supports Human Mesenchymal Stem Cell Proliferation and Chromosomal Stability. *Cell Transplant.* **20**, 797–811 (2011).
 161. AventaCell BioMedical: Products: BSSub™-XF. Available at: <http://www.atcbiomed.com/BSSub-XF.html>. (Accessed: 5th August 2016)
 162. Ssemaganda, A. et al. Characterization of Neutrophil Subsets in Healthy Human Pregnancies. *PLOS ONE* **9**, e85696 (2014).
 163. Han, J. et al. Adipose tissue is an extramedullary reservoir for functional hematopoietic stem and progenitor cells. *Blood* **115**, 957–964 (2010).
 164. Li, C. et al. Comparative analysis of human mesenchymal stem cells from bone marrow and adipose tissue under xeno-free conditions for cell therapy. *Stem Cell Res. Ther.* **6**, 55 (2015).
 165. Simões, I. N. et al. Human mesenchymal stem cells from the umbilical cord matrix: successful isolation and ex vivo expansion using serum-/xeno-free culture media. *Biotechnol. J.* **8**, 448–458 (2013).
 166. Leite, C. et al. Differentiation of human umbilical cord matrix mesenchymal stem

- cells into neural-like progenitor cells and maturation into an oligodendroglial-like lineage. *PLoS One* **9**, e111059 (2014).
167. Melief, S. M., Zwaginga, J. J., Fibbe, W. E. & Roelofs, H. Adipose Tissue-Derived Multipotent Stromal Cells Have a Higher Immunomodulatory Capacity Than Their Bone Marrow-Derived Counterparts. *Stem Cells Transl. Med.* **2**, 455–463 (2013).
 168. Shawki, S. *et al.* Immunomodulatory effects of umbilical cord-derived mesenchymal stem cells. *Microbiol. Immunol.* **59**, 348–356 (2015).
 169. Bá *et al.* What Makes Umbilical Cord Tissue-Derived Mesenchymal Stromal Cells Superior Immunomodulators When Compared to Bone Marrow Derived Mesenchymal Stromal Cells? *Stem Cells Int.* **2015**, e583984 (2015).
 170. gelifesciences. *Understanding Design of Experiments (DoE) in Protein Purification (Part 1)*.
 171. Hatami, J. *et al.* Developing a co-culture system for effective megakaryo/thrombopoiesis from umbilical cord blood hematopoietic stem/progenitor cells. *Cytotherapy* **17**, 428–442 (2015).
 172. StemSpan™ SFEM II | STEMCELL Technologies. Available at: <https://www.stemcell.com/products/stemspan-sfem-ii.html#section-data-and-publications>. (Accessed: 13th August 2016)
 173. Kent, D. *et al.* Regulation of hematopoietic stem cells by the steel factor/KIT signaling pathway. *Clin. Cancer Res. Off. J. Am. Assoc. Cancer Res.* **14**, 1926–1930 (2008).
 174. Broudy, V. C. Stem cell factor and hematopoiesis. *Blood* **90**, 1345–1364 (1997).
 175. Waskow, C. *et al.* The receptor tyrosine kinase Flt3 is required for dendritic cell development in peripheral lymphoid tissues. *Nat. Immunol.* **9**, 676–683 (2008).
 176. Christensen, J. L. & Weissman, I. L. Flk-2 is a marker in hematopoietic stem cell differentiation: A simple method to isolate long-term stem cells. *Proc. Natl. Acad. Sci.* **98**, 14541–14546 (2001).
 177. Adolfsson, J. *et al.* Upregulation of Flt3 Expression within the Bone Marrow Lin–Sca1+c-kit+ Stem Cell Compartment Is Accompanied by Loss of Self-Renewal Capacity. *Immunity* **15**, 659–669 (2001).
 178. Solanilla, A. *et al.* Flt3-ligand induces adhesion of haematopoietic progenitor cells via a very late antigen (VLA)-4- and VLA-5-dependent mechanism. *Br. J. Haematol.* **120**, 782–786 (2003).
 179. de Graaf, C. A. & Metcalf, D. Thrombopoietin and hematopoietic stem cells. *Cell Cycle* **10**, 1582–1589 (2011).
 180. What is a block? Available at: <http://support.minitab.com/en-us/minitab/17/topic-library/modeling-statistics/doe/basics/what-is-a-block/>. (Accessed: 24th August 2016)
 181. Pinho, S. *et al.* PDGFR and CD51 mark human Nestin+ sphere-forming mesenchymal stem cells capable of hematopoietic progenitor cell expansion. *J. Exp. Med.* **210**, 1351–1367 (2013).
 182. Ratajczak, M. Z. & Suszynska, M. Emerging Strategies to Enhance Homing and Engraftment of Hematopoietic Stem Cells. *Stem Cell Rev. Rep.* **12**, 121–128 (2016).